UNIVERSITÁ DEGLI STUDI DI PADOVA

DIPARTIMENTO DI INGEGNERIA INDUSTRIALE

CORSO DI LAUREA MAGISTRALE IN

INGEGNERIA ENERGETICA

CYCLIC AND CONTINUOUS FLOW SYSTEMS: ANALYTICAL AND NUMERICAL MODELS

Relatore:

Prof. Michele De Carli

Correlatori:

Ing. Angelo Zarrella

Ing. Mirco Donà

Prof. Gudrún Sævarsdóttir

Laureando:

Alessandro Bellini

matricola 1019829

Anno Accademico 2012 - 2013

Acknowledgements

La pagina dei ringraziamenti è dedicata in primo luogo ai miei genitori Antonio e Cecilia, i quali hanno avuto sempre fiducia in me, nonostante il mio carattere non sia dei più trasparenti nei loro confronti. Ringrazio i miei fratelli Francesco, Marco e Lucia con i quali ho vissuto tanti anni sotto lo stesso tetto con tanti litigi amorevoli. Infine una persona speciale, la mia Enrica, senza la quale non sarei qui a scrivere l'atto finale di laurea; la ringrazio per tutto l'appoggio, il sostegno nei momenti difficili che sono stati e saranno. La tesi è frutto del lavoro svolto in parte all'estero, quindi ringrazio le persone che mi sono state vicine in questa mia prima esperienza di vita che mi ha portato a vivere per diversi mesi distante dalla sicurezza delle mie abitudini. Luca e Alberto come compagni di viaggio e tutte le persone che mi sono venute a trovare in quel luogo dimenticato dal sole, Francesca, Paolo e l'instancabile Roberto.

Ringrazio tutti gli amici che ci sono e che ci saranno, quelli perduti con cui ho condiviso comunque delle esperienze. Una speciale citazione per ringraziare Giulio, che ancora mi sopporta. Per concludere ringrazio Sandra e la pazienza avuta nel leggere e cercare di rendere umane queste pagine.

Contents

Introduction

This work wants to present different aspects and problems relating to Underground Water Systems. Underground Water Systems initially were used especially where there were geothermal anomalies (Continuous Flow Systems); but now there are new different utilizations, as ATES (Cyclic Flow Systems), driven by energy storage concept, thus also areas with normal aquifer situation, without any geothermal anomaly, could be exploited. With increasing of Energy Savings ideas these Underground Water Systems had become more studied and utilized. It is possible to identify two different way of exploitation the Underground Water Systems: one exploitation of aquifer due on geothermal anomaly, that is use of underground system as big heat exchanger, or use of underground water as Storage material of cold and heat which can be useful in other circumstances[1]. For these systems two points are important: the first is represented by the geological analysis and field characterization study, and the second study is represented by the modeling of systems using simulation programs to predict how the system will go. After this pre-feasibility studies a pilot system can be prepared. In this work, after an background and introduction chapter, the focus is on the simulation, analytical and numerical analysis. There are two main parts of this document: numerical and analytical modeling of Continuous Flow Water Systems and Cyclic Flow Systems. The objectives of this thesis are the comparison between analytical and numerical solution and also to find a simple numerical model which can be used to predict the underground water situation under different state, for a good pre-feasibility study. Differently to several articles in literature, the focus, takes into account axial symmetric solutions that represent the real situation of a well drilled in the ground; normally to compare analytical and numerical solutions, the numerical one is usually simulated under the same condition of the analytical one; here, instead the numerical solution is built as close as possible to the real phenomena. This work is divided in chapters whose content is introduced by an abstract section.

[1]These storage systems present several advantages to other storage systems, indeed they need minimum one well to store already a great amount of energy. The disadvantage is represented by the several and expensive pre-feasibility analysis.

Chapter 1

Background

Abstract

The word Aquifer, from Latin language, means water-bearing and it is easy to understand how its normal structure is made by a porous media strata only with an impermeable under burden for the swallow aquifer (unconfined aquifer) and also an impermeable overburden for confined aquifer. To understand better the origin and the structure of the aquifer it is appropriate to talk about minerals and rocks and the formation of unconsolidated materials. Than the macrostructure of the underground formations will be explained, hence the aquifer typology as well. Also in this chapter some theory elements about the hydraulic properties will be introduced. For more information see (Delleur et al. 2007) and (Banks 2008).

1.1 Rocks

Rocks are formed by one or more minerals conglomerate under different type of crystallization that are due to a different types of formations. Minerals are made as singles chemicals elements or as a compound. There are three main classes of rocks: igneous rocks, sedimentary rock and metamorphic rocks.

Igneous Rocks are very common all over the world indeed they are formed as cooled products from the molten state (magma that is get out during volcanic eruptions from earth fractures); the most known type of igneous rock is basalt, an extrusive rock cooled by a rapid process near the earth surface crust.

Pyroclastic rocks is a part of sedimentary rock and igneous rocks formed by accumulation of particular types of rocks as extrusive lighter lava or pumice, erupted just as lapilli (type of rock that usually cools in air incorporating a lot of hair in its crystals formation, this cause the typical characteristic of lightness).

Sedimentary rocks are the most common class of formation, this type is usually formed by the deposition of rocks from air or water.

	Porosity (n) %	Specific yield (S_Y) %	Hydraulic conductivity (K) m s^{-1}
Clay	30–60	1–10	10^{-12}–10^{-8}
Silt	35–50	5–30	10^{-9}–10^{-5}
Sands	25–50	10–30	10^{-7}–10^{-3}
Gravel	20–40	10–25	10^{-4}–10^{-1}
Sandstone	5–30	5–25	10^{-9}–10^{-4}
Most unweathered crystalline silicate rocks (granites, schists, gneisses)	<1 0.1** <0.05*	<1	10^{-13}–10^{-5} depending on degree of fracturing
Basalt	<1–50	<1–30	10^{-13}–10^{-2}
British Chalk	10–45	0.5–5	10^{-10}–10^{-6}# (median 7×10^{-9})#

* Olofsson (2002) cites an effective (kinematic) porosity of crystalline rock aquifers of <0.05%.
** Domenico and Schwartz (1990) cite values as low as 0.1% for porosity and 0.0005% for effective porosity in granite.
# These figures refer to Chalk matrix hydraulic conductivities. Bulk transmissivities of the Chalk aquifer are typically in the range 10–10 000 m^2 day^{-1} (10^{-4}–10^{-1} m^2 s^{-1}), which provides some impression of the importance of fracture flow in the Chalk (Allen *et al.*, 1997).

Figure 1.1: Typical hydraulic properties of geological formations (Banks 2008)

The last main class is named Metamorphic, these are formed by rocks from all the category (parent rocks) under transformation due particular external conditions (pressure and temperature stress). Note that metamorphic rocks have the same chemical composition of the parent rocks, but a different structure.

Obviously groundwater can be found in all of the three rocks formation, but commonly the greatest amounts of water stands in the sedimentary accumulation. The cause of that is because in sedimentary formations the porosity is higher than the other classes of rocks.

1.2 Underground General Characterisation

It is possible to classify underground formation in three macro structure: Aquifers, Aquitards and Fractures. There are two important hydraulic properties that are useful to understand the differences in these categories: Hydraulic conductivity (K) and storage (S). The first one represents the maximum velocity that a water flow can assume. The second one represents the maximum volume of water that is possible to absorb (or release) under specific condition in hydraulic head about 1 m for a specific volume of material. Thus a material with an high value of K (Hydraulic conductivity) can absorb a great amount of water during a specific time and it is easy to think that a material with a good value of S (storage coefficient) can stock a high amount of water (Figure1.1). With the word Aquifer it is assumed every underground system that is a strata or body of rocks or sediments that produces an economically useful amount of groundwater; these structures are usually characterized by great values of K and S. Thus these formations are usually identify as porous-medium or inter-granular flow aquifers.

An underground system characterised, with poor value of K and S, is identified as Aquitard,

Figure 1.2: A groundwater cascading out of a fissure in a pumped borehole in the Chalk aquifer of southern England (Banks 2008)

usually this consist in Fine-grained sediments[1] e.g. silt and clay formations.

The third underground rock formation lays where rocks structures are crystalline as granite, slates and gneiss. In these types of rocks it is easy to expect a very poor porosity and high value of impermeability, however there are different events to be taken into account. The main one is the high value of stress, made by earth movements during geological time, which cause several permeable structures like joints and fractures; these formations are usually named Fractures-Aquifers and have the ability to use an enormous amount of water (magnitude of hundreds liters per hour until thousands).

Also there are other typical rocks structures like limestone, dolomite or chalk formations that have, as the formation just introduced, a very poor permeability and very poor porosity as well. It is typical to find in these types of rocks formation some erosion phenomena. Indeed the solubility of the salt in the water and the capability of water erosion power conduct, during the years, to form underground channel typically named Karsic phenomena (Figure1.2). These types of structure produce a different Aquifer just named Karstidied Aquifer (it is easy to understand that these formation are High K and low S characterized).

1.3 Aquifers Characterisation

The word Aquifer derives from Latin language and means water-bearing, therefor it is easy to understand how the normal Aquifer structure is characterized with a porous media strata with an impermeable under burden (for the swallow aquifer, unconfined aquifer) and also an impermeable overburden for confined aquifer. One important difference when talking about aquifers is represented by the difference between *Confined* and *Unconfined* concepts (Figure1.4).

Unconfined aquifers (Figure1.3 (a)) are not under pressure and there is not a defined cover

[1]Characterised with low porosity which consists in a very small pore dimension formation, or in the worst cases with very low interconnection between pores. Thus there is a very low effective porosity.

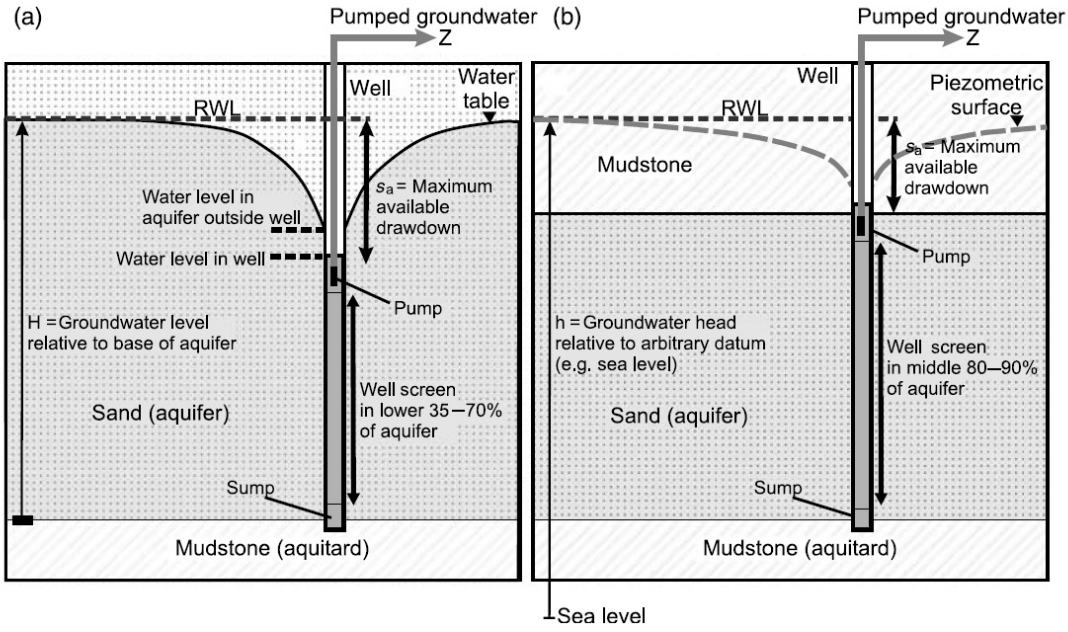

Figure 1.3: (a) Unconfined aquifer (b) Confined aquifer (Banks 2008).

layer indeed the cover part is "free": in other words without any constraints. Thus the upper boundary is free and the water surface is named water-table. This water-table can vary during the time so it is difficult to define precisely a saturated zone. Also the recharge water (from rainfall) enters from the top of the aquifer and moves for gravity, so there is a portion of strata in which the aquifer is unsaturated, "the vadose zone".

Confined aquifers (Figure1.3 (b)) are made by a strata of medium material between two impervious layers on the bottom and on the top. That structure is typically made with porous media and two clay layers bounded. This type of aquifer is kept under pressure; this pressure depends on depth and the natural pressure of the formation. Sometimes the hydraulic head is greatest than the depth, so water starts to gush from the ground; this phenomena is well known as artesian aquifer.

1.4 Hydraulic Properties

1.4.1 Porosity

Porosity is a property that represents the ideal capacity of a solid volume to storage water, it is done by the follow expression:

$$n = \frac{V_p}{V_s} \tag{1.1}$$

where:

V_p is pores(voids) volume $[m^3]$.

V_s is solid volume $[m^3]$.

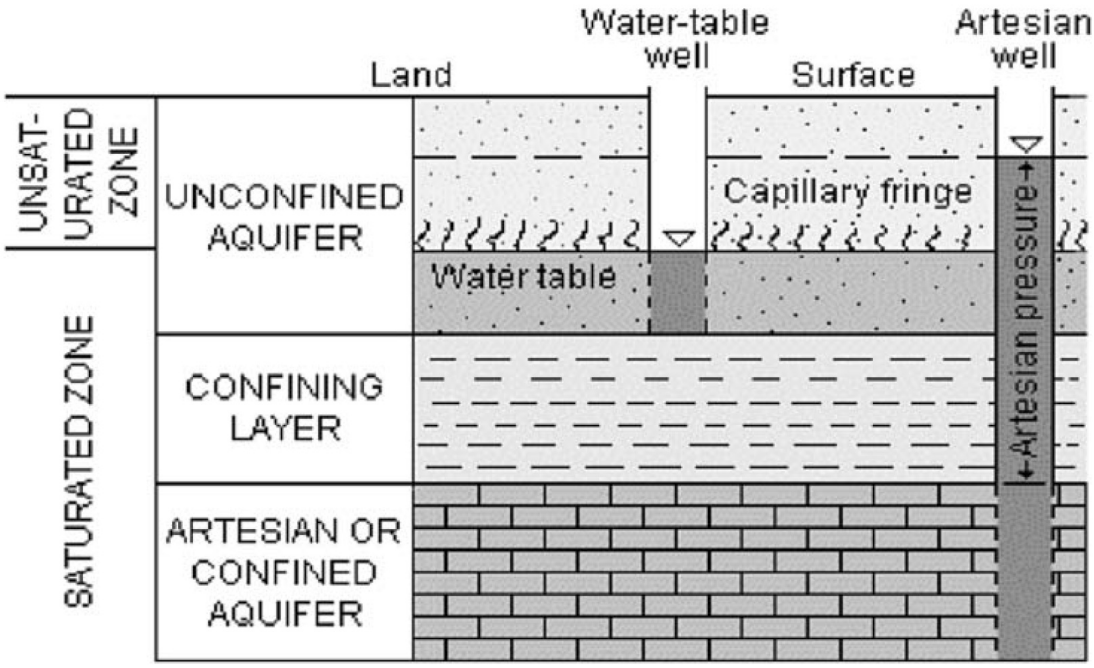

Figure 1.4: Another representation of Confined and Unconfined aquifer.

n is porosity.

There are two different types of porosity: *Primary porosity* and *Secondary porosity*. The first one represents the value of porosity that it is possible to find after the first event of the rocks formation (e.g. after precipitation or other causes typically weathering or biological); the second, Secondary porosity, is obtained after a subsequent process that induces new cavities formation (e.g. due to animals or vegetables decomposition). If we are consider the porosity of a single rock and do not talk about a conglomerate of gravel, it is useful to use the term of *Effective porosity*. Effective porosity represents the ratio between all connected pores (of the sample considered) and all the sample solid volume. To determine the entity of n a very simple test is used and it is based on Archimede's rule. One volume of rock (our sample) is considered, it is known in shape dimension; this volume is absorbed in a well known water volume and after that some times it must be wait to permit that water fills all the void spaces of the sample. After waiting some time (saturation time), we have to measure the different high variation of water level due only by the rock volume that represents the real sample rock part volume. It is possible to find the void volume by the difference between the volume of the rock sample and the real volume of the sample rock part. If we talk about single rock, there is the difference between porosity and effective porosity, but if the strata taken into account is formed by a conglomerate (e.g. coarse gravel), these two parameters are the same. To determine the conglomerate porosity two factors have to be considered: the arrangements of its grains and the uniformity of the grain-size distribution.

To better understand these concepts, it is useful to consider one ideal model to represent the gravel conglomerate: the greatest value of porosity for a conglomerate is analytically found using a spherical grains laying in a parallelepiped shape, as represented in Figure1.5 it amounts at 47.65%.

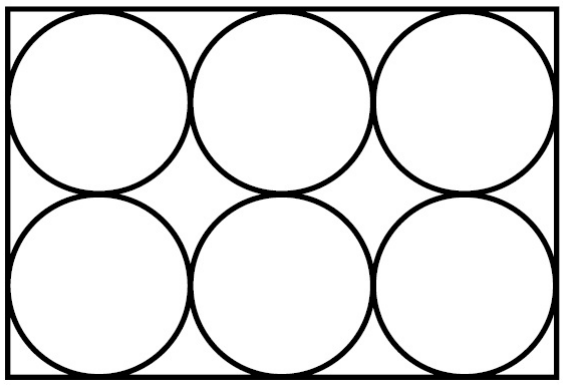

Figure 1.5: Cubic packing spherical grains.

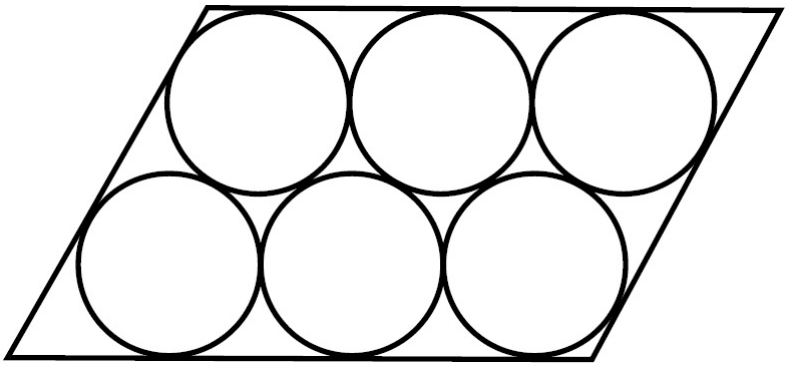

Figure 1.6: Rhombohedral packing spherical grains.

On the other hand, if the same spherical grains are in a different pack as rhombohedral packing, the value of porosity is 25.95%(Figure1.6). It is useful to define others coefficients like *Uniformity coefficient* C_u that is indicating the quality (due to the inhomogeneous size of the grains) of the stored volume:

$$C_u = \frac{D_{60}}{D_{10}} \tag{1.2}$$

where

D_{60} is diameter below of which 60% of the grains are finer.

D_{10} is diameter below of which 10% of the grains are finer (real grains diameter).

If C_u is less than four it means that the D_{10} and D_{60} are nearest and the conglomerate is well stored, but if C_u is greater than six it means that the D_{10} and D_{60} are considerably very various and the composition of the conglomerate is very different in grains size, thus this is a poor stored volume. Another parameter is e *Void ratio* represented as follow:

$$e = \frac{V_p}{V_s} \tag{1.3}$$

Porosity using e become:

$$n = \frac{1}{(1 + e^{-1})} \tag{1.4}$$

1.4.2 Moisture Content

Usually the water content is considered in a underground porous media system to better forecast its behavior under given hydraulic situation. The water content is given in two ways: as in weight ratio or in volume ratio. The moisture content gravimetrically and volumetrically are the following:

$$\phi_m = \frac{W_w}{W_s} \tag{1.5}$$

$$\phi_v = \frac{V_w}{V_s} \tag{1.6}$$

where:

W_w is water weight of sample volume $[kg]$.

W_s is the weight of the dry volume $[kg]$.

V_w is water volume of the sample $[m^3]$.

V_s is the sample volume $[m^3]$.

Usually these parameters are less used, the most used and common parameters are *Saturation Ratio* and *Degree of Saturation*. The first represents the ratio between the volume of the water and the volume of the voids and the latter is the saturation ratio percentage form:

$$\phi = \frac{V_w}{V_v} \tag{1.7}$$

$$\phi_{\%} = 100\phi \tag{1.8}$$

Lithology	Porosity (percent)	Hydraulic conductivity (cm/sec)	Compressibility, α(m^2/N or Pa $^{-1}$)
Unconsolidated			
Gravel	25–40	10^{-2}–10^{2}	10^{-8}–10^{-10}
Sand	25–50	10^{-4}–1	10^{-7}–10^{-9}
Silt	35–50	10^{-7}–10^{-3}	no data
Glay	40–70	10^{-10}–10^{-7}	10^{-6}–10^{-8}
Glacial Till	10–20	10^{-10}–10^{-4}	10^{-6}–10^{-8}
Indurated			
Fractured Basalt	5–50	10^{-5}–1	10^{-8}–10^{-9}
Karst Limestone	5–50	10^{-4}–10	not applicaple
Sandstone	5–30	10^{-8}–10^{-4}	10^{-11}–10^{-10}
Limestone, Dolomite	0–20	10^{-7}–10^{-4}	$< 10^{-10}$
Shale	0–10	10^{-11}–10^{-7}	10^{-7}–10^{-8}
Fractured Crystalline Rock	0–10	10^{-7}–10^{-2}	—10^{-10}—
Dense Crystalline Rock	0–5	10^{-12}–10^{-8}	10^{-9}–10^{-11}

Source: Adapted from Domenico, P.A. and Schwartz, F.W 1990. *Physical and Chemical Hydrogeology*, John Wiley and Sons, Inc., New York; Freeze, R.A. and Cherry, J.A., 1979. *Groundwater.* Prentice-Hall, Inc., Englewood Cliffs, NJ; Fetter, C.W., 1994. *Applied Hydrogeology*, 3rd ed. Macmillan College Publishing Co. Inc., New York; Narashimhan, T.N., and Goyal, K.P., 1984. Subsidence due to geothermal fluid withdrawal, in Man-Induced Land Subsidence, *Reviews in Engineering Geology, v.* VI, 35–66, Geological Society of America, Boulder, Co.

Figure 1.7: Soil and Rock Physical Properties.

If ϕ reaches the unity and $\phi_{\%}$ reaches 100% the volume of the soil is saturated, otherwise it would be unsaturated and part of the voids would be filled with air.

1.4.3 Capillarity

When a volume of soil is unsaturated, some water will fill those voids where there is not the presence of water and it is called capillarity effects. Capillary forces firstly have a major role and permit the movement of the water between solids grains by adhesion phenomenon. There are two interesting phenomena that insist in the capillarity process: one is the molecules attraction and the second one is the surface tension. The first is responsible for water adhering to soil or rock particle surfaces and the second is the water cohesion toward each other when water is in contact with air. In the saturated formation these two phenomenon are perfectly balanced, thus their effect do not cause any water movement. There are numerous phenomena that permit the water movement, specially when the underground systems nearest the free surface is treated (e.g. evaporating and drying), fortunately all of these can be neglected in saturated formations as will be done in this work.

1.4.4 Compressibility

To study the groundwater processes is useful know about the water and soil behaviours, first of all their compressibility.

Compressibility of Water

Water is a fluid and it is slightly compressible. To identify this properties is useful the use of isothermal compressibility (Domenico and Schwartz 1990):

$$\beta_w = K_w^{-1} = \frac{-1}{V_w} \cdot \frac{\partial V_w}{\partial P} \tag{1.9}$$

where

K_w is the water bulk module of compressibility $[N/m^2]$.

V_w is the water bulk volume $[m^3]$.

P is the pressure $[Pa]$.

NOTE: Typical value of β_w for water at 25℃ is $4.8 \cdot 10^{-10}$ $[m^2/N]$.

Compressibility of Solid

The matrix solid Compressibility factor is different from the water compressibility factor because for solid there are different stress in action, thus it is given a stress balance equation between external and internal stress due to the pore pressure and the stress from the skeleton of the solid

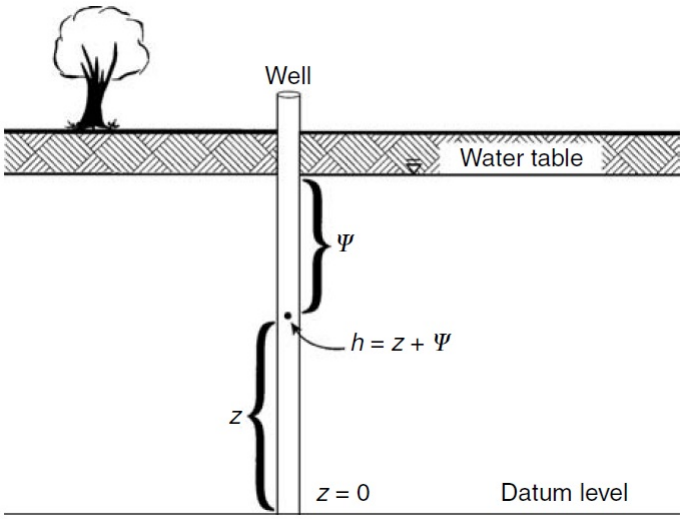

Figure 1.8: Illustration of Hydraulic Head

grains. Under constant temperature and incompressible grains the bulk matrix compressibility can be represented as (Domenico and Schwartz 1990):

$$\beta_b = K_b^{-1} = \frac{-1}{V_b} \cdot \frac{\partial V_b}{\partial \sigma_t} \tag{1.10}$$

where:

K_b is the rock bulk module of compressibility $[N/m^2]$.

V_b is the rock bulk volume $[m^3]$.

σ_t is the total vertical stress acting $[N]$.

(NOTE: sign minus identify the situation that under a compression the volume decrease itself).

1.4.5 Hydraulic Head

Hydraulic Head (Figure1.8) is an important variable because it represents the energy in a specific point of groundwater; by identifying this value for each point of the system it is easy to identify the value of the groundwater movements (water moves from a point with high value of hydraulic head to a point with less, the hydraulic gradient (Figure1.9) well describes the variation of Hydraulic head $I = \frac{\partial h}{\partial l}$ where h is hydraulic head and l is the length in which is considered the variation of h). Typically in hydraulic head expression the kinetic value is neglected and it can be represented:

$$h = Z + \frac{P}{\rho \cdot g} \tag{1.11}$$

where:

Z is the elevation head [m].

P is the pressure $[Pa]$.

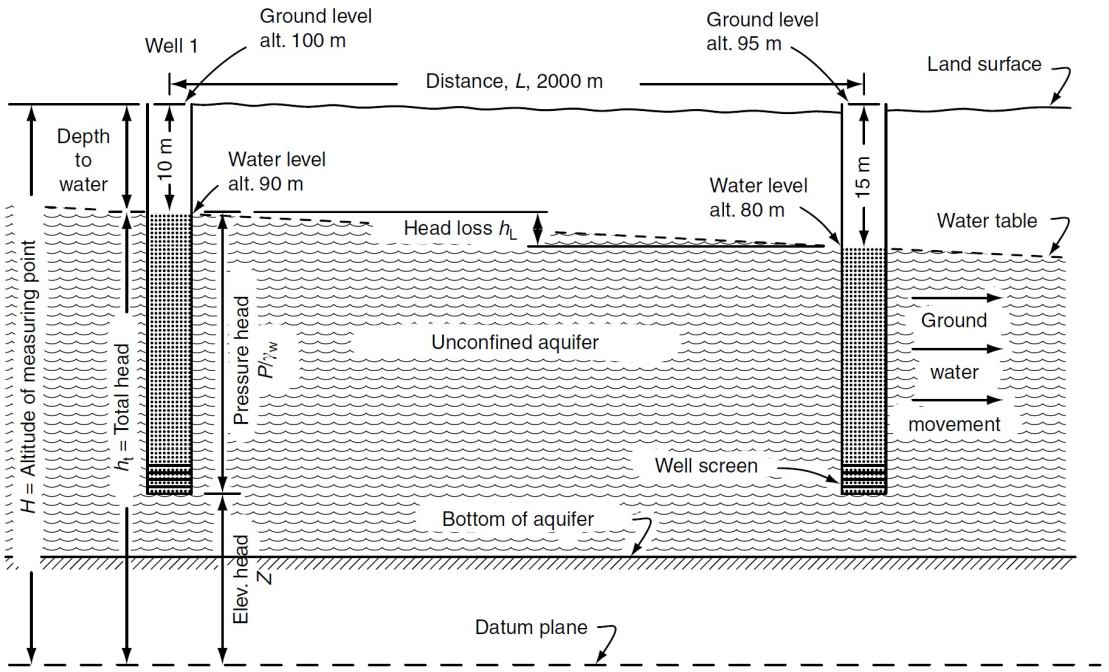

Figure 1.9: Illustration of Hydraulic Head

rho is the water density $[\frac{kg}{m^3}]$.

g is the gravitational velocity $[\frac{m}{s^2}]$.

NOTE: $\frac{P}{\rho \cdot g}$ can be identify with PSI called pressure head.

1.4.6 Storage

Storage is an important parameter that would represent the capacity of a single volume of aquifer to accept or release water under a specific condition of hydraulic head variation ($1[m]$). In other words, Storage represents the maximum volume of water that is possible to take up (or release) under specific condition in a specific volume of material under $1[m]$ of hydraulic head. The concept of storage it is useful to apply in a flow rate balance, when the injection flow rate is different from the pumping flow rate. The flow rate balance can be expressed as follow:

$$Q_{out} \cdot \Delta t = Q_{in} \cdot \Delta t \pm \Delta S \cdot \Delta t \tag{1.12}$$

(NOTE: during a Δt time) where:

Q_{in} is the Injection flow rate $[\frac{m^3}{s}]$.

Q_{out} is the Pumping flow rate $[\frac{m^3}{s}]$.

t is the Time $[s]$.

S is the Volume for unit of time accepted or released from the aquifer $[\frac{m^3}{s}]$.

In saturated porous media there are two important phenomena that cause the storage phenomenon: the compressibility of water and the expansion of the matrix. These two phenomena can be used in the definition of *Specific Storage* (that is the volume of water store or released from a volume of saturated porous media under $1m$ of increase or decrease in hydraulic head) as follow:

$$S_s = \rho \cdot g \cdot (\alpha + n \cdot \beta) \tag{1.13}$$

where:

Q_{in} is the Injection flow rate $[\frac{m^3}{s}]$

ρ is density of water $[\frac{kg}{m^3}]$

g is acceleration of gravitation $[\frac{m}{s^2}]$

β is water compressibility coefficient $[\frac{m^2}{N}]$

α is aquifer compressibility $[\frac{m^2}{N}]$

Another coefficient *Storativity* consider the specific characteristic of the aquifer, the thickness:

$$S = S_s \cdot b \tag{1.14}$$

where:

b is the aquifer thickness $[m]$

b is the aquifer thickness (NOTE: in confined aquifer under saturated condition the value of S ranges from 0.005 to 0.00005. Obviously when S is big the aquifer can be store more than an aquifer with low value of S).

1.5 Permeability

One important characteristic of the aquifer is the capacity to transmit fluid. The most important parameter to describe the transmittance of the fluid is *Intrinsic Permeability* (k); this parameter depends only by the characteristics of the media and does not depend from the media condition state or pressure and temperature values. The follow equation indicates the Intrinsic Permeability:

$$k = C \cdot d^2 \tag{1.15}$$

where:

d is the average diameter of the pores $[m]$.

C is an empirical variable depending from the aquifer characteristics (as packing sorting).

The unit of measurements is $[darcy]$ (from the name of Henry Darcy the author of the Darcy's Law for porous media). One $[darcy]$ is the area through which one fluid with 1 centipoise of will flow at a rate of one cubic centimeter per second per square centimeter under 1 atmosphere as pressure gradient per centimeter:

$$1darcy = \frac{1centipoise\frac{cm^3}{(sec \cdot cm^2)}}{(1atm/1cm)}$$

Usually the relationship between one darcy and one cm^2 is:

$$1darcy = 9.87 \cdot 10^{-10} cm^2$$

NOTE: this relationship is well used for every Newtonian liquids or gases through the medium.

1.6 Hydraulic Conductivity

As just explained, the intrinsic permeability is an aquifer attribute and does not depend on the type of liquid and the media condition; to have a complete description of transmittance fluid phenomena it is taken into account the *Hydraulic Conductivity*. Hydraulic Conductivity considers the medium behavior (using k) and also the liquid properties:

$$K = k \cdot \rho \cdot \frac{g}{\mu} \tag{1.16}$$

where:

k is intrinsic permeability $[D]$.

ρ is fluid density $[\frac{kg}{m^3}]$.

μ is fluid dynamic viscosity $[Pa \cdot s]$.

The dimension of this parameter is velocity $[\frac{m}{s}]$ and it is easy to understand that it represents the volume of fluid flowing perpendicular to a unit area of porous medium per unit time and per unit of hydraulic gradient. (NOTE: to see some typical value look Figure1.7) Henry Darcy was the first to use this parameter, he had found that the coefficient K is proportional value between the flow rate and the hydraulic gradient per unit of length. Sometimes it is useful consider one parameter to generalized the concept for entire aquifer, thus using *Trasmissivity* it is easy to know the amount of water through an aquifer of b thickness:

$$T = K \cdot b \tag{1.17}$$

It is simple to identify the definition of trasmissivity as "the volume of water per unit time passing through a unit width area of aquifer perpendicular to flow integrated over the thickness". If we consider an area A of the aquifer, it is possible to calculate the value of the total flow rate Q through this area under the gradient I as follow:

$$Q = T \cdot I \cdot A \tag{1.18}$$

1.7 Water Underground Movement

As already illustrated, the energy for a ground water system can be express as hydraulic head usually with dimension of meter, also it is already known that only with a variation of energy

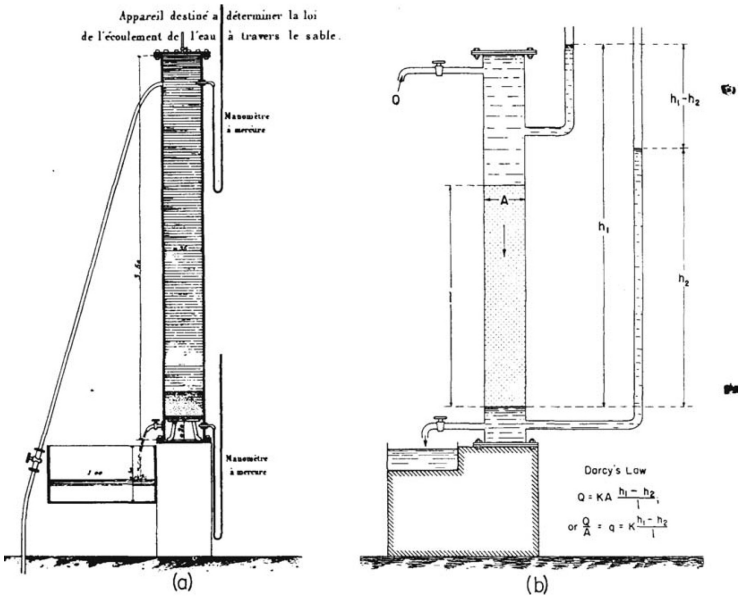

Figure 1.10: Darcy's original apparatus with mercury manometer and (b) equivalent apparatus with water manometers (Delleur et al. 2007).

there is the possibility to have a variation of equilibrium state. To have ground water movement we must have a hydraulic head gradient, this can be caused by geodetic variation and velocity or pressure variations (particularly important are those during an human exploitation).

1.7.1 Darcy's Law

Henry Darcy, French engineer, found in 1586 the relationship between hydraulic gradient and the flow rate in a porous media volume. Considering a sample of porous media with Hydraulic conductivity K, Darcy's Law says that the flow rate across an area A of the sample under an hydraulic gradient $i = -\frac{\partial h}{\partial s}$ (in s direction) is given by the follow equation:

$$Q = q \cdot A = -K \cdot i = k \cdot \rho \frac{g}{\mu} \cdot A \cdot i \tag{1.19}$$

where:

k is intrinsic permeability $[D]$.

ρ is fluid density $[\frac{kg}{m^3}]$.

μ is fluid dynamic viscosity $[Pa \cdot s]$.

q is Darcy's velocity (or specific discharge) $[\frac{m}{s}]$.

NOTE: the minus sign indicates that the flow moves from high to low head (along the direction of decreasing head). The parameter q is not the real water velocity (named pore velocity), indeed q represent the flow velocity in porous media like the water crossing all the surface A. To find the

real velocity of the water it is advantaged the use of effective porosity:

$$v = \frac{q}{n_e} \tag{1.20}$$

The one dimensional form of Darcy's Law is:

$$q = K \cdot \frac{(h_1 - h_2)}{L} \tag{1.21}$$

The limit of validity can be introduced with Reynolds number N_r:

$$N_r = \frac{q \cdot D}{\nu} \tag{1.22}$$

where:

q is Darcy's velocity (or specific discharge) $[\frac{m}{s}]$.

D is representative length $[m]$.

ν is kinematic viscosity $[\frac{m^2}{s}]$.

NOTE: Darcy's Law can be used only in the porous media formation; it cannot be used in karstic and in fracture formations (and all the formations with big average pores diameter). For the porous media systems the deviation from Darcy's Law stars at $N_r \approx 5$ and the turbulent flow starts at $N_r = 60$ (Schneebeli 1955).

1.7.2 Flow Toward Circular Well

Following Darcy's Law it is possible to analyze the behaviour of confined aquifer under pumping condition from a circular well (Figure1.11). If we consider a confined aquifer with an hydraulic conductivity K, during a pumping session it is possible to identify the variation of the piezometric level due to the variation of the water velocity, that is initially close to the well and subsequently further away than the well. With a constant flow rate pumped out from the well, a steady state situation can be analyzed; In this situation Darcy's Law is (at radial distance from well, r_1 and r_2):

$$Q = 2 \cdot \pi \cdot r_1 \cdot b \cdot K \cdot i_1 = 2 \cdot \pi \cdot r_2 \cdot b \cdot K \cdot i_2 \tag{1.23}$$

where:

r is is the radial distance from the well $[m]$.

b is the aquifer thickness $[m]$.

K is hydraulic conductivity $[\frac{m}{s}]$.

K is hydraulic gradient $(\frac{\partial h}{\partial r})$.

Integrating this equation from r_1 to r_2 (remembering the gradient definition $(\frac{\partial h}{\partial r})$) we find the *Thiem's equation* for confined aquifer:

$$Q = 2 \cdot \pi \cdot b \cdot K \cdot \frac{(h_2 - h_1)}{ln(r_2 - r_1)} \tag{1.24}$$

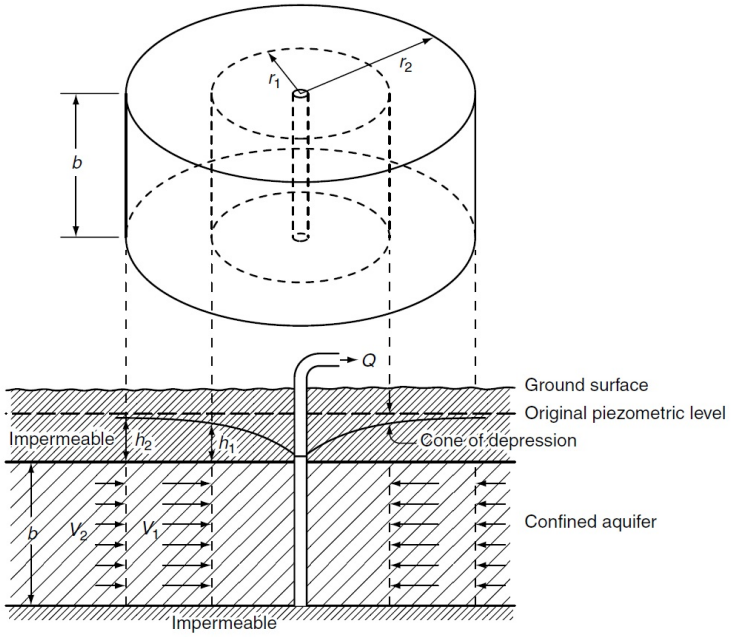

Figure 1.11: Fluid toward a circular well in a confined aquifer.

It is possible replace the product $b \cdot K$ with T, trasmissivity. The limit of the solution is represented by the choice of r_1 and r_2 indeed $r_1 \geq r_w(radiusofwell)$ and $r_2 \leq R$ (radius of influence that is the radius after which the pressure dropdown is near to zero).

1.8 Heat transport in Groundwater Systems

As well known the three ways for heat exchange are conduction, convection and radiation. Usually, considering the underground typical temperature[2], the major effect is conduction (obviously where there is not the groundwater presence). In the underground system radiation can be omitted because the normal temperature of underground is very low. It will be easier to treat heat exchange for closed system that it can be represented as heat exchanger, with this system without groundwater flow the only major effect is conduction. When a groundwater system is treated the heat exchange mechanisms are different; usually the main component of heat exchanged it is due by advection of groundwater. In an ATES system, where some water is directly injected and extracted from the aquifer, the system cannot be represented as heat simple exchanger because the phenomenon is more difficult to model. In these system it must be taken into account the presence of the underground water and the injection water; thus advection take the major role and conduction can be neglected. The injection water exchanges with the water in the aquifer and directly with the porous media. Another issue to contemplate is the natural advection caused by the difference of water density at different temperature; that can cause the typical effect of thermal

[2]Typically to identify the underground temperature it is useful consider the average annual temperature of the air. These simplification is right for a specific depth condition: from 10 m to the depth where geothermal heating is uninfluenced.

plume floating. Usually the natural advection can be neglected both for forced system, like ATES, and for natural system, like energy piles (closed circular pipe without any mass interaction). The heat exchange for doublet wells system will be explain in the ATES chapter 2.

Chapter 2

Underground Energy Storage

Abstract

In this chapter we introduce the most important thermal energy storage systems. In particularly we will focus on the A.T.E.S. (Aquifer Thermal Energy Storage) of its state of art design, taking in to account its main problems and further considerations. Furthermore general information on basic operation principles are going to considered and the modeling of ATES will be introduced.

2.1 U.T.E.S.

U.T.E.S is the acronym of Underground Thermal Energy Storage, and indicates all the systems used to store thermal energy in an Underground Formations. In Schmidt, Mangold, and MullerSteinhagen 2003 some different types of U.T.E.S. [1] are introduced, these are below listed (see Figure2.1):

- Hot-water Heat Stored.
- Gravel-water Heat Stored.
- Duct Heat Store.
- Aquifer Heat Store.

These are briefly summarized below with the explanation of their main characteristics.

2.1.1 Hot-water Heat Store

The concept of this technology is very simple. An insulated tank with water has to store the energy under hot or cold water form. With this technology uses only water as storage material because of water has good thermal properties as high specific heat capacity and the high difference

[1] In this case it is better the use of word STES, like author suggestion (Seasonal Thermal Energy Storage).

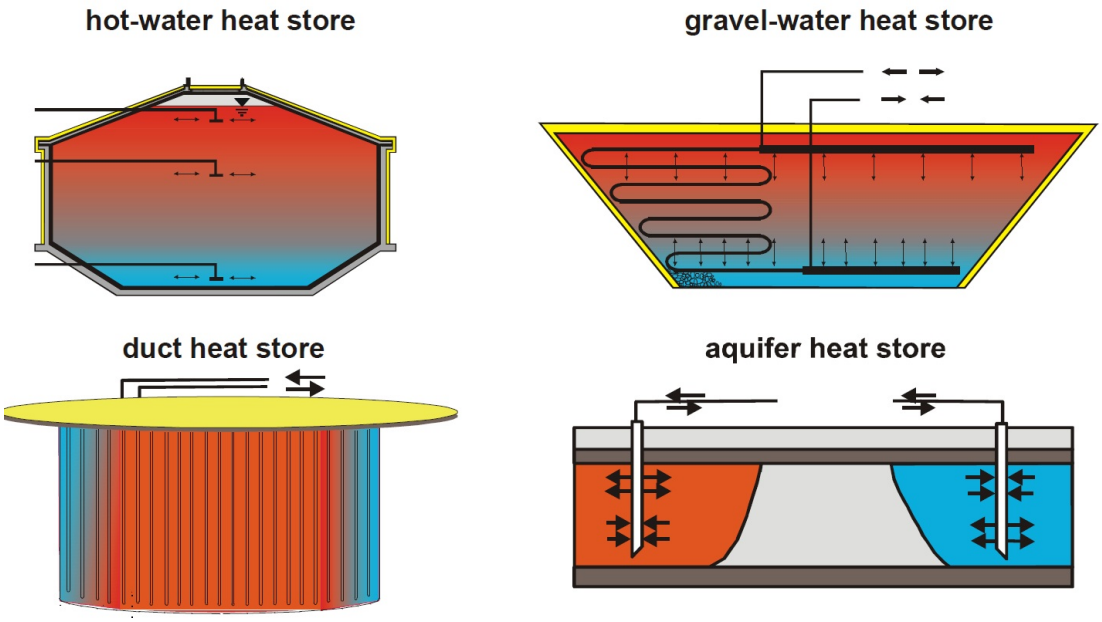

Figure 2.1: Different technology for Thermal Energy Storage.

of density under different temperature[2]. Hot-water tank is a very simple structure but needs a good insulated tank with a relatively high cost. The typical size of these tank can reach more than 12000 m^3 [3].

2.1.2 Gravel-water Heat Store

As cited previously, the Hot-water store is an expensive system because of the tank complexity. To reduce this cost Gravel-water heat store system can be used. In this technology a simpler tank is used; indeed there is a single thin plastic layer that is used only as water barrier and it is not used as insulation. This confined system contains a mixture of gravel and water, consequently heat storage capacity is lower than the previous system because of the presence of gravels with a lower specific heat coefficient than water. Therefore to stock the same amount of energy using gravel-water system, the volume has to be bigger than the volume for an hot-water system, approximately 50% more. To exploit Gravel-water system it is possible to use it directly: water charging and discharging, or use it indirectly with plastic pipes as heat exchanger.

2.1.3 Duct Heat Store

This system is the cheapest and use a different concept than the previous explained technologies. The ground stores heat that is exchanged using vertical or horizontal pipes in which the thermal fluid runs (Heat exchangers). In this system heat transfer is driven by conduction and

[2]It is possible to use two different water taking point, one on the bottom of the tank and the other one on the top.

[3]The Size is not a good parameter for a sensitive analysis, more useful parameters can be Water equivalent volumetric heat capacity kWh/m^3 and also a economic parameters as Investment per m^3 of water equivalent.

hot-water	gravel-water	duct	aquifer
storage medium			
water	gravel-water	ground material (soil / rock)	ground material (sand/gravel…-water)
heat capacity in kWh/m³			
60 - 80	30 - 50	15 - 30	30 - 40
storage volume for 1 m³ water equivalent			
1 m³	1.3 - 2 m³	3 - 5 m³	2 - 3 m³
geological requirements			
• stable ground conditions • preferably no groundwater • 5 - 15 m deep	• stable ground conditions • preferably no groundwater • 5 - 15 m deep	• drillable ground • groundwater favourable • high heat capacity • high thermal conductivity • low hydraulic conductivity (k_f<1•10^{-10} m/s) • natural ground-water flow < 1 m/a • 30 - 100 m deep	• natural aquifer layer with high hydraulic conductivity (k_f>1•10^{-5} m/s) • confining layers on top and below • no or low natural groundwater flow • suitable water chemistry at high temperatures • aquifer thickness 20 - 50 m

Figure 2.2: Comparison between four U.T.E.S. concepts

not by convection, like it happens in the other cases. This system is easy to install but needs a good pre-faseability study because of the possibility of temperature interference between different vertical heat exchangers. Also a preliminary study has to forecast the thermal drift. Usually using numerical models it is easy to predict the magnitude of thermal drift or thermal interferences.

2.1.4 Aquifer Heat Store

Aquifer is briefly introduced in Chapter1. With this system it is possible to use directly ground water as thermal source; it is possible to use the high porosity and the low natural areal flow to store thermal energy without any containment. The density of energy for this system is not high (same consideration of Gravel-water Heat Store systems). They are usually coupled with high thermal loads and due to the great amount of water, they can accept. Aquifer needs good thermal and physical properties to be used in this system (see Chapter1).

In the Figure2.2 the main difference between the two systems are indicated. To conclude this brief introduction: every single system, above illustrated, need a good preliminary analysis and a pre-faseability phase to be well performed and to avoid financial loss. Moreover under given thermal loads condition, the choice of the better system to be used is driven by relevant conditions as local geological situation, system integration, required size of the store, temperature levels, power rates and, equally important, legal restrictions and economics analysis (Schmidt, Mangold, and MullerSteinhagen 2003) .

2.2 A.T.E.S. State of the Art

The following paragraphs will introduce the A.T.E.S. technology. And will cover the history, the principal types of A.T.E.S. and the main affected factors, the main problems and the importance of modeling.

2.2.1 Story

A.T.E.S. has been used for the first time in China in the 1960s. The first important plant started in Shangai in 1965; it has been exploited only for water extracting with firstly a land subsidence problem. To solve that problem a cold water injection system was adopted; in that occasion the capacity of the aquifer to store cold water was observed. Indeed water had maintained for long time its cool temperature and after it was used for industrial cooling. Then ATES was used both for heating and cooling systems in the way to have two balanced loads to avoid the aquifer warming or cooling.

In Europe the main countries where ATES is used are Germany, Sweden, Belgium, Switzerland and Netherlands. The latter is probably the leader country in Europe, because of popularity of ATES plants due by the fact that aquifer can be found everywhere. Recently the use of groundwater heat pumps induced increasing in ATES plants (K. S. Lee 2010).

2.2.2 Operational Principles

Typical ATES plants have two wells or groups of wells, one for pumping and the other one for injecting water. Essentially there are two important operational principles to conduct ATES plant:

1. Continuous Regime (Figure2.3 (a)).
2. Cyclic Flow (Figure2.3 (b)).

The first one indicates those plants where one well (or one group of wells) injects water and another well (or one group of wells) pumps during all the operation time. The second one indicates that plants where one well (or one group of wells) injects and pumps water in an alternative way during all the exploitation time, the second well, instead, works in a symmetrical manner[4]. With Cyclic Flow it is possible to store energy all around each well, but this system is more complicated to conduct. The Continuous flow can be used only with systems that produce water with temperature close to the groundwater temperature; also this system is easier to control. An example of Continuous flow will be used and explained in the Chapter4.

2.2.3 Design

Following Paksoy, Snijders, and Stiles 2009 these are factors affecting A.T.E.S. design:

- Stratigraphy;
- Grain size distribution;
- Aquifer and fracture distribution;
- Aquifer depth and geometry;
- Storage coefficient;

[4]Usually during winter *the Heat well* pumps water and *the Cold well* injects cold water, in the summer viceversa.

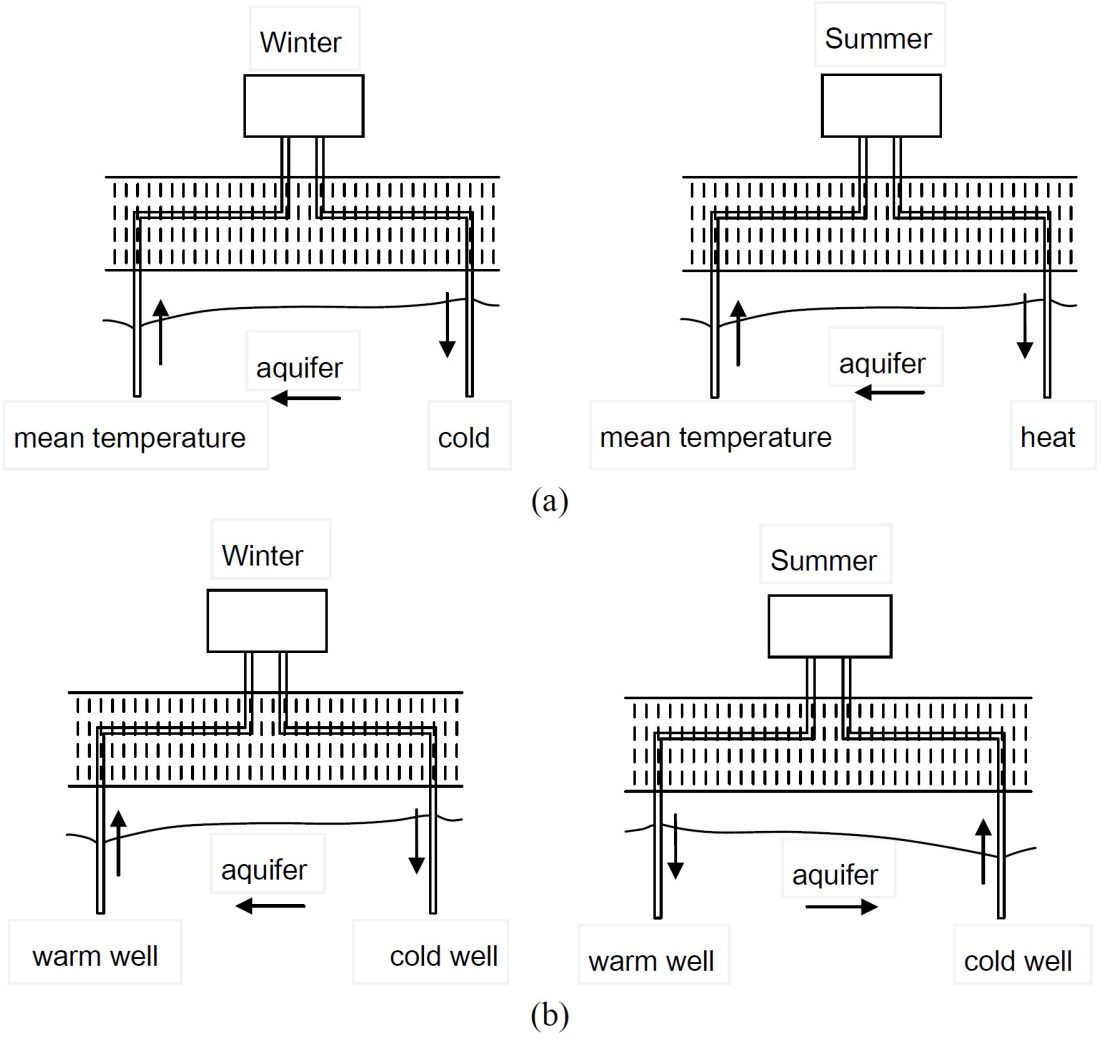

Figure 2.3: (a) Continuous regime (b) Cyclic Flow (K. S. Lee 2010)

Aspect	Lower limit	Typical	Upper limit
Aquifer thickness (m)	2-5	25	None (partial use)
Aquifer depth (mbgs)	5 (injection pressure)	50	150 (economic)
Aquifer permeability (m/s)	3 10exp-5	3 10exp-4	1 10exp-3
Groundwater flow (m/d)	0	0.1	0.3
Static head (mbgs)	50	10	-5

Figure 2.4: Lower,upper and typical values for exploitable aquifer.

- Permeability;
- Leakage factor confining layers;
- Degree of consolidation;
- Thermal gradient;
- Static Head;
- Natural ground water flow;
- Direction of flow;
- Water chemistry;

each of these items has to be checked during a pre feasibility study to forecast the Aquifer behaviour during operation time. Also the major criteria for unconsolidated aquifer are presented in Figure2.4. As reported in K. S. Lee 2010 there is a general procedure for designing and construction of ATES system:

- pre feasibility studies to describe the principal issues;
- feasibility study to tell the technical and economical feasibility and environmental impact compared to more than one reference systems;
- the first permit applications to local authorities;
- definition of hydrogeological conditions by site investigations and measurements of loads and temperatures, etc on the user side;
- evaluation of results and modeling for technical, legal, and environmental purposes;
- final design for tender documents;
- final permit application for court procedures.

The most important and problematic part of A.T.E.S. is the well (Figure2.5); in a unconsolidated formation it is important prevent the clogging of pores that could be conduct an high back pressure. Usually a thin gravel pack surrounds the screen, with a good hydraulic conductivity, is located to keep the flow inlet velocity low enough to ensure a good aquifer absorbtion .

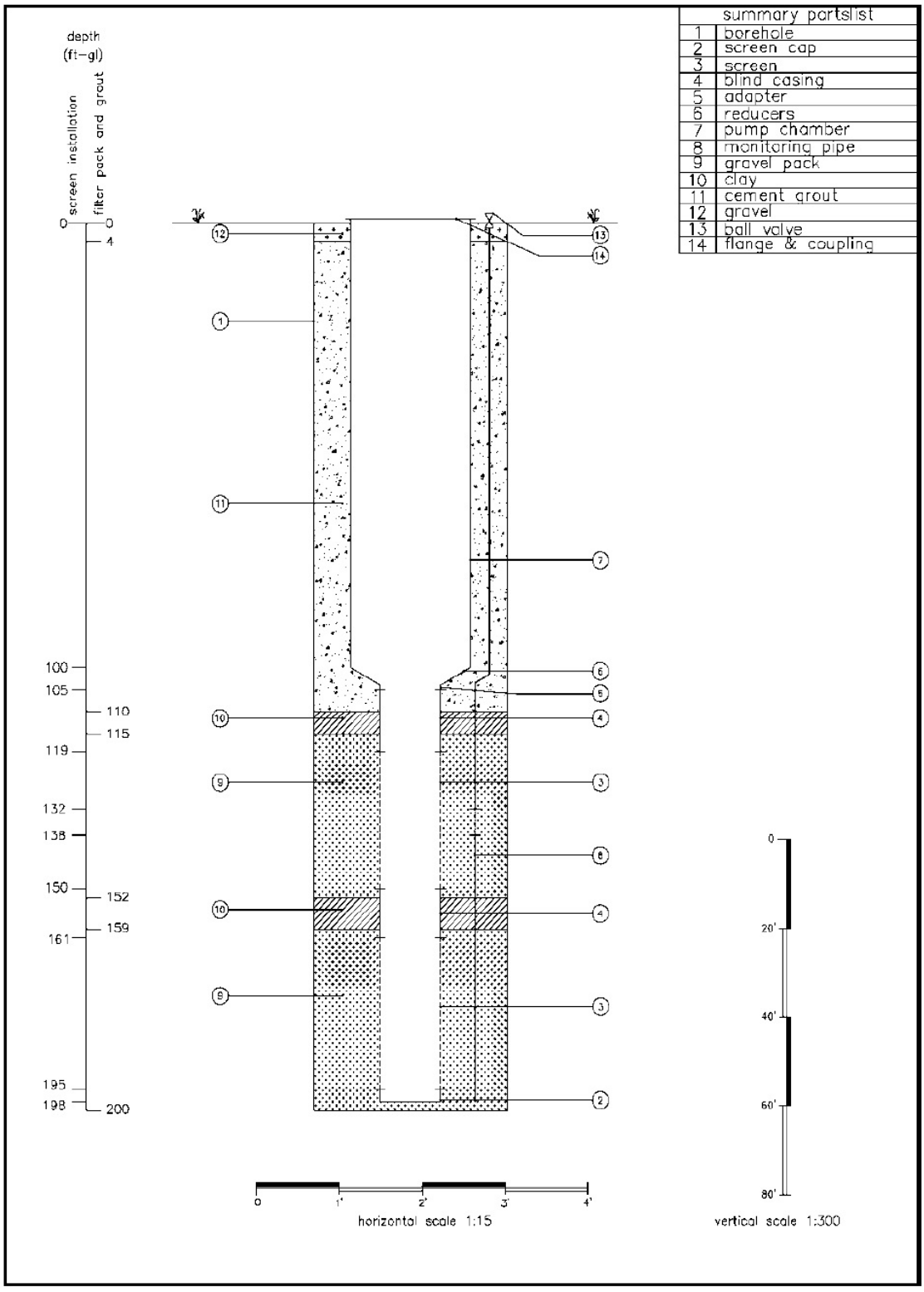

Figure 2.5: Well cross section fur unconsolidated formation.

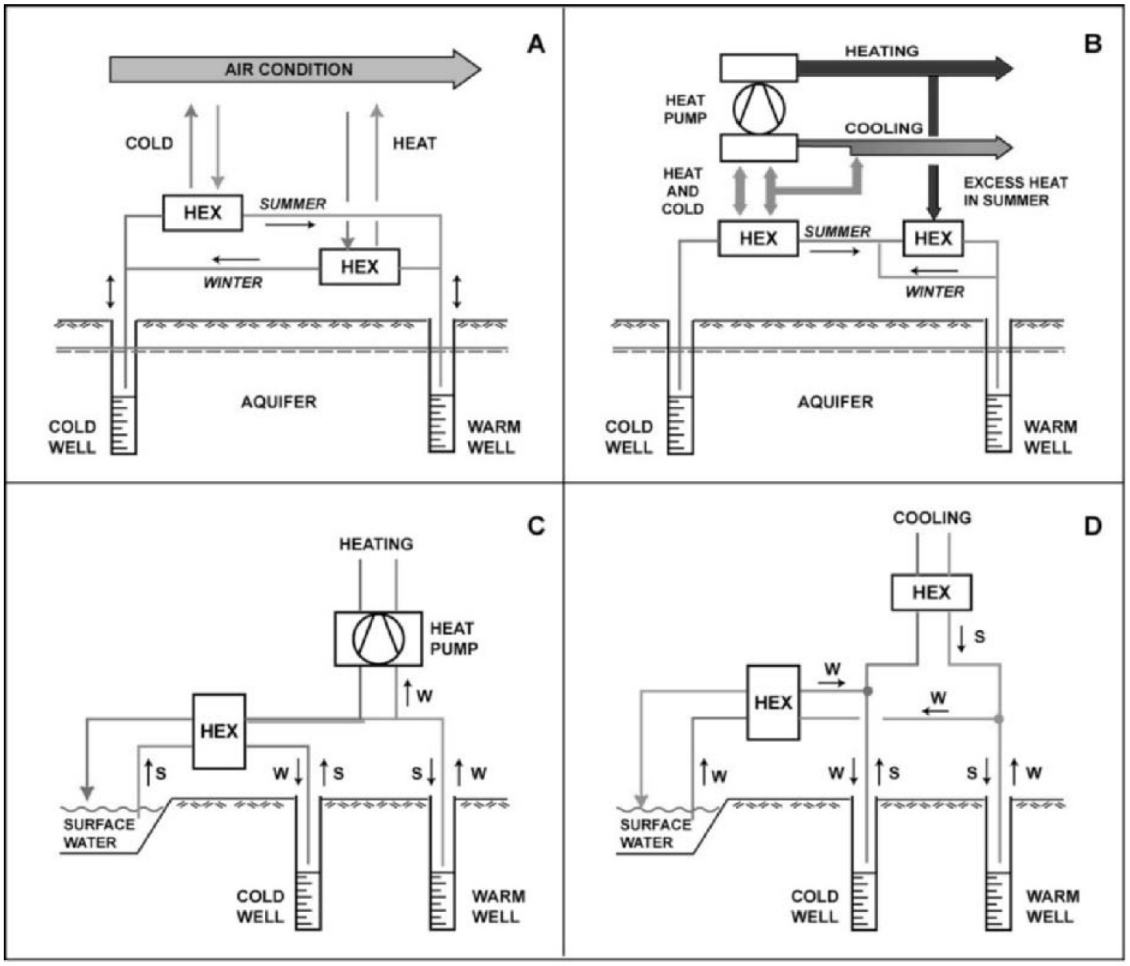

Figure 2.6: Different ATES configurations.

2.2.4 Configurations

ATES systems can be used with an external system, that has the capacity to exploit the A.T.E.S. potential. These secondary system can be summarized in four configurations (according with Andersson 2007a):

- Direct use of groundwater (Figure2.6 (A)).
- Indirect use of groundwater (Figure2.6 (B)).
- Indirect use of groundwater and natural energy storage (Figure2.6 (C)).
- Direct use of groundwater ad natural energy storage (Figure2.6 (C)).

The case A uses groundwater to preheating and cooling air in ventilation system. The case B presents systems coupled with a heat pump; these systems are common, they produce a great amount of energy (also with high quality). In the third case, C, the water from warm well is used as source for the heat pump during winter and the water from cold well is heated using the surface water during summer. Finally, the system D uses the surface water to cool the water from the warm well that will go into the cold well to be used in summer as free cooling. Obviously the most

System application	PF	Energy saving (%)	Payback (years)
A. Direct heating and cooling	20–40	90–95	0–2
B. HP supported heating and cooling	5–7	80–87	1–3
C. HP supported heating only	3–4	60–75	4–8
D. Direct cooling only	20–60	90–97	0–2

Figure 2.7: Example of difference in Economics and Energy Savings field for A.T.E.S.

used system is the case B, but it is also the more complicated; in recent years the cold storage from natural source (case D) is increasingly been used in cooling process (Andersson 2007a).

To have an idea of different configurations performances of previous systems, it is useful look at Figure2.7 in which are represented some differences using different parameters. PF (*Performance Factor*) represents the average coefficient of performance (COP) , the resulting Energy Savings and the calculated Payback time [5].

2.2.5 ATES Problems

A.T.E.S. technology is already well known in advantages but also in disadvantage. Literature reports a lot of example in which ATES technology has found some maintenance problems or failures (Lau et al. 1986), (Andersson 2007c). To avoid these inconveniences every A.T.E.S. project must be good designed and good tested. Thus it is possible to predict in a good way problems (obviously an important part is done by field Tests); the main problems are below summarized. The most probably problem is clogging of wells. This clogging cause an increase in resistance of flowing and consequently an increase of pressure drop. Closure of the wells is easily to find with a simple pressure investigation during the time (monitoring flow rate program) and with a comparison of an observation well pressure data to evaluate false clogging.

To better understand the clogging process there are three main events that can occurred:

- Clogging by fines.
- Hydro-chemical clogging.
- Biochemical clogging.

The first one is good presented in Figure2.8. This type of pores closure happens during two moments: during well perforation by bentonite injection or mud or during gravel-packed injection and also during exploitation of the reservoir with migration of the fines.

The second one, Hydro chemical clogging, cause a precipitation of chemicals (iron and calcium compounds) due by chemicals reaction (see Figure2.9). These chemicals reaction can be caused by quickly variation in pressure or temperature during production.

[5] Figure2.7 refers on Swedish application presented in Andersson 2007a.

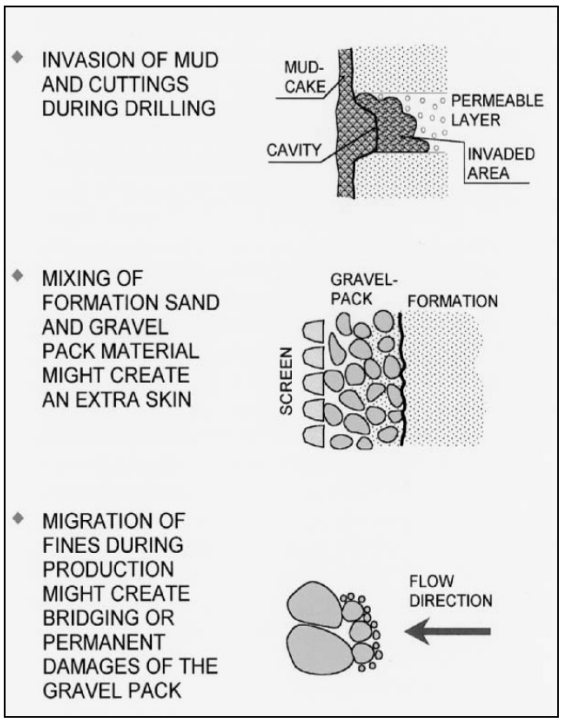

Figure 2.8: Clogging by fines during well drilling, gravel-packed positioning and during exploitation.

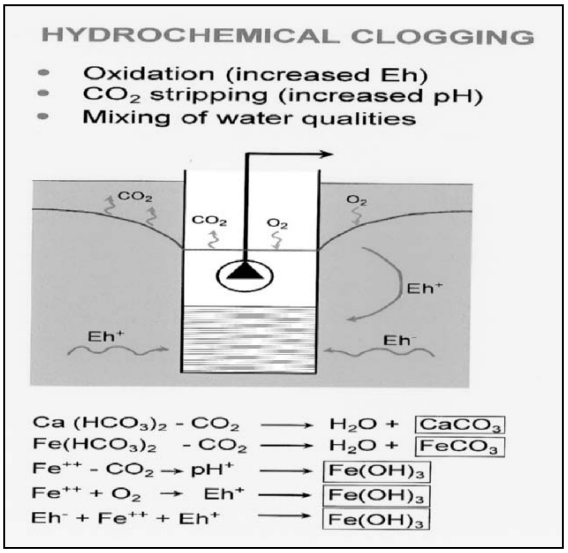

Figure 2.9: Clogging by hydro-chemical reactions

2.2.6 Modeling

An important part for the pre-feasibility study for A.T.E.S. systems is the modelisation. As just remembered, to avoid some problems and to have a good behaviour prediction, models are useful. The study wants to compare different situations (under given geophysical data derived by field tests) that are different well distance and various flow rate. All the simulation want to find the better situation using acceptable and real compromises. All the simulations obtain two relevant results: one for hydraulic head distribution and the other for the temperature field. A.T.E.S. modeling is one of the issue of this work so the importance of modeling will be treat below. To have an idea about mass and heat transport model that are already done in literature, see Figure2.10.

Model	Creator	Numerical Scheme	Description
AQUA3D	Vatnaskil Consulting Engineers, Reykjavik, Iceland	finite-element method	developed mainly for simulation of mass transport problems, but can be adapted to model heat transport without density-dependent groundwater flow
HST3D	United States Geological Survey (USGS)	finite-difference method	capable of simulating mass and heat transport in variable-density groundwater flow system
FEFLOW	DHI-WASY GmbH, Berlin, Germany	finite-element method	capable of simulating both mass and heat transport in density-dependent groundwater flow systems
SUTRA-MS	United States Geological Survey (USGS)	hybrid finite-element and finite-difference method	simulated fluid movement and the transport of either energy or dissolved substances in the subsurface environment
THETA 3.0	Nuclear Engineering Laboratory, Helsinki University of Technology, Finland	finite-difference method	coupled transport of fluid and energy in porous media
TOUGH2	Earth Sciences Division, Lawrence Berkeley National Laboratory	integral finite difference method	simulating the coupled transport of water, vapor, non-condensable gas, and heat in porous and fractured media
SHEMAT	Applied Geophysics and Geothermal Energy E.ON Energy Research Center, RWTH Aachen University	finite difference method	simulating coupled flow, heat transfer, transport and chemical water-rock interaction in hydro-geothermal reservoirs in two and three dimensions
UTCHEM	Center for Petroleum and Geosystems Engineering, Austin, Texas, U.S.A.	finite difference method	developed mainly for modeling multiphase, multicomponent, compositional simulation of chemical flooding processes, but can be used to model heat transport

Figure 2.10: Numerical models used for groundwater simulation.

Chapter 3

Analytical Models

Abstract

This chapter will analyse the main analytical methods for temperature distribution in a porous media. There is plenty of literature about analytical solutions for both for planar symmetric and axial symmetric models. This chapter is focused on the second type of model: the axial symmetry; it is representative of injection well cases. Before talking about analytical solutions, an heat transfer introduction will be presented to conclude the background paragraph (par. 1.8). Analytical solutions can be presented in a direct or indirect form; in other words, with an explicit form (direct solution, easy to calculate) or with an integral form, more complicated. Obviously direct forms are easier and preferable than indirect forms which need calculator as support. In any case whichever form is treated, the purpose of each one is to individuate the temperature trend in space or time varying. There are different various articles in which analytical solutions are compared with FEM solutions under the same hypothesis(Barends, Daltares, et al. 2010) ,(Tan, Cheng, and Guo 2012), (Kim, Y. Lee, et al. 2010). The purpose of this chapter is to compare analytical solutions with a *real case*(that is done with a complete FEM models).

3.1 Heat Transfer

Considering an injection well with which a water flow rate get in a aquifer formation: the heat cannot travel at the same velocity of the water because of the heat exchange principles. In a underground formation water is driven by three main phenomenon (Banks 2008):

- Conduction through mineral grains and water filled pores;
- Advection with groundwater flow;
- Exchange between moving groundwater and the matrix of aquifer.

Employing an energy balance of a small volume of aquifer it is possible to describe the heat transfer with the three mechanism just introduced; therefor following the assumption of "instantaneous

thermal equilibrium", energy balance (for one dimension) is:

$$\lambda_e \cdot \frac{d^2\theta}{dx^2} - S_{VCw} \cdot \frac{d(q \cdot \theta)}{dx^2} = S_{VCaq} \cdot \frac{d\theta}{dt^2} \tag{3.1}$$

where:

x is spatial variable $[m]$.

λ_e is the effective thermal conductivity $[W/mK]$.

$S_{VCwo} or S_{VCaq}$ is the Specific volumetric heat capacities of aquifer and groundwater $[J/m^3K]$.

q is the Darcy's velocity $[m/s]$.

t is time $[s]$.

θ is temperature $[K]$.

To understand better the importance of the above energy balance, it is useful to read the mathematical equation as follow: heat transfer by convection (first term) plus heat transfer by convection (second term) = variation of heat stored in a unit of aquifer at the time considered.
An important parameter to consider when talking about temperature distribution is *Thermal Breakthrough*. The concept of Thermal breakthrough describes the variation of temperature from the normal and boundary condition of the field. For the Analytical solution it is possible to find thermal breakthrough. By the fixing space it is possible to find the time of Temperature Breakthrough or viceversa; by the fixing time it is possible to find space distribution using a retardation factor; thus an hydraulic continuity equation can help, considering a volume of aquifer and a flow rate:

$$V_{aq} \cdot n_e = A \cdot x_{hyd} \cdot n_e = Q \cdot t \tag{3.2}$$

where:

V_{aq} is the volume of aquifer considered $[m^3]$.

n_e is aquifer porosity $[m^3]$.

A is the area which the Q flow rate is crossing $[m^2]$.

Q is flow rate $[m/s]$.

Obviously heat has not the same velocity of the groundwater, therefor considering that during t time, the injected water transports (having $\delta\theta$ higher than aquifer) $Z \cdot t \cdot S_{VCw} \cdot \delta\theta$ as amount of energy, and that amount of energy is instantaneously absorbed with the ambient, absorbed by the volume of aquifer named V_{th} results:

$$V_{th} \cdot S_{VCaq} \cdot \delta\theta = Q \cdot S_{VCw} \cdot \delta\theta \tag{3.3}$$

There is a delay between the water front and the heat front, this is represented using R, the *Retardation Factor*[1]:

$$R = \frac{x_{hyd}}{x_{th}} = \frac{S_{VCaq}}{n_e \cdot S_{VCw}} \tag{3.4}$$

These relations can correlate the distribution of the fluid injected and the distribution of the heat, also the temperature field, using analytical solutions.

Before introducing analytical models, an important variable has to be introduced, named *Peclet's Number*: it represents the ratio between heat transferred by convection and heat transferred by conduction. The Peclet's number can assume the follow forms:

$$Pe = \frac{heattransferredbyconvection}{heattransferredbyconduction} = \frac{L \cdot v}{D} = \frac{Q \cdot R}{4\pi \cdot n \cdot H \cdot D}$$

where:

L is a Characteristic Length for convection $[m]$.

v is a Thermal heat front velocity $[m/s]$.

R is Retardation Factor.

D is the Thermal Diffusivity defined $[m^2/s]$.

3.2 Analytical Models

There is a lot of analytical solutions for heat distribution in aquifer, however there are some articles that present a good summarization and comparison of main methods (Noyer 1977),(Barends, Daltares, et al. 2010),(Tan, Cheng, and Guo 2012). Lauwerier's solution was the first analytical model to represent the distribution of heat in a horizontal aquifers. Usually the heat transport studies are done for the Oil and Petroleum field, first of all Lauwerier's study has been done to increase the oil extraction using injection of heat in the feed zone. All the studies start using differential equation, hence to reach an explicit solution the Laplace transformation has been used (this methods is not herein presented). However the results (from Laplace anti transformation) are presented as explicit form. Temperature is as direct form in some cases and as indirect in others (using integral form). As already said, in the abstract there are two important types of analytical solutions, one for planar and one for axial symmetric formation. The Table3.1 introduce all the main methods. Some methods will be analysed in detail.

The purpose of this work is to compare some analytical solution with a real case found with FEM[2] simulations. Below is be introduced only the radial methods[3] made by Lauwerier, Rubistein-Advonin and Barends. The symbols used in the chapter are:

h Aquifer thickness $[m]$.

[1] This factor is not a constant, indeed as the volumetric heat capacity depends on temperature.

[2] See Chapter4

[3] Only radial methods because only those are well representing the well injection mode.

Table 3.1: Main analytical solutions

SOLUTION	PLANAR	RADIAL	NOTE	TREATED
Lauwerier	yes	yes	Radial = Planar	yes
Ogata e Banks	yes	no	-	-
Rubistein-Advonin[a]	yes	yes	-	yes
Barends	yes	yes	Two formulations of radial solution	yes
Haochen	yes	no	-	-

[a]This solution is the *schéma B* of Noyer 1977 the only one method that was easy to reproduce.

r Radial distance from the center of the well $[m]$.

r_w Radius of the well (here assumed 0.5m) $[m]$.

x Spatial horizontal coordinate $[m]$.

z Spatial vertical coordinate $[m]$.

T Temperature (i=injection 0=initial A=Aquifer temp. R=Rock temp.) [].

λ Thermal Conductivity (A=Aquifer, F=fluid,R=rock [4])$[W(mK)^{-1}]$.

ρ Specific mass $[kg(m^3)^{-1}]$.

α_L is the Longitudinal Dispersivity coefficient $[m]$.

c is the Heat specific coefficient $[J(kgK)^{-1}]$.

Q Volumetric flow rate $[m^3 s^{-1}]$.

S Surface of stream flow rate $[m^2]$.

t Time $[s]$.

n Porosity

w_0 is thermal bleeding Heat Flux

v is a Thermal heat front velocity $[ms^{-1}]$:

$$v = q \cdot \frac{(\rho c)_F}{(\rho c)_A}$$

q is Darcy's velocity $[ms^{-1}]$:

$$q = \frac{Q}{2 \cdot \pi \cdot r \cdot h}$$

ϵ is Heat Capacity ratio:

[4]In the following analysis we consider the overburden (Aquitard) formed by rocks only.

$$\epsilon = \frac{(\rho \cdot c)_R}{\rho \cdot c)_A}$$

R is Retardation Factor[5].

$$R = n \cdot \frac{(\rho \cdot c)_F}{\rho \cdot c)_A}$$

D is the Thermal Diffusivity $[m^2 s^{-1}]$:

$$D = \frac{\lambda}{\rho \cdot c} + \alpha_L \cdot v$$

D_r is the Radial Dispersivity $[m^2 s^{-1}]$:

$$D_r = \frac{Q \cdot R}{4 \cdot \pi \cdot n \cdot h}$$

θ is Radial apparent time $[s]$:

$$\theta = \frac{r^2 - r_w^2}{4 \cdot D_r}$$

The Dimensionless number are:

T_D Dimensionless temperature

$$T_D = \frac{T_A - T_0}{T_i - T_0} \tag{3.5}$$

Pe Radial Peclet's Number

$$Pe = \frac{Q \cdot \rho_F \cdot c_F}{2 \cdot \pi \cdot h \cdot \lambda_A} \tag{3.6}$$

t_D Special time [6]

$$t_D = \frac{\rho_F \cdot c_F \cdot Q \cdot t}{\rho_A \cdot c_A \cdot h \cdot \pi \cdot r^2} \tag{3.7}$$

3.2.1 Lauwerier's solution

Like every Analytical solution it is a good thing to declare the initial assumptions. Lauwerier's assumptions are indicated below:

- in Aquifer Heat conduction along flow direction is neglected (heat transfer is due only by convection) ($\lambda_{hz} = 0$);
- in Aquitard Heat conduction in horizontal direction is neglected ($\lambda_{hz} = 0; \lambda_v = finite$);
- temperature distribution in the Aquifer cross-section is constant, thus changes only along the fluid flow direction ($\lambda_v = \text{inf}$);
- thickness, porosity, inlet flow rate and permeability are constant.

Under the above assumption, the Aquifer equations for heat transfer are below described. To obtain the energy balance the following 3 items are needed:

[5] In other words Retardation factor exist because of energy loss for heating -up (or cooling down) the solid matrix.
[6] It is used only for Lauwerier and Rubistein solutions as used in (Noyer 1977).

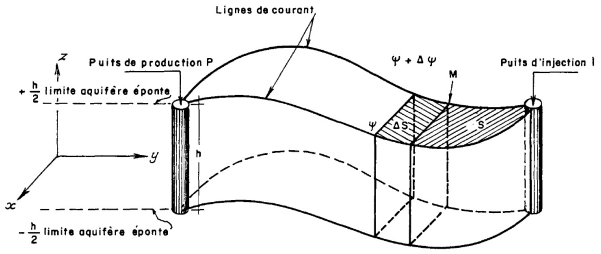

Figure 3.1: Infinitesimal Stream line flow.

Convection term, under hypothesis

$$\rho_F \cdot c_F \cdot u_x \cdot \frac{\partial T_A}{\partial x} \cdot h \cdot \delta S \tag{3.8}$$

Variation of internal energy term

$$\rho_A \cdot c_A \cdot \frac{\partial T_A}{\partial t} \cdot h \cdot \delta S \tag{3.9}$$

Crossing Heat transfer the aquifer bounds

$$2 \cdot \lambda_R \left(\frac{\partial T_R}{\partial z} \right)_{z=h/2} \tag{3.10}$$

Considering a (x,y) coordinates system, where x is the direction parallel to the flow and y is perpendicular, it is useful consider the infinitesimal stream flow line (Figure3.1) in which is flowing infinitesimal flow rate dq.

$$dq = u_x \cdot h \cdot dy \tag{3.11}$$

The temperature variations in surface variation is:

$$\frac{\partial T}{\partial S} = \frac{\partial T}{\partial x} \cdot \frac{\partial x}{\partial S} + \frac{\partial T}{\partial y} \cdot \frac{\partial y}{\partial S} \tag{3.12}$$

following the hypotesis $\frac{\partial T}{\partial y} = 0$, thus $\frac{\partial T}{\partial x} = \frac{\partial T}{\partial S} \cdot dy$ and $u_x \cdot \frac{\partial T}{\partial x} = \frac{dq}{h} \cdot \frac{\partial T}{\partial S}$. Thus the convection term will be:

$$\rho_F \cdot c_F \cdot dq \cdot \frac{\partial T_A}{t} \cdot h \cdot dS \tag{3.13}$$

The temperature of fluid ($T_A(S,t)$) and temperature of rocks ($T_R(S,t,z)$) are determined for the aquifer, using the thermodynamic equilibrium equation:

$$\frac{h}{2} \cdot \rho_A \cdot c_A \cdot \frac{\partial T_A}{\partial t} + \frac{dq}{2} \cdot \rho_F \cdot c_F \cdot \frac{\partial T_A}{\partial S} - \lambda_R \cdot \left(\frac{\partial T_R}{\partial z} \right)_{z=h/2} = 0^7 \tag{3.14}$$

The initial conditions are:

$$T_A(S,0) = T_0$$

$$T_A(0,t) = T_i$$

[7] S is spatial variable.

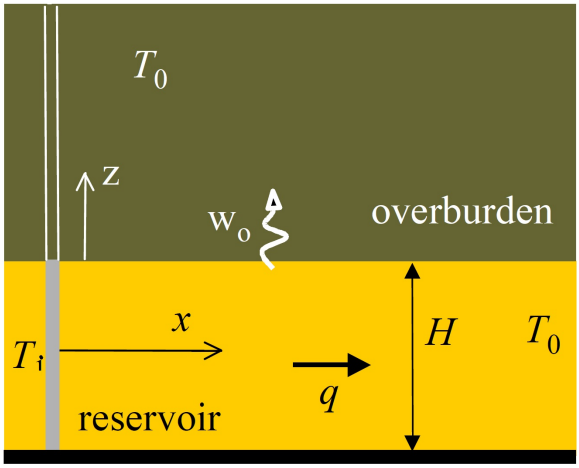

Figure 3.2: Lauwerier's scenario, with Aquifer (reservoir) and Aquitard (overburden).

Using Laplace transformation it is possible to find the Aquifer Temperature variation under the above listed assumptions, they becoming[8]:

$$T_D(t_D > 1, \phi, Pe/2) = erfc\left(\frac{1}{\sqrt{\phi \cdot (t_D - 1)}}\right) \tag{3.15a}$$

$$T_D(t_D < 1, \phi, Pe/2) = 0 \tag{3.15b}$$

The Aquitard temperature variation is not important for this work; but it is good to know that every single analytical solution forecast the temperature trend for both Aquifer and Aquitard (Figure3.2).

3.2.2 Rubistein-Advonin

This method is presented in Noyer 1977 under the name *Schéma B*. The Rubistein's assumptions are below listed:

- Aquifer is homogeneous, with constant thickness, with infinite horizontal length.
- Aquitard is homogeneous and vertical infinite extension.
- Initial temperature T_0 is equal everywhere.
- Injection temperature T_i is constant.
- Aquifer physical parameters does not change with temperature variation.
- There is temperature continuity between Aquifer and Aquitard.
- Aquifer Heat conduction along flow direction is not neglected ($\lambda_{hz} = finitevalue$).
- Aquitard Heat conduction in horizontal direction is neglected ($\lambda_{hz} = 0; \lambda_v = finite$).

[8]Remembering that ϕ is named *Loss parameter*: $\phi = \frac{\rho_A \cdot c_A \cdot \rho_F \cdot c_F \cdot Q \cdot h}{\rho_R \cdot c_R \cdot \lambda_R \cdot \pi \cdot r^2}$.

- Temperature distribution in the Aquifer cross-section is constant, thus change only along the fluid flow direction ($\lambda_v = \text{inf}$).
- Injection of water toward an infinitesimal point.

Using a radial geometry the flow velocity is $u_r = \frac{Q}{2\cdot\pi\cdot r\cdot h}$, thus the convection term eq. (3.9) becomes $\rho_F \cdot c_F \cdot \frac{Q}{2\cdot\pi\cdot r\cdot h} \cdot \frac{\partial T_A}{\partial r} \cdot \frac{h}{2}$. To find the Aquifer temperature trend for radial problem under Rubistein's hypothesis the follow equations have to be solved:

$$\frac{h}{2}\cdot\rho_A\cdot c_A\cdot\frac{\partial T_A}{\partial t}+\frac{Q}{4\cdot\pi\cdot r}\cdot\rho_F\cdot c_F\cdot\frac{\partial T_A}{\partial r}-\lambda_R\cdot\left(\frac{\partial T_R}{\partial z}\right)_{z=h/2}-\lambda_A\cdot\left(\frac{\partial^2 T_A}{\partial r^2}+\frac{\partial T_A}{r\cdot\partial r}\right)=0 \tag{3.16a}$$

$$T_A(r,t=0)=T_0 \tag{3.16b}$$

$$T_A(r=0,t)=T_i \tag{3.16c}$$

$$\frac{\partial^2 T_R}{\partial z^2}=\frac{\rho_A\cdot c_A}{\lambda_R}\cdot\frac{\partial T_R}{\partial t} \tag{3.16d}$$

$$T_R(r,z,t=0)=T_0 \qquad z\geq h/2 \tag{3.16e}$$

$$T_R(r,z=h/2,t)=T_R(r,t) \qquad \forall \quad r,t \tag{3.16f}$$

$$\lim_{z\to\text{inf}} T_R(r,z,t)=T_0 \tag{3.16g}$$

Using Laplace transformation it is possible to find the Aquifer Temperature variation under the above listed assumptions, this become the Rubistein's radial solutions [9]:

- For $\nu \leq 5$

$$T_D(\phi,\nu,t_D)=\frac{1}{\Gamma(\nu)}\cdot\left(\frac{\nu}{t_D}\right)^{\nu}\int_0^1 \quad \exp\left(\frac{-\nu}{t_D\cdot s}\right)\cdot erfc\left(\sqrt{\frac{t_D}{\phi}}\cdot\frac{s}{\sqrt{1+s}}\right)\cdot\frac{ds}{s^{\nu+1}} \tag{3.17}$$

- For $\nu > 5$

$$T_D(\phi,\nu,t_D)=\sqrt{\frac{\nu}{2\pi}}\int_0^1 \quad \exp\left(\nu\cdot\left(\log\frac{1}{t_D\cdot s}1-\frac{1}{t_D\cdot s}\right)\right)\cdot erfc\left(\sqrt{\frac{t_D}{\phi}}\cdot\frac{s}{\sqrt{1+s}}\right)\cdot\frac{ds}{s} \tag{3.18}$$

NOTE: Rubistein's solution when $\nu \to \text{inf}$ (that is when $\lambda_A \to 0$) assume the same form of Lauwerier's solution.

3.2.3 Berends

Barends' theory (Barends, Daltares, et al. 2010) for axial-simmetric fluid distribution follows the Lauwerier's theory. The solution, that is here taken into account, is similar to the Dunn and Nlson's solution (Dunn and Nilson 1981).

Barends uses Laplace transform for situation of constant temperature in injection and he takes into account two cases: first without thermal bleedings in the Aquitard from the aquifer and the second without conduction in the Aquifer (reservoir). The main Assumptions are the same of

[9] Remembering that $\nu = Pe/2$ and $\Gamma(x)$ is a mathematical function *gamma function*, see Abramowitz and Stegun 1972.

Lauwerier's; the only difference is the main rule for every case. The equation that represents the energy balance in the aquifer for a a single well as follow:

$$\frac{\partial}{r \cdot \partial r} \cdot r \cdot D \frac{\partial T}{\partial r} - v \cdot \frac{\partial T}{\partial r} = \frac{\partial T}{\partial t} + \frac{w_0}{\rho \cdot c \cdot h} \quad r > r_w \quad t > 0 \tag{3.19}$$

Also Berends considers for the boundary condition at r_w (that is the well radius) the Danckwerts' condition; thus under the assumption that at time $t = 0$ the injection temperature jumps to T_i. The system needs time before the heat front starts, this period is t_0. So the condition at well-bore are:

$$\frac{\partial T_A}{\partial r} = -\frac{Q \cdot R \cdot (T_i - T_A)}{2 \cdot \pi r_w \cdot n \cdot D \cdot h} \quad r = r_w \quad t < t_0 \qquad T_A = T_i \quad r = r_w \quad t \geq t_0 \tag{3.20a}$$

The t_0 value can be found with some expressions (Barends, Daltares, et al. 2010), but in this work they are not presented. All the following analysis using Barends' solution will take into account only the second well bore boundary condition. In other words, t_0 is considered equal to 0.

Barends case 1.

This paragraph will introduce the Barends' solution under the assumption of Aquifer without thermal bleedings in overburden. Under this condition, $w_0 = 0$ and the Aquifer governing equation is:

$$\frac{\partial}{r \cdot \partial r} \cdot r \cdot D \frac{\partial T}{\partial r} - v \cdot \frac{\partial T_A}{\partial r} = \frac{\partial T_A}{\partial t} + 0 \quad r > r_w \quad t > 0 \tag{3.21}$$

Barends Applied the separation of variable technique and found as result (for $t > t_0$ (so $t > 0$ under our assumption) and $r > r_w$)[10]:

$$T_D = \frac{\Gamma[Pe, \eta]}{\Gamma[Pe]} \quad t > t_0 \quad r > r_w \tag{3.22}$$

Barends case 2.

This paragraph will introduce the Barends' solution under the assumption of Aquifer with thermal bleedings in overburden. Under this condition, $w_0 \neq 0$ and $D = 0$ and the Aquifer governing equation is:

$$-v \cdot \frac{\partial T_A}{\partial r} = \frac{\partial T_A}{\partial t} + \frac{w_0}{\rho \cdot c \cdot h} \quad r > r_w \quad t > 0 \quad r > r_w \tag{3.23}$$

Barends Applied the separation of variable technique and found as result (for $t > t_0$ (so $t > 0$ under our assumption) and $r > r_w$)[11]:

$$T_D = erfc\left(\frac{\epsilon \cdot \theta \sqrt{D_R}}{2 \cdot h \cdot \sqrt{D_R} \cdot \sqrt{t - \theta}}\right) \quad t > t_0 \quad r > r_w \tag{3.24}$$

[10] Where $\Gamma[x, y]$ is the Incomplete Gamma function and $\Gamma[x]$ is Complete Gamma function under Abramowitz and Stegun 1972 nomenclature.

[11] D_R is the diffusivity of the overburden

3.2.4 Comparison between Analytical solution and Numerical solutions

The purpose of this work is not only for analytical models presentation, indeed in this paragraph it is presented as a comparison between a FEM[12] model and analytical models. The FEM model is done using COMSOL Multhypisics (see Chapter4) and the analytical models tested are only the axial-simmetric (Lauwerier, Rubistein, Barends 1, Barends 2). In this paragraph we introduce the physical and condition of use data that are used for analytical models and the numerical model. Then we present the main results found, and finally the conclusions and synthesis to comment the results. All the analytical models have been implemented using Matlab code with a spreadsheet input and output file to make the data variations easier. All the results have been elaborated using a spreadsheet and they are presented as graphical comparison.

Simulation Data

[13] Herein there are all the physical data that have been used in the numerical and analytical simulations. Also there are all the simulation conditions. The cases taken into account are 15 in which there are Peclet's number variations and thickness variations (all the cases are summarized in Table3.2). The physical data is summarized in Table3.3. Considering the same Pe case with different thickness, note that the volume flow rate is different, but velocity is the same for every considered case. For the simulation it has been assumed that :

- Aquifer is saturated;
- Aquifer is made with rock and water, the percentage depends on porosity n. Fraction n is water made and 1-n is rock made;
- Aquitard (overburden)is made rocks only;
- All the properties are constant with temperature variation;
- The simulation time is 20 years and all the results refer to a temperature distribution along the Aquifer after the simulation time.

Simulation results

In this sub-section all the results are presented. A matlab code has been used; that program is made to get out the Aquifer temperature vs radial distance from injection well. The Analytical models have been implemented as listed below [14]:

Lauwerier implementation of eq.3.15.

Rubistein implementation of eq.3.17.

[12] Finite Element Method.

[13] Just to remember the subscripts mean: A refers to Aquifer, r refers to Rock, w refers to water and O to overburden.

[14] This list represent the Legend for the graphics solutions.

h[a] $[m]$	**Pe** [b]	**Q** [c]$[m^3/day]$	V_{in} [d] $[m/s]$
10	0.1	0.655	2.41E-7
10	1	6.55	2.41E-6
10	10	65.5	2.41E-5
10	100	655.	2.41E-4
10	200	1310.	4.827E-4
25	0.1	1.64	2.414E-7
25	1	16.4	2.414E-6
25	10	164.	2.414E-5
25	100	1638	2.414E-4
25	200	3276	4.827E-4
50	0.1	3.28	2.414E-7
50	1	32.8	2.414E-6
50	10	328	2.414E-5
50	100	3276	2.414E-4
50	200	6552	4.827E-4

Table 3.2: Cases take into account for simulations.

[a]Thickness.

[b]PECLET'S Number; refer to References3.6.

[c]Volume Flow rate.

[d]Inlet Velocity represent the value of velocity assumed by the water at the boundary screen(the separation strata between well and aquifer, at r=0.5 m) of the well.

n	ρ_r	ρ_w	ρ_A	c_r	c_w	c_A	λ_r
λ_w	λ_A	D_A	D_O	ϵ	R	T_0	T_i
0.2	2700	1000	2360	840	4186	1509.2	3
0.63	2.526	9.5263E-7	1.3227E-6	0.86	0.3157	80	30

Table 3.3: Simulations data.

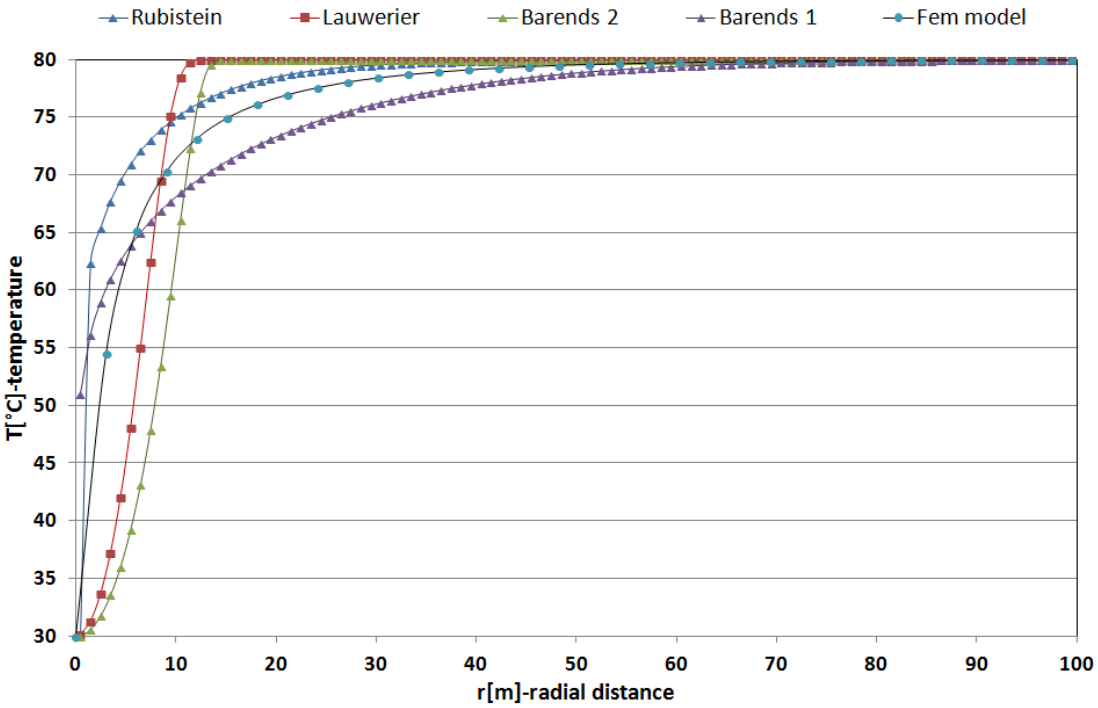

Figure 3.3: Case: Thickness = 10m, Pe = 0.1

Barends 1 implementation of eq.3.22.

Barends 2 implementation of eq.3.24.

For the Fem model it has been used a 3D geometry (see the Chapter4 where are explained all the boundary conditions); Temperature trend-vs-space is represented with a curve named *Fem model*. This curve represents the situation in the middle of the Aquifer after 20 years of transient simulation. The line in the middle of the Aquifer, where temperature data are read, connects injection and production well (because the 3D model use two wells one for injection and the second one for production to have a realistic pressure field[15]). In the "Conclusion and synthesis" section there the consideration of comparison between analytical and numerical models will be presented. Every figure presented below represents one case of those indicated in Table3.2.

[15]The connecting line of the two wells has the bigger pressure gradient that cause more flow in that direction. Thus that is the main direction of thermal plume progression.

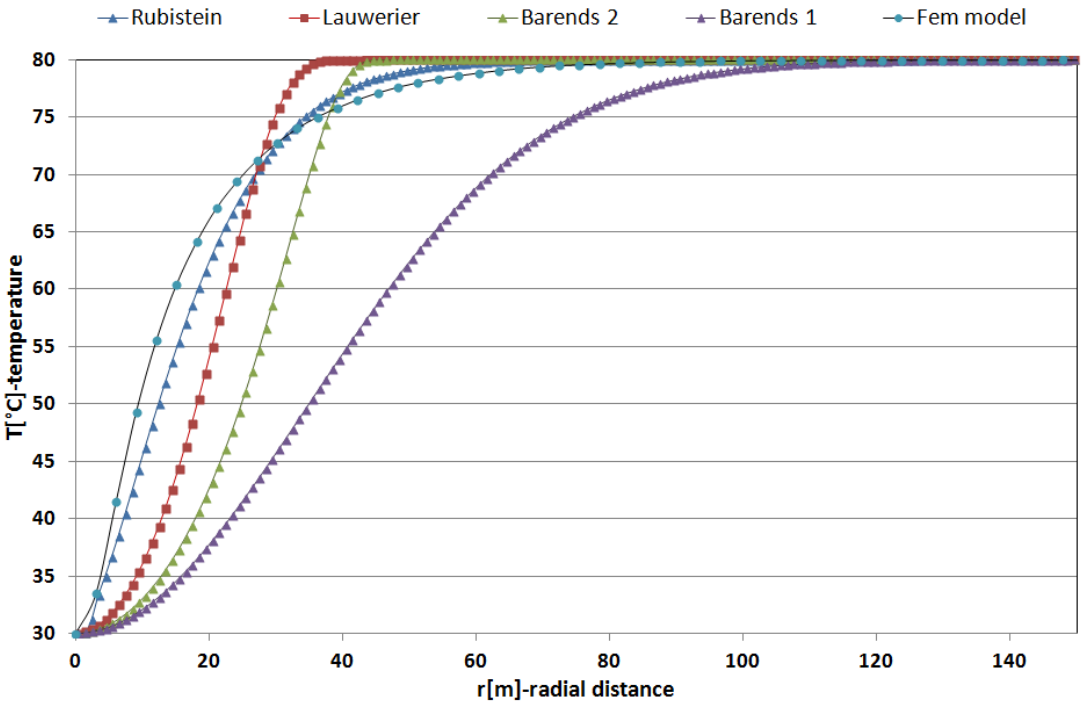

Figure 3.4: Case: Thickness = 10m, Pe = 1

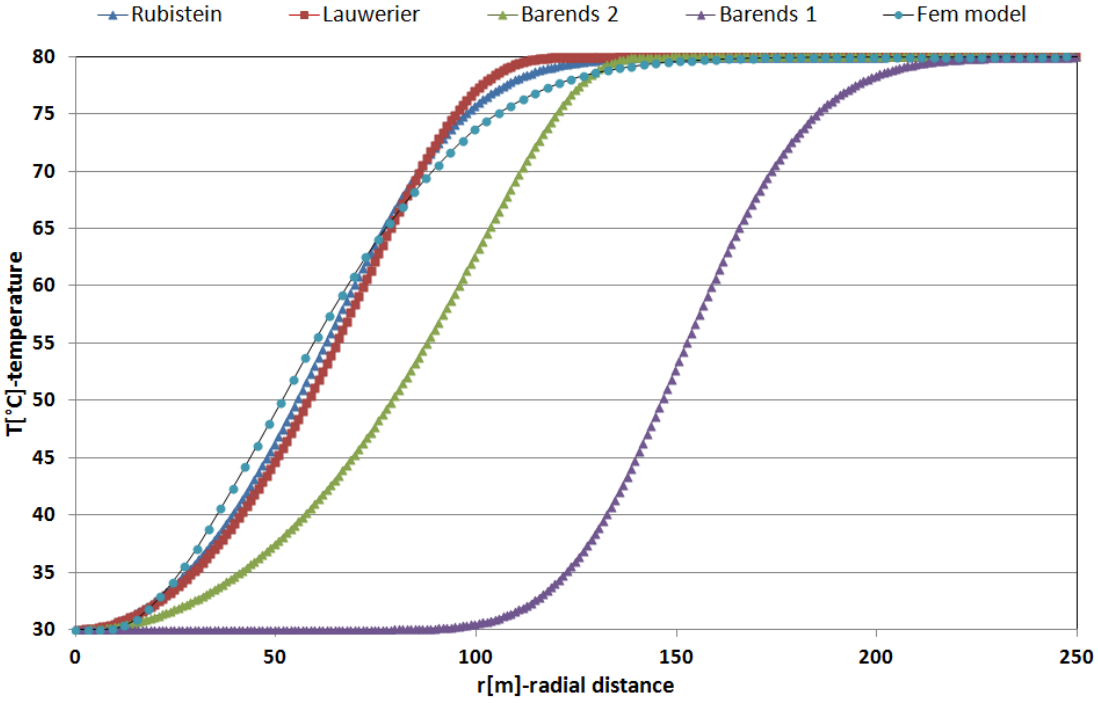

Figure 3.5: Case: Thickness = 10m, Pe = 10

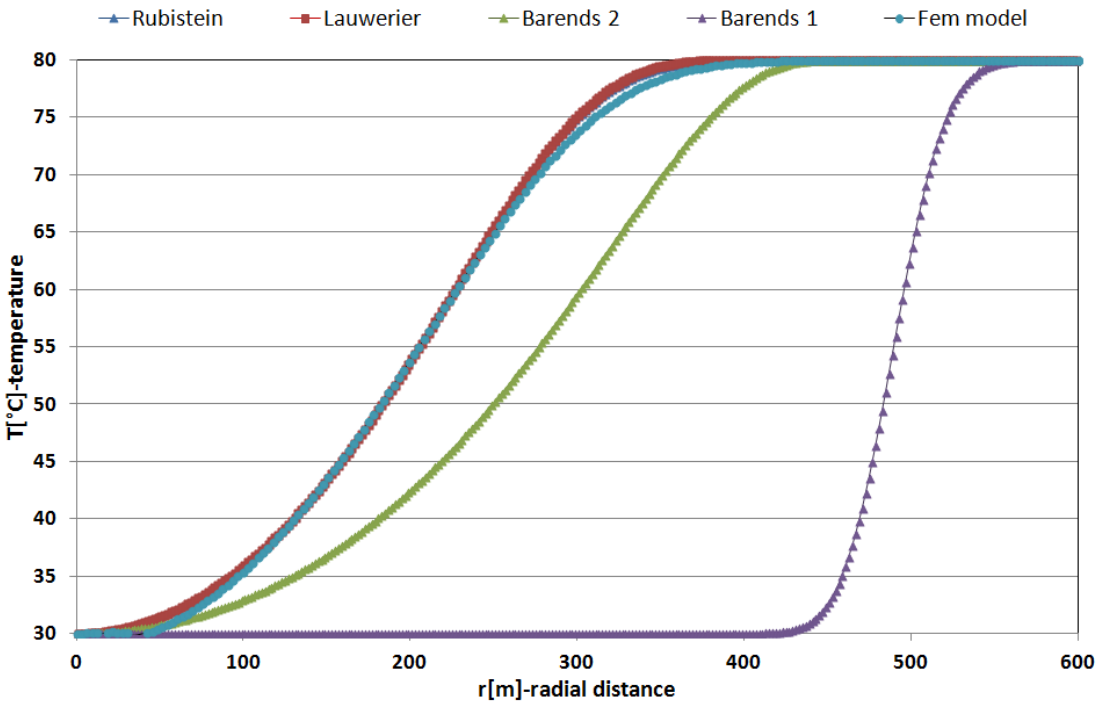

Figure 3.6: Case: Thickness = 10m, Pe = 100

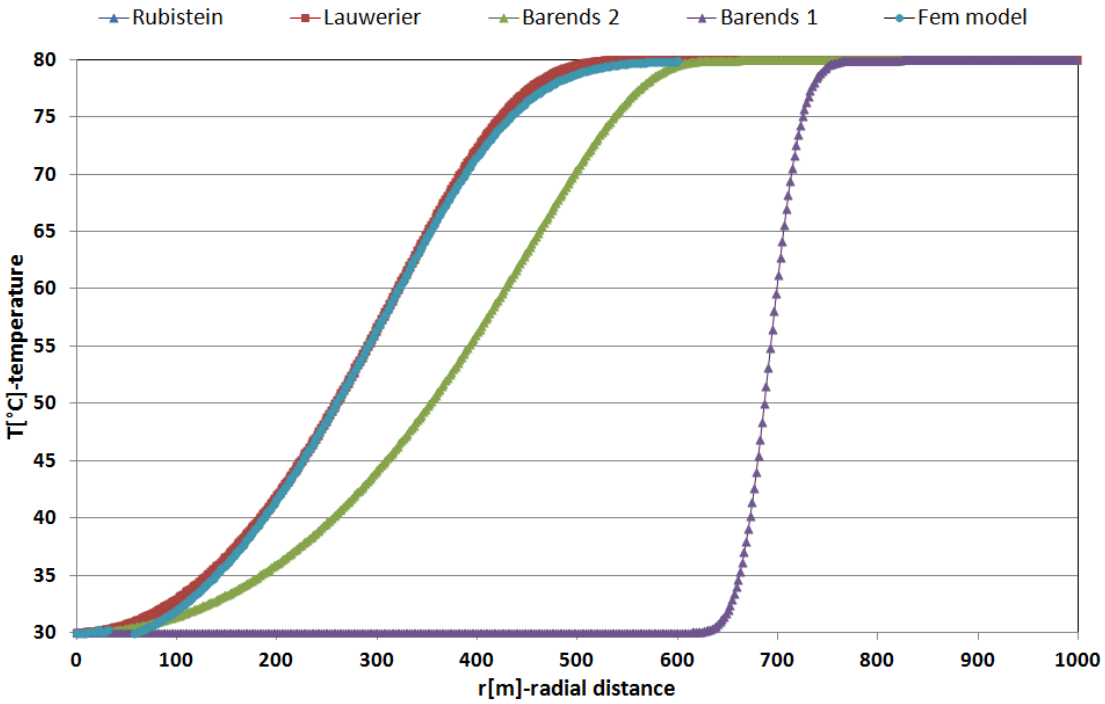

Figure 3.7: Case: Thickness = 10m, Pe = 200

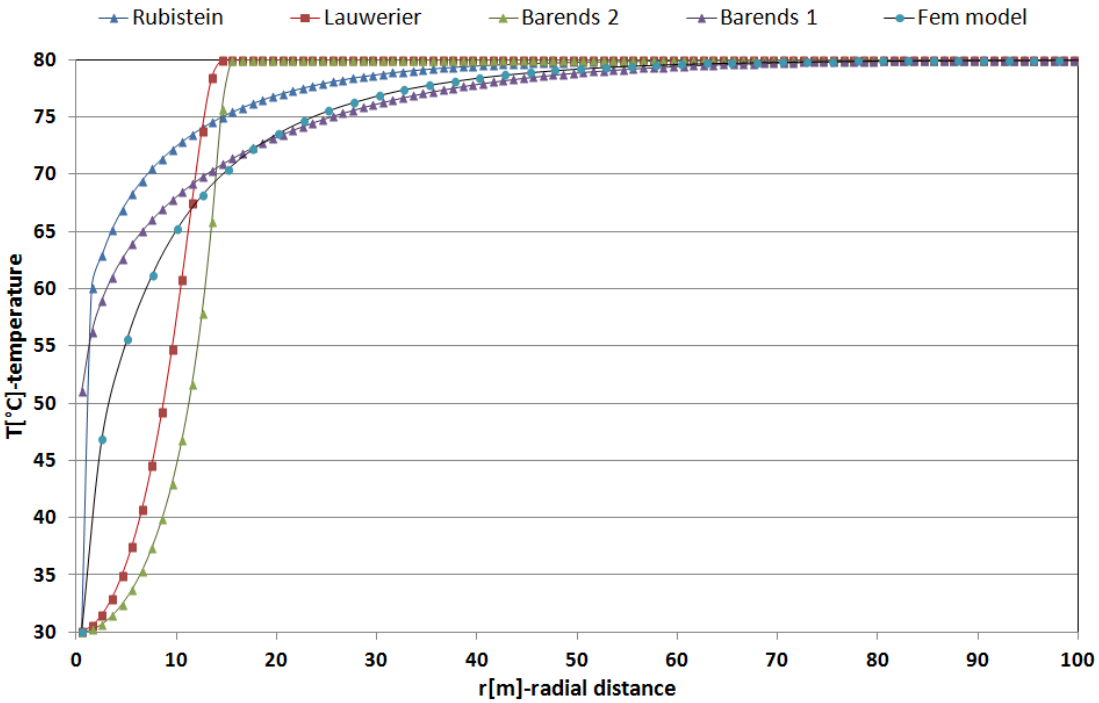

Figure 3.8: Case: Thickness = 25m, Pe = 0.1

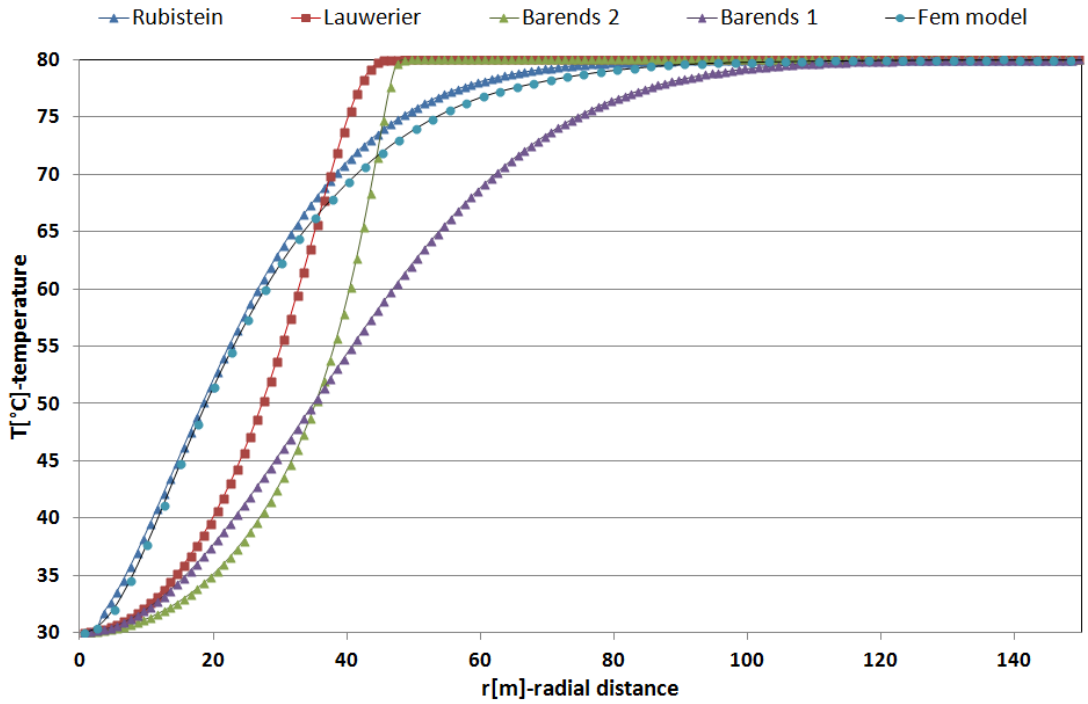

Figure 3.9: Case: Thickness = 25m, Pe = 1

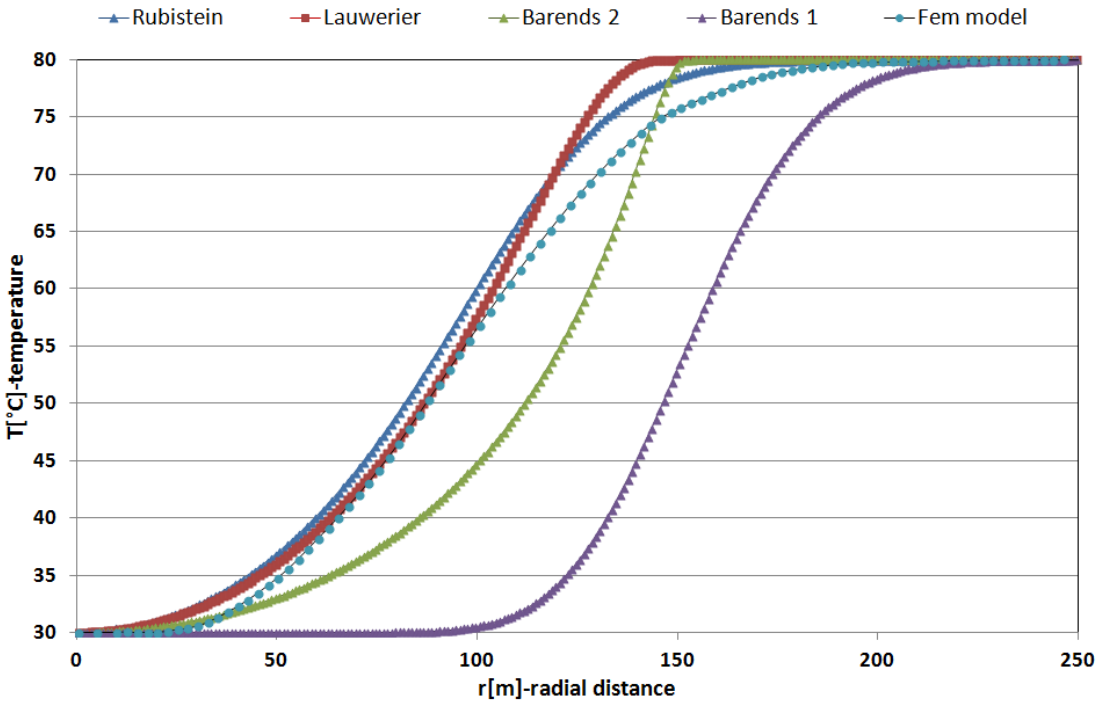

Figure 3.10: Case: Thickness = 25m, Pe = 10

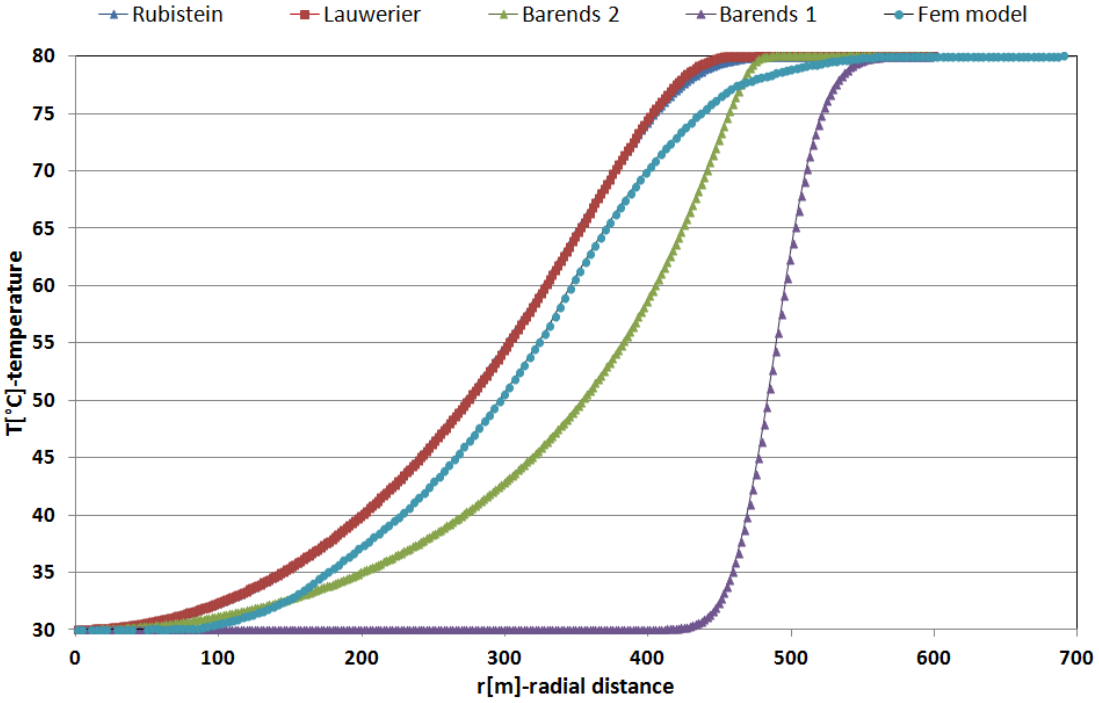

Figure 3.11: Case: Thickness = 25m, Pe = 100

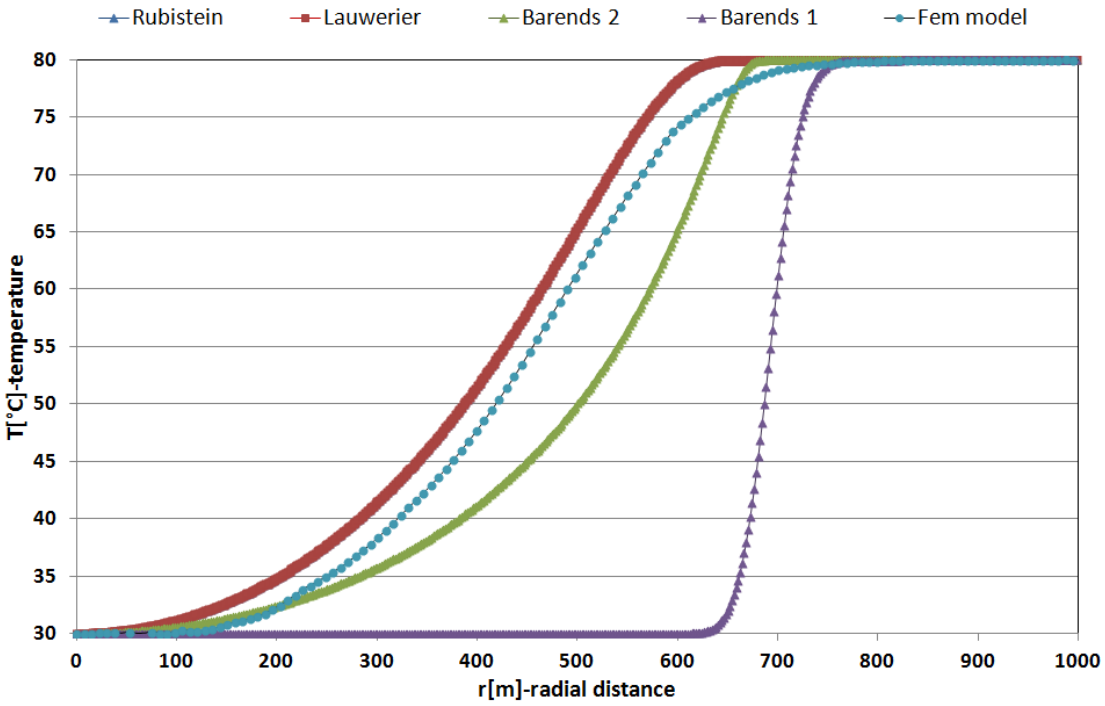

Figure 3.12: Case: Thickness = 25m, Pe = 200

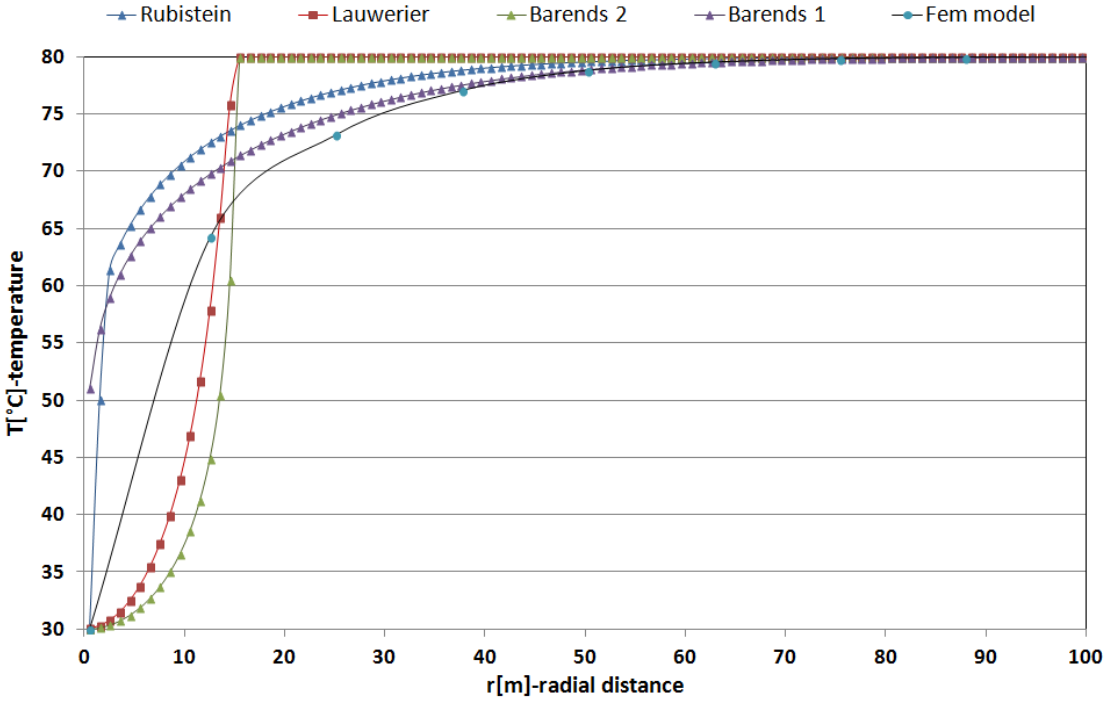

Figure 3.13: Case: Thickness = 50m, Pe = 0.1

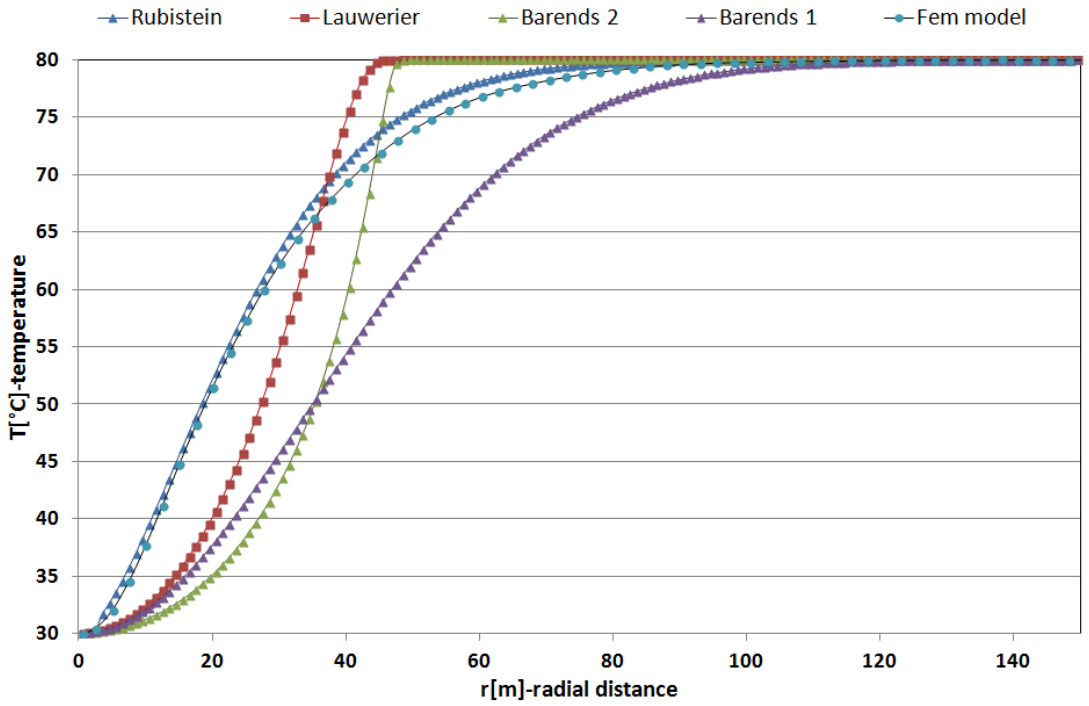

Figure 3.14: Case: Thickness = 50m, Pe = 1

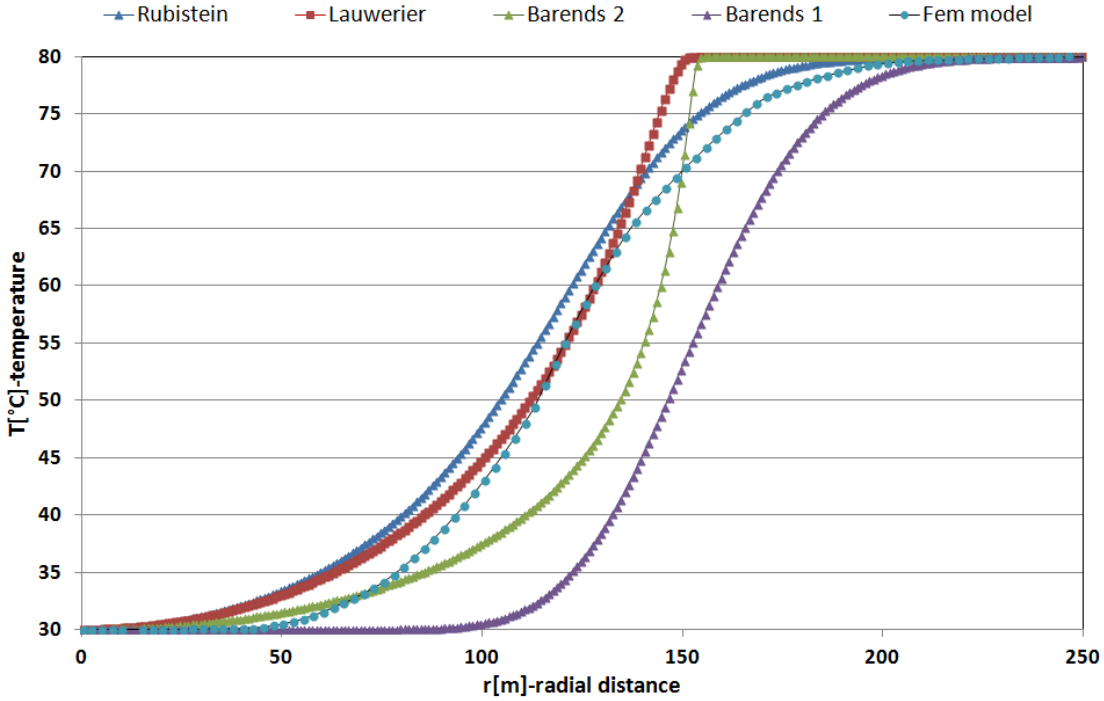

Figure 3.15: Case: Thickness = 50m, Pe = 10

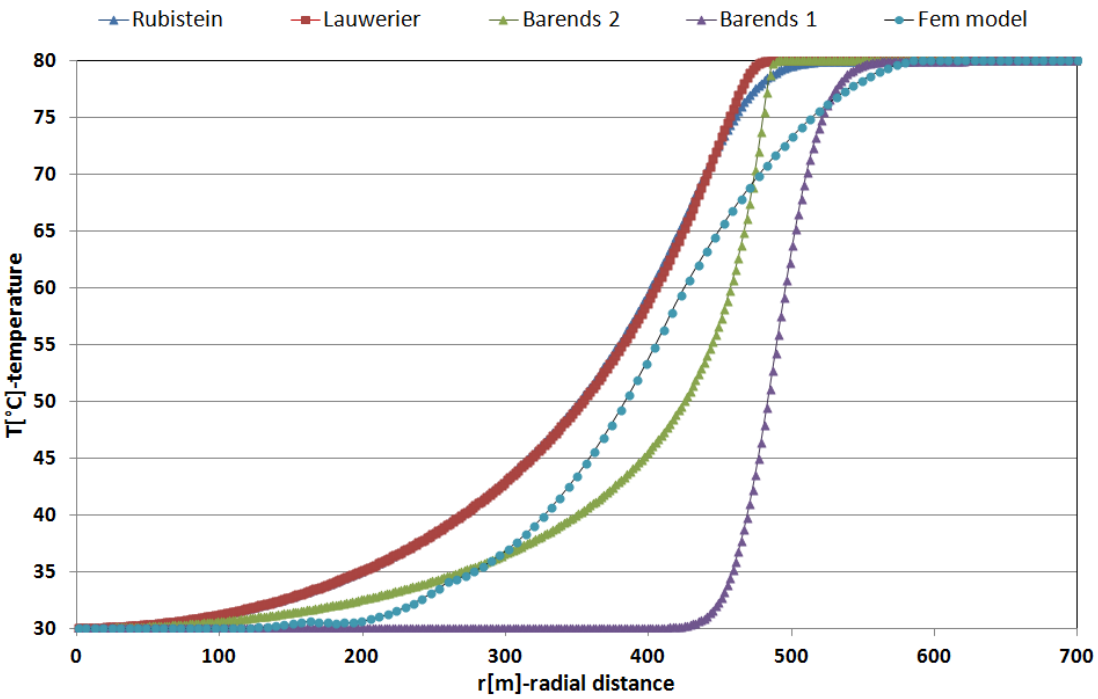

Figure 3.16: Case: Thickness = 50m, Pe = 100

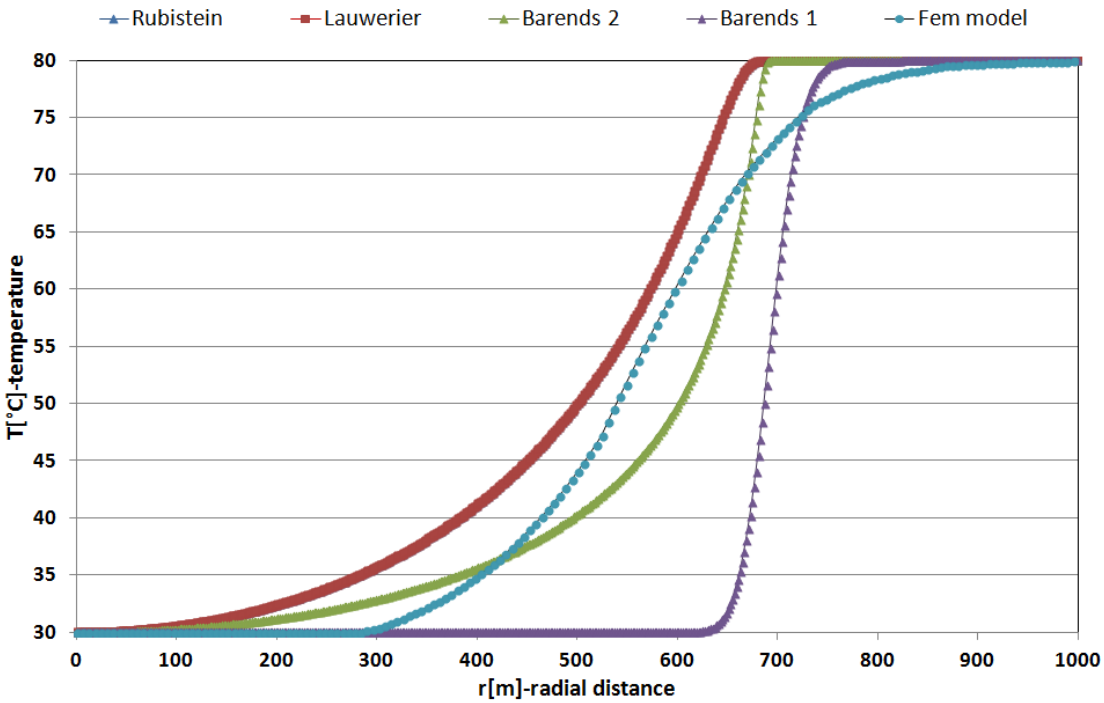

Figure 3.17: Case: Thickness = 50m, Pe = 200

Synthesis & Conclusions

For the graphics presented above it is possible to take some considerations. Before any further consideration it is useful introduce the concept of *Thermal Front*. *Thermal Front* in this work representing a distance reached, in a given time, by the temperature variation from the initial condition of the Aquifer.

Thickness=10m:

The best fitting is between Rubistein's solution and the numerical solution in every cases, with Pe variation.

Thickness=25m:

For Pe=0.1 the best fitting between analytical solution and numerical solution is done by Barends with out thermal bleedings (Barends 1).

For Pe from 1 to 200 the best fitting between analytical solution and numerical solution is done by Rubistein's solution.

For Pe=100 and 200 the best fitting is provided by Rubistein only for the temperature variation trend. Indeed there is a constant different between numerical and Rubistein solutions named *Delay*. This gap can be explained with the asymmetry of the water flow in the numerical simulation different from the analytical solution done for axial-symmetric system. The asymmetry is given by the hydraulic head asymmetry in a specific zone (in the middle of the two wells, injection and production [16]); the hydraulic gradient in that direction is more than in the others. Along this zone there is an asymmetry in the thermal plume, that is most probably the cause of the *Delay*.

For Pe=100 and 200 the best fitting only for the Thermal Front is between analytical solution and numerical solution and is provided by Barends 1 solution. Most probably the not consideration of the thermal bleedings pulls the thermal front more distant than the other solutions; this situation fills the gap caused by the asymmetry of the numerical models.

Thickness=50m:

For Pe=0.1 the best fitting between analytical solution and numerical solution is done by Barends with out thermal bleedings (Barends 1).

For Pe=1 the best fitting between analytical solution and numerical solution is done by Rubistein's solution.

For Pe=10 the best fitting between analytical solution and numerical solution is done by Rubistein's solution. The Thermal Front best fitting is done by Berends 1.

For Pe=100 The Thermal Front best fitting is done by Berends 1.

[16] See Chapter4.

For Pe=200 there is no best fitting. None of Analytical models approximate, in a good way, the numerical solution.

General considerations It has been observed that there are different behaviours of the analytical solutions under different cases.

Increasing thickness at same inlet velocity, the best fitting get worse.

Increasing inlet velocity at same thickness the best fitting gets worse. This is imputable of the increasing of the hydraulic gradient in the middle of the wells for the numerical model that has been used.

The thermal front analysis in some unfavorable conditions (as increase thickness and high inlet velocity) is well fitted by the unrealistic Barends 1 solution;this solution does not consider the thermal bleedings.

To conclude, it is possible to say that for Continuous Flow case regime, just presented, the analytical solutions can be useful. Analytical solutions, indeed, are a good help to predict the magnitude of the Worst thermal front (the major one that is the main size of the thermal bubble). Also to understand the temperature space distribution some analytical solutions (Rubistein and Lauwerier for high Pe value) are good forecaster.

Chapter 4

Numerical Models

Abstract

The objective of this chapter is to present the importance of numerical solution for Aquifer exploitation introducing numerical models that have been made by Finite Element Methodology. COMSOL Multiphysics version 3.5a has been used as FEM software. Also we introduce two numerical models that are used for different purposes, one for comparison with Analytical solution (used in Chapter3) and one for A.T.E.S simulations (used in Chapter5).

4.1 F.E.M

It is clear that every single natural process[1]can be considered a continuous problems. Humanity with mathematics and physics tools, tries to approximate and model these natural problems to understand and predict the natural behaviour of everything. There are two ways to do this: one using differential equation to find an exact solution of the problem with mathematical tools and the other one using a finite number of defined components. To note that, the first solution implies using an infinite number of elements,*continuous* method, whereas the second one is named *discrete* because of the use of finite number of elements. The main problem of these mathematical solutions is the needs of a simplified situation.

FEM is the acronym of Finite Element Method. This is a technique mainly used by engineer to model and solve numerous processes. FEM is a discrete analysis and this model method has development with increasing computers power. The FEM can be identify with the follows sentence from the introduction of Zienkiewicz, Taylor, and Zhu 2005, *Finite element method is a general discretization procedure of continuum problems posed by mathematically statements* . In FEM analysis there is a procedure to find the behaviour of whole finite investigated elements, indeed that procedure is founded in the local equilibrium at each node[2] of the elements. For Zienkiewicz,

[1]With *natural* we intend every single process that is driven by natural law, every man-made process follows natural law.

[2]Node is the connecting point of an element.

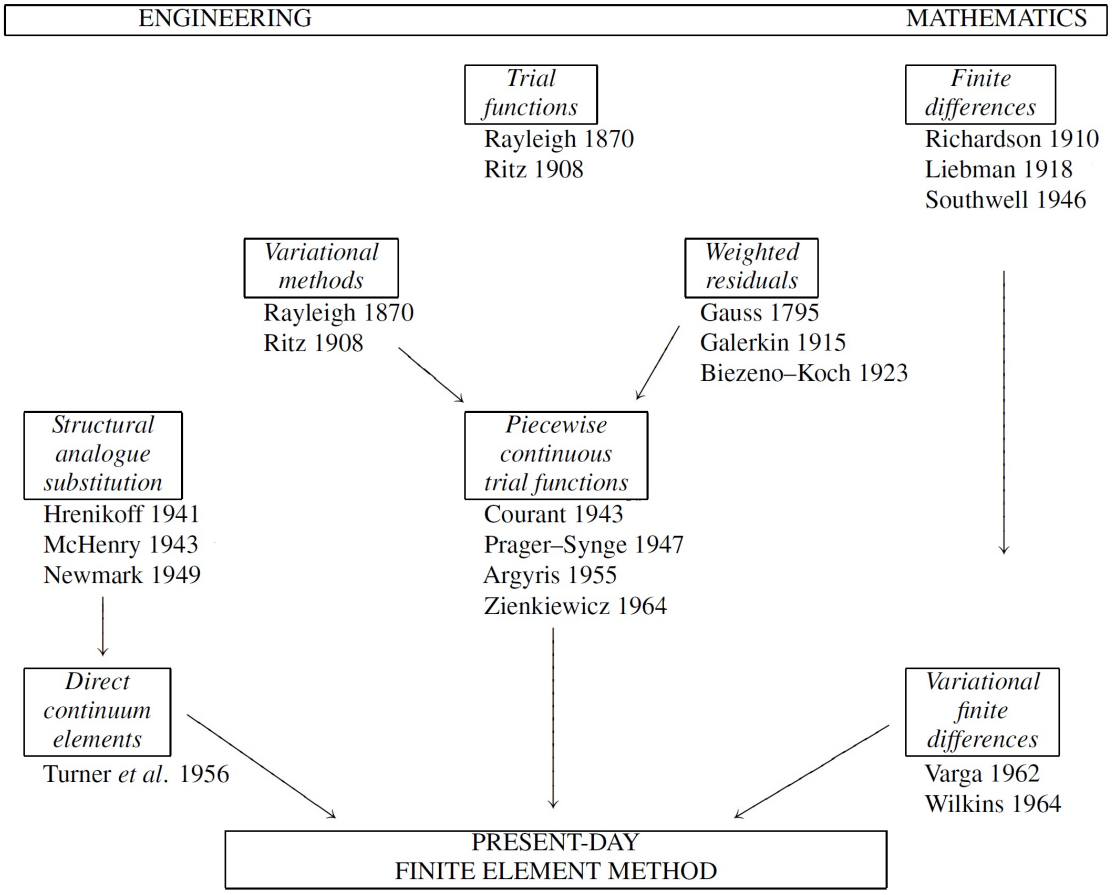

Figure 4.1: History of approximate methods (Zienkiewicz, Taylor, and Zhu 2005).

Taylor, and Zhu 2005 FEM has two main characteristics:

- *the continuum is divided into a finite number of parts (elements), the behaviour of which is specified by a finite number of parameters;*
- *the solution of the complete system as an assembly of its elements follows precisely the same rules as those applicable to standard discrete problems.*

Thus to apply the FEM methodology needs several information about the model:

- Governing Equations;
- Model domain;
- Model parameters;
- Boundary and initial condition;
- Mesh size and number of elements;
- Operation conditions;

For every model treated, these information will be presented. These information are fundamentals for FEM analysis to allow the reproduction of the model.

4.2 COMSOL®Multiphysics

In this section we introduce the software COMSOL®Multiphysics and in particular two packages used the models below presented. In "COMSOL textsuperscript®Multiphysics user guide", Comsol is presented as a *powerful interactive environment for modeling and solving all kinds of scientific and engineering problems based on partial differential equations.* This software is very useful and it is possible to use it stand alone or using a script programming in the MATLAB®language. A standalone way is used to create the follows models. Comsol is very useful because of several reasons:

- CAD package to directly design geometry;
- Possibility to use simultaneously more than one PDE packages;
- Several PDEs are already done in the software;
- There is a good meshing tool;
- Results are easily extrapolated;
- It is possible to do steady state and transient simulations;
- Properties can be time varying[3].

For this work we use two COMSOL environment, one for pressure field and a second one for the temperature field. In Earth science using the modules we use follows Kim, Y. Lee, et al. 2010 directions and they are Darcy's Law-Head PDEs and Heat transfer in porous media PDEs. Below, these two PDE's package are explicated.

4.2.1 Darcy's Law application

Darcy's Law application as already explained in the Chapter1 describes fluid movement in a porous medium. Using the head application, fluid flow in porous medium driven by gradients in hydraulic head (that is a way to represent pressure with equivalent height of fluid). The relationship between hydraulic head HH, pressure head H_p, elevation H_e, and pressure p is:

$$\frac{p + \rho_F \cdot g \cdot H_e}{\rho_F \cdot g} = H = H_p + H_e \tag{4.1}$$

where:

g is the magnitude of gravitational acceleration $[m/s^2]$.

ρ_F is fluid density $[kg/m^3]$.

[3]In this work none property is time varying

Remembering from 1Chapter, the K, that is Hydraulic conductivity a Aquifer properties,the velocity u according to Darcy's Law is, $u = -K \cdot \bigtriangledown H$, thus the governing equation becomes:

$$S \cdot \frac{\partial H}{\partial t} + \bigtriangledown[-K \cdot \bigtriangledown H] = Q_s \tag{4.2}$$

where:

S is the storage coefficient $[m^3]$.

Q_s is a fluid source.

The boundary conditions can be Dirichlet condition, Neumann condition,Chauchy conditions, these are:

Hydraulic Head: $H = H_0$,

Free surface: $H = H_e$;

Zero flux: $n \cdot K \cdot \bigtriangledown H = 0$[4];

Symmetry: $n \cdot K \cdot \bigtriangledown H = 0$;

Flux: $n \cdot K \cdot \bigtriangledown H = N_0$[5];

Mixed: $n \cdot K \cdot \bigtriangledown H = N_0 + R_b \cdot [H_b - H]$[6].

4.2.2 Heat transfer application

Heat transfer application is used for heat transferred by convection and conduction in porous medium system. The equation describes heat transfer by convection and conduction is:

$$\delta_t s \cdot C_{eq} \cdot \frac{\partial T}{\partial t} + \bigtriangledown(-\lambda_{eq} \cdot \bigtriangledown T) = -C_L \cdot u \cdot \bigtriangledown T + Q_H + Q_G \tag{4.3}$$

where:

δ_{ts} is a weight coefficient;

C_{eq} is "effective"[7] volumetric heat capacity;

λ_{eq} is the effective thermal conductivity;

T is temperature;

C_L is the volumetric heat capacity of moving fluid;

u is the fluid velocity[8];

[4]Where n is the normal to the boundary.

[5]Where N_0 is a specific flux.

[6]Where R_b represents conductance to flow in a semi-pervious layer adjacent to the boundary.

[7]Effective represents the average value of a complex system made with different type of matter with different characteristics.

[8]In this work models u "value" is calculated using Darcy's Law application.

Q_H is general heat source;

Q_H is geothermal heat source.

The boundary conditions can be Dirichlet conditions, Neumann conditions,Chauchy conditions, these are:

Temperature $T = T_0$;

Heat Flux $N = N_0$;

Convective Flux This boundary condition represents a boundary where heat flows in or out with a fluid;

Thermal insulation $N = 0$;

Symmetry $N = 0$.

Where N is *Total Heat Flux*, due to conduction(driven temperature gradient) and convection (driven fluid velocity):

$$N = -\lambda_{eq} \cdot \bigtriangledown T + C_L \cdot u \cdot T \tag{4.4}$$

4.3 Model 1:

Double well with a Continuous Flow

This model is used in the Chapter3 as numerical model to compare with analytical models. There are three Comsol models each one for different Aquifer thickness. This section will be presented only the 25 m Aquifer thickness, the 10 m and 50 m have the same characteristics of 25 m, with the exception of the size of the thickness. The model is studied in a symmetric way to reduce computation, thus every figure represents half of the model. The symmetric line cuts the model along the connecting line of the two wells. The model is made so extensive to avoid possible problems with the boundary conditions during the simulation time (20 years). Meshing is an important part for a FEM analysis. In this model automatical Comsol meshing was used. Thus we have been using normal size almost for all the simulation. For the operational condition, in this model, continuous flow is chosen, thus one well is for injection and the other is as a pump.

4.3.1 Governing Equations

The governing equations adopted are treated in the previous section (section 4.2); they are:

- Darcy's Law applied only to Aquifer strata;
- Heat transfer in porous media Applied to each strata (Aquifer, overburden and Underburden).

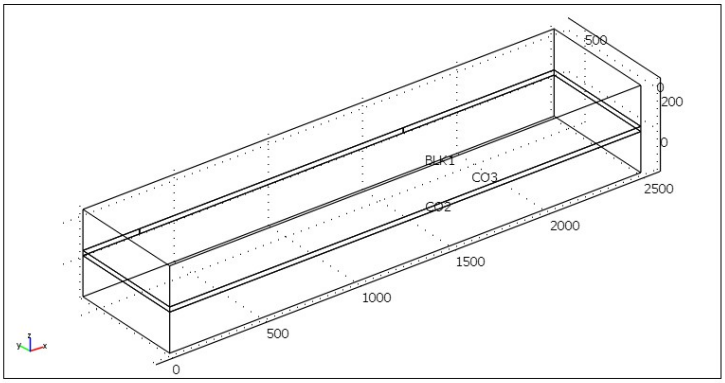

Figure 4.2: Three-dimensional finite element model.

K^a	${\chi_f}^b$	χ_s
1E-3	4.4E-10	1E-8

[a]Saturated Hydraulic Conductivity $[m/s]$.
[b]Compressibility of fluid and solid $[1/Pa]$.

Table 4.1: Hydraulic properties have been used in model 1.

4.3.2 Model Domain

This section will present the dimension of the three strata and of the wells along in order x,y and z direction. The domain is in Figure4.2

Overburden and Underburden: 2500m x 600m x 200m

Aquifer: 2500m x 600m x 25m

Wells: radius= 0.5m high=25m; all high is the active part for injecting and pumping fluid (Figure4.3)

4.3.3 Model Parameters

The main model parameters are summarized in Table3.3; however to use the Darcy's Law package in Comsol multiphysics other parameters are necessary,in particular hydraulic properties; see Table4.2.

4.3.4 Boundary and Initial conditions

In Table4.2 and Table4.3the initial and boundary hydraulic and thermal conditions are presented.

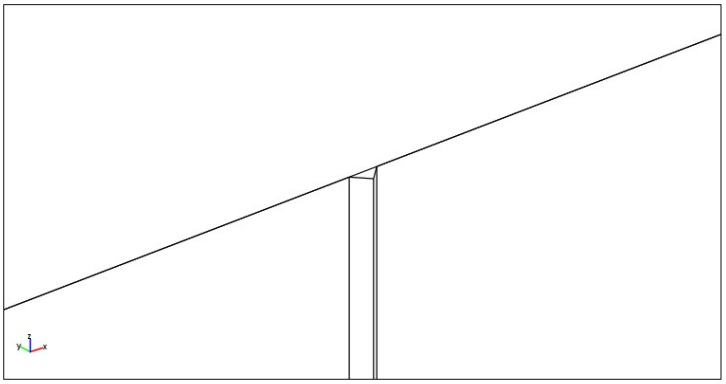

Figure 4.3: Particular of the model, well.

T_0 [a]	80
H_0 [b]	50

[a] Initial Temperature $[C]$.
[b] Initial Hydraulic head $[m]$.

Table 4.2: Hydraulic properties have been used in model 1.

		Hydraulic				**Thermal**		
	Surface Type	H [a]	v_{in} [b]	Symm [c]	Cont.[d]	T [e]	Symm [f]	Cont.[g]
	Lateral surface						yes	
Aquitard[h]	Horizontal surface					80		
	Symmetrical surface[i]						yes	
	Lateral surface	50					yes	
Aquifer	Horizontal surface			yes				yes
	Symmetrical surface			yes			yes	
	Lateral surface		Q/S_L [j]					
Wells	Symmetrical surface			yes			yes	

[a] Hydraulic Head $[m]$.
[b] Inlet Flow $[m/s]$.
[c] Condition of Symmetry or No Flux.
[d] Condition of internal boundary: Continuity.
[e] Temperature [°C]
[f] c
[g] d
[h] Refers both underburden and overburden.
[i] It is the surface of geometrical symmetry.
[j] Where Q is Volume flow rate $[m^3/s]$ and S_L is lateral surface $[m^2]$

Table 4.3: Boundary conditions for model 1.

4.4 Model 2:
Double well with cycling Flow (A.T.E.S. System)

This model is used in Chapter5 as numerical model to reproduce ATES system and to compare with analytical models. There are three Comsol models, each one for different wells distance. This section will be presented only the 80m wells distance; the 40 m and 120 m have the same characteristics of 80 m. The model is studied in a symmetric way to reduce computation, thus every figure represents half part of the model. The symmetric line cuts the model along the two wells line connected. Meshing is an important part for a FEM analysis. In this model automatic Comsol meshing was used. Hence we have been used normal size almost for all the simulation. The simulation time is 20 years and, with normal mesh size, the computational time is between 3 and 4 hours each simulation.

NOTE:Model 2 is different then model 1, boundary conditions are different as well as the operational conditions. Model 2 works with cyclic flow and the well's temperature condition is constant only 3 months per year; during the rest of the year the well temperature has to be unknown to simulate a real condition of the simulation. In other words, with this model it is possible to answer the question: what is the temperature of the water pumped from the aquifer ? To reach the condition of unknown temperature on the well's surface a trick is used, a fake circular crown is positioned in the middle of the well. The temperature condition of injection water is applied on the cylinder crown internal lateral surface; the Conductivity Coefficient of this fake circular crown is varying to permit the condition just illustrated, in fact the circular crown material become extremely conductive during injection period and insulated during pumping period(this way to avoid interference of boundary temperature condition).

4.4.1 Governing Equations

The governing equations adopted are treated in the previous section (4.2); they are:

- Darcy's Law applied only to Aquifer strata;
- Heat transfer in porous media Applied to each strata (Aquifer, overburden and Underburden).

4.4.2 Model Domain

This section present the dimension of the three strata and of the wells along in order x,y and z direction. The domain is in Figure4.4

Overburden and Underburden: 300m x 150m x 25m (for underburden 50m)

Aquifer: 300m x 150m x 50m

Wells: radius= 0.5m height=50m; the active part is only half all height (Figure4.5)

Circular Crown radius= 0.2m height=25m

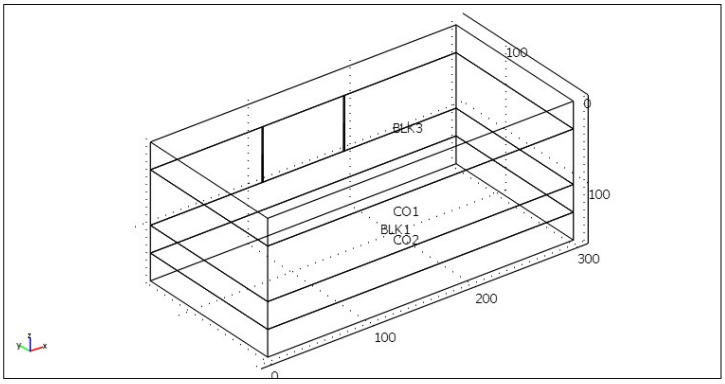

Figure 4.4: Three-dimensional finite element model 2.

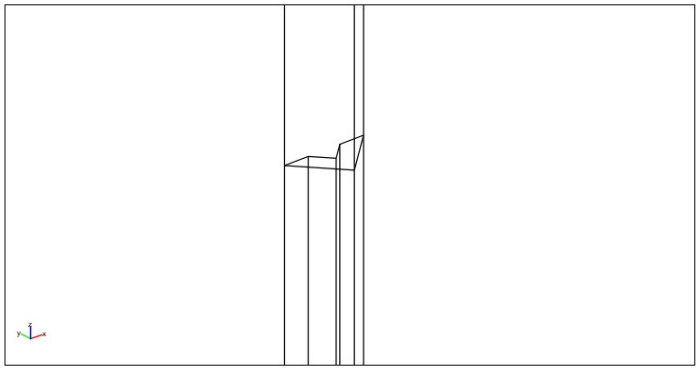

Figure 4.5: Particular of the model, well and circular crown.

n	ρ_r	ρ_w	c_r	c_w	λ_r	λ_w
T_0	T_{i_hot} [a]	T_{i_cold} [b]	K	χ_f	χ_s	
0.3	2700	1000	2360	840	4186	3
0.63	15	10	1E-3	4.4E-10	1E-8	

[a] Refers to the hot well inlet condition.
[b] Refers to the cold well inlet condition.

Table 4.4: Model 2 simulation data.

T_0 [a]	15
H_0 [b]	50

[a] Initial Temperature $[C]$.
[b] Initial Hydraulic head $[m]$.

Table 4.5: Initial condition used in model 2.

4.4.3 Model Parameters

The main model parameters are summarized in Table4.4;.

4.4.4 Boundary and Initial conditions

In Table4.5 and Table4.6the initial and boundary hydraulic and thermal conditions are presented. In these tables general data is presented, to have an idea of specific data see next chapter 5.

		Hydraulic				Thermal		
	Surface Type	H [a]	v_{in} [b]	Symm [c]	Cont.[d]	T [e]	Symm [f]	Cont.[g]
Aquitard[h]	Lateral surface						yes	
	Horizontal surface					15		
	Symmetrical surface[i]						yes	
Aquifer	Lateral surface	50					yes	
	Horizontal surface			yes				yes
	Symmetrical surface			yes			yes	
Wells	Lateral surface		Q/S_L [j]					
	Symmetrical surface			yes			yes	
C.Crown[k]	Lateral surface				T_in			yes
	Symmetrical surface						yes	

[a] Hydraulic Head $[m]$.
[b] Inlet Flow $[m/s]$.
[c] Condition of Symmetry or No Flux.
[d] Condition of internal boundary: Continuity.
[e] Temperature [°C]
[f] c
[g] d
[h] Refers both underburden and overburden.
[i] It is the surface of geometrical symmetry.
[j] Where Q is Volume flow rate $[m^3/s]$ and S_L is lateral surface $[m^2]$
[k] Circular Crown.

Table 4.6: Boundary conditions used in model 2.

Chapter 5

A.T.E.S Modeling

Abstract

In this chapter details of A.T.E.S Numerical models will be explained. The used model, Model 2 was already introduced in paragraph 4.4, here it is explained in details and for each case specifications. All the boundary conditions will be presented, also with initial conditions. The main parameters are already explained in Table4.4, here are also considered in more details in respect to underground water conditions. The main idea is to compare a vast number of results with different geometry, flow rate and aquifer conditions, using several investigation parameters utilization. Finally, after the cases presentation, some considerations are taken into account regard the utilisation of analytical solutions, commonly used for continuous flow systems, and here employed with cyclic flow systems (A.T.E.S.).

5.1 Model

The model 2, here explained in details, represents the typical A.T.E.S system plant. A.T.E.S mechanism is briefly explained in Chapter2. As well known there are two wells named respectively hot and cold. The Hot well represents that in which hot water is injected during a cooling period (summer), whereas the Cold well represents well in which cold water is injected during heating period (winter)[1]. It is possible to define two different important periods in which groundwater flow changes direction. In fact, during one period, groundwater is pumped from hot well and re-injected, after heating process, in a cold well; instead, during another period, groundwater is pumped from cold well and re-injected in hot well. As presented below, in this work, these two situations are used in the middle of two specific periods; these two specific periods are static situation without any pumping or injecting work (no operational period). The purpose of this section is to present various detailed cases with a particular attention in boundary and initial conditions of the simulation. The

[1]Obviously cooling and heating period refer to the possibility of use underground water as natural source for heating or cooling process.

model geometry and sub-domain data has been presented in Figure4.4 and Table4.4. Also general boundary conditions have been presented in Table4.6.

The main idea is to compare a many results between different cases, which are characterized by different geometrical, operational and aquifer characterisation.

5.1.1 Operational Conditions

This subsection are presented of all the operational conditions used for every case. The idea was to reproduce a typical year of thermal load necessary to cover a typical energy demand, for heating and cooling a building. To do that it was more acceptable to consider a oscillatory trend of thermal load (e.g. using sine wave), but it was very difficult do that because of convergence problems in Comsol model. Thus a step wave condition was adopted, this situation is represented in Figure5.1 as symmetrical situation. The thermal loads injected in the aquifer are considered with constant temperature and constant mass flow rate. Hence the power that can be useful depends on pumping well temperature level. This is an unreal situation, but it is a critical situation for the aquifer; indeed the aim of this work concern the Aquifer behaviours. To test the aquifer behaviors, different situations have been used, that are done with symmetrical or asymmetrical (Figure5.2) situations of thermal loads [2]. Note the parameter Power injected P is calculated as:

$$P = \dot{m} \cdot c_w \cdot (T_{in} - T_{aq}) \tag{5.1}$$

where:

P is Thermal power injected $[W]$.

$\dot{m}$ is Mass flow rate $[kg/s]$.

c_w is specific heat $[J/kgK]$.

T_{in} is inlet temperature [].

T_{aq} is aquifer temperature [].

The main characteristics of the symmetric and asymmetric operational conditions are:

- The wells operational curve represent the flow rate;
- injection temperature is constant;
- the periodisation of operational condition is (considering a year).

  3 months (spring) of no operation;

  3 months (summer) in which hot well injects and cold well pumps;

  3 months (autumn) of no operation;

[2] Symmetrical situation means that injected power is symmetrical in the initial aquifer temperature; the symmetry of injected thermal load is due only flow rate magnitude as above explained.

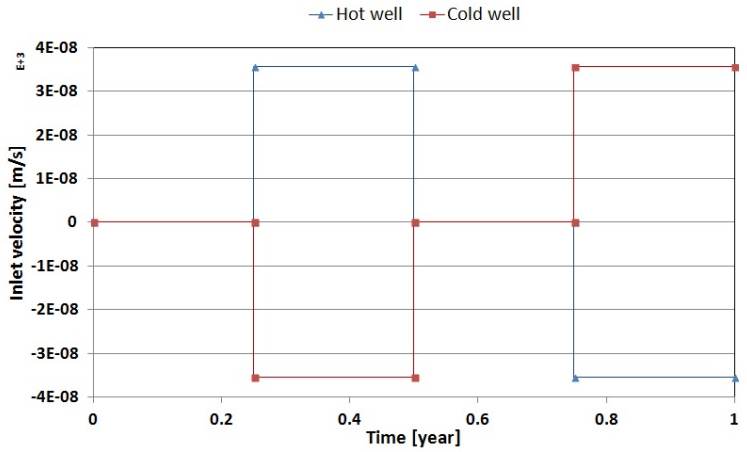

Figure 5.1: Specific Flow rate input for hot and cold wells (Symmetric case).

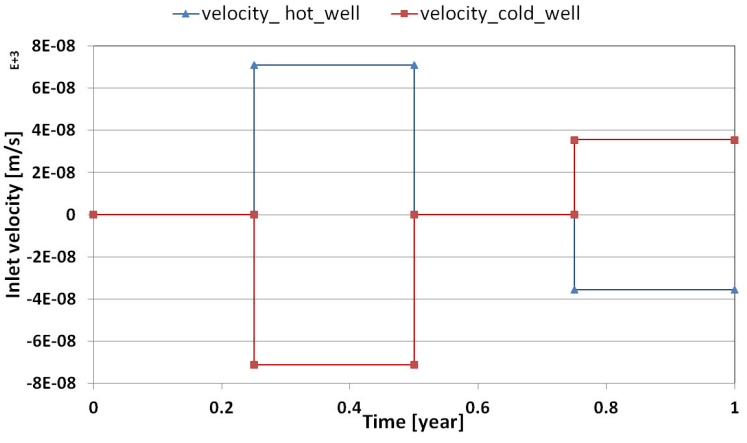

Figure 5.2: Specific Flow rate input for hot and cold wells (Asymmetric case).

3 months (winter) in which hot well pumps and cold well injects.

In this work every case is studied under different mass flow values. The values used are listed below[3]:

Symmetric load All the symmetric load cases are studied with two mass flow values:

10 m^3/h for both hot and cold wells.

20 m^3/h for both hot and cold wells.

Asymmetric load They are studied only with one mass flow configuration:

10 m^3/h during cold well injection and 20 m^3/h during hot well injection.

The choice of mass flow rate is quite casual, typical values for each injection well are 20-30 m^3/h (Lau et al. 1986), (Andersson 2007c), (Andersson 2007b). With these values of mass flow rate, the minimum value of power that it is possible to extract by underground water is calculated using eq. 5.1. Considering the injected temperature for hot well (20^oC) and considering the worst level of temperature of pumping well, that is the aquifer natural temperature (in this work 15^oC), the minimum power can be available is almost 58 kW (for a mass flow rate of 10 m^3/h) and almost 116 kW (for a mass flow rate of 20 m^3/h)[4].

There are others two operational conditions: wells distance and underground natural flow velocity (areal flow). Thus the second aquifer characterisation is the underground water natural movement. Three values of underground natural flow have been chosen, 0 m/year, 30 m/year and 100 m/year. These values are considered because they are respectively ideal value, most common and upper limit for areal flow velocity (Figure2.4). To put the underground natural flow in the model an indirect way has been used. Indeed, under the assumption of homogeneity of the aquifer with permeability K, it is easy to find the underground water velocity by Darcy's velocity using (1.20). In these cases we already know the underground natural velocity, hence the objective is to find the hydraulic head variation which is oriented as the same direction of the areal flow. The hydraulic gradient is found with Darcy's Law (**??**):

$$\Delta H = q \cdot \frac{L}{K}$$

where:

ΔH is the hydraulic gradient that has to be applied as boundary condition to have the wanted areal flow $[m]$.

q is Darcy's velocity $[m/s]$.

L is the distance between the surface which hydraulic gradient is applied $[m]$.

K is hydraulic conductivity $[m/s]$.

[3]With the word Load we intend the injected power in the aquifer.

[4]To note that these values are calculated with assumption of no thermal interaction between hot and cold wells.

Well Distance[b]	Type of Thermal Load	Mass flow Magnitude[c]	Areal flow[a]		
			0	30	100
40	Sym	10	✓	✓	✓
	Sym	20	✓	✓	✓
	Asymm		✓	✓	✓
80	Sym	10	✓	✓	✓
	Sym	20	✓	✓	✓
	Sym	40	✓		
	Sym	60	✓		
	Asymm		✓	✓	✓
120	Sym	10	✓	✓	✓
	Sym	20	✓	✓	✓
	Asymm		✓	✓	✓

[a] $[m/s]$
[b] $[m]$
[c] $[m^3/h]$

Table 5.1: Cases done for with Fem model.

Also there is a differentiation on wells distance. Three values are used: 40,80 and 120 m distance that can be used in ATES applications; for every well distance is varying as the mass flow rate and areal flow rate.

All the thermo-physical-hydraulic properties are given in Table4.4. All the cases are summarized in Table5.1. Totally they are 29 simulations.

5.1.2 Boundary Conditions

A general boundary condition are presented in Table4.6, but in this paragraph, boundary conditions are presented in a detailed form. Referring to the figures 5.3, 5.4 and 5.5, table 5.2 report all boundary conditions.

5.2 Postprocessing Analysis

To evaluate the postprocessing data of every simulation some parameters are used. In literature there are not typical parameters to evaluate ATES situation, thus this section presents some different coefficients to do that. Some of these are new and others are taken from different article as Kim, Y. Lee, et al. 2010, Andersson 2007a and Courtois and Grisey 2007. All parameters are listed below. To note that the post processing analysis want to evaluate the temperature distribution and the Aquifer behaviour as A.T.E.S system.

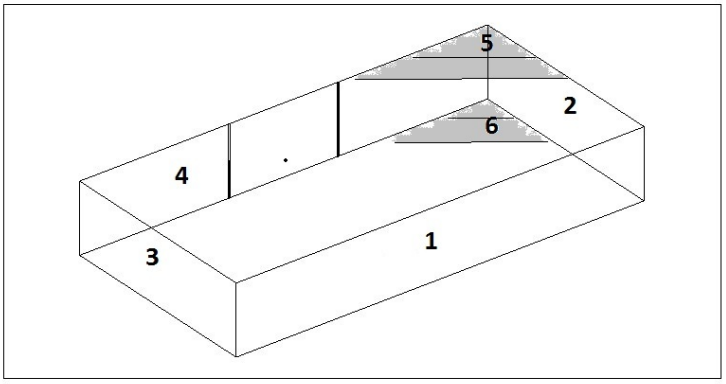

Figure 5.3: Aquifer numerical references for boundary specifications.

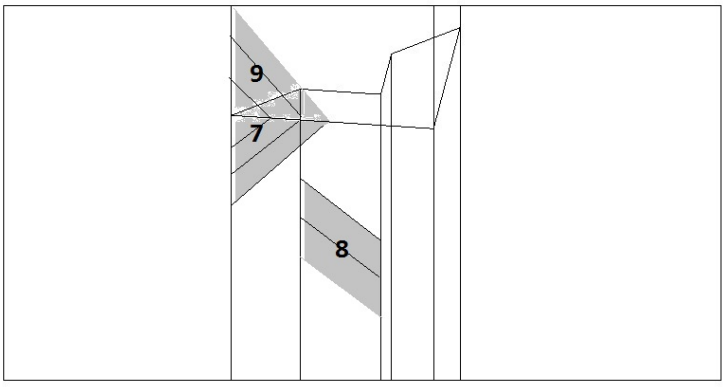

Figure 5.4: Well numerical references for boundary specifications.

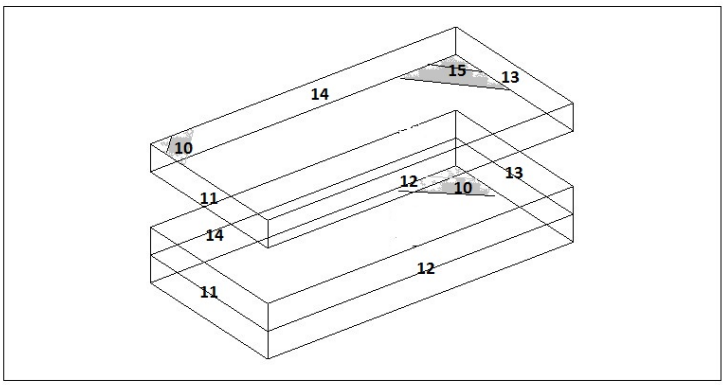

Figure 5.5: Overburden and underburden numerical references for boundary specifications.

	Hydraulic Boundaries			Thermal Boundaries		
Surf.Nr	HH[a]	Inlet flux[b]	Sym[c]	T[d]	Sym[e]	Cont.[f]
1	50	(✓)			✓	
2	50				✓	
3	50+($\triangle$ H)				✓	
4		✓			✓	
5						✓
6						✓
7			$v(t)$			
8				10/20		
9			✓			
10				15		
11					✓	
12					✓	
13					✓	
14					✓	
15						✓

[a]It is Hydraulic head condition, with hydraulic head value for the surface. Usually surface is considered quite far by the injection or pumping well do not cause any errors in pressure trend. Obviously dimension of HH is [m].

[b]represent Inlet or outlet velocity [m/s].

[c]Sym Refers both to symmetry conditions and no flux conditions.

[d]Temperature in .

[e]c

[f]represent Continuity condition.

Table 5.2: Boundary conditions for every single case; between bracket are the boundary conditions of case with natural underground water movements.

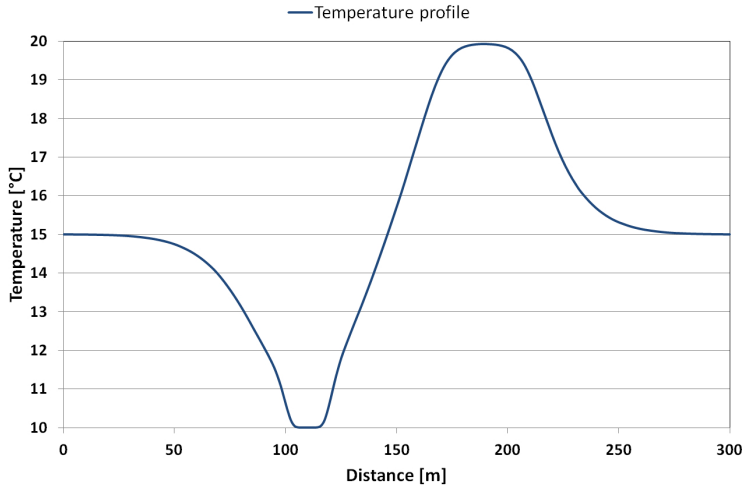

Figure 5.6: Temperature profile with distances indications using same reference of (5.2).

5.2.1 Parameter η

This parameter represents the ratio between length of thermal front and distance between two boreholes in a given time (usually after 20 years of operativity). In the Figure5.6 is presented a temperature vertical section of the aquifer with a simple explicative thermal length indications.

Length of Thermal Front This value represents the main radius[5] of thermal bubble developed all around every well.

Distance between boreholes It is the distance between two wells center, in this work assumes 40, 80, 120 m as value.

$$\eta = \frac{LengthofThermalfront}{Distancebetweenboreholes} = d/D \tag{5.2}$$

5.2.2 Parameter MWT

MWT means Middle Wells Temperature and indicates the temperature trend in a zone which is situated in the middle of two boreholes. Thus MWT presents temperature variation of one point or one zone (as average value) varying time. In this work MWT was chosen as temperature trend of one point in the middle of two wells [6]. In Figure5.7 there is an example of MWT.

5.2.3 Parameter WT

WT means Well Temperature and indicates the temperature of the water, injected and pumped. Using $Comsol^{®}Multiphysics$ WT value is found as average value at the well surface. Indeed using

[5]Usually main radius, in an homogeneous system, is found in the middle of the well height.

NOTE: the Thermal front length is individuate when there is al least $0.1^{o}C$ between temperature profile and the undisturbed temperature of the aquifer.

[6]Point coordinate are for the height,in the middle of the well active part, for the wells distance, same distance from two wells and for depth, in the plane of geometry symmetry.See Figure5.3 where this point is good indicated.

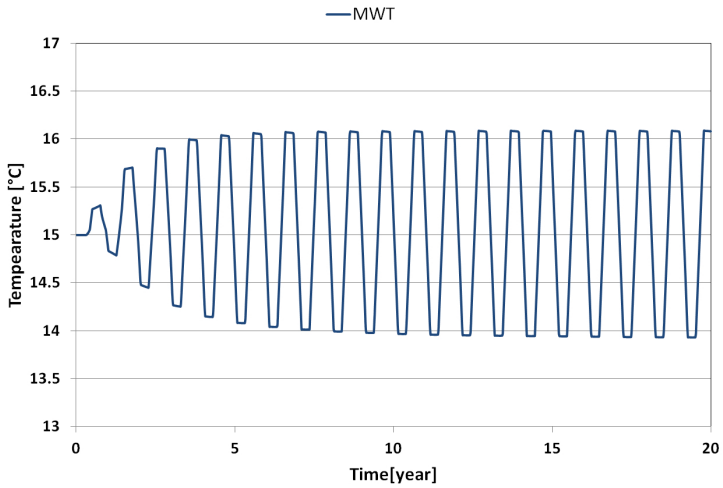

Figure 5.7: MWT evaluation.

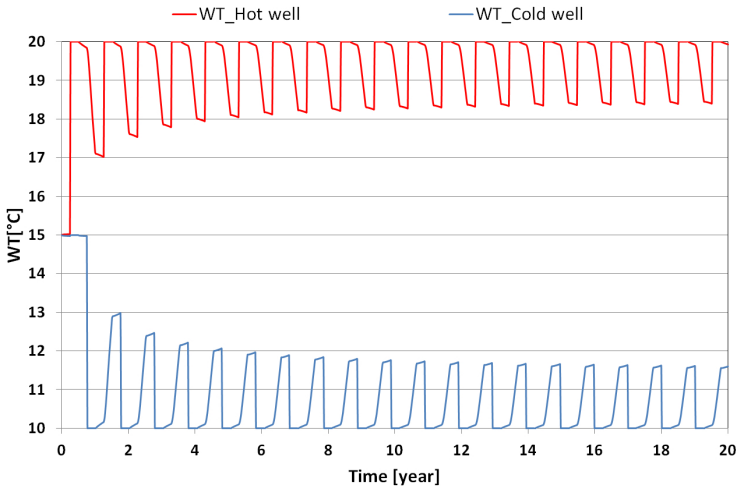

Figure 5.8: WT evaluation for hot and cold boreholes.

temperature surface integration it is possible to find a value with the dimension of $T \cdot L^2$, then using the value of entire surface given by Comsol postprocessing analysis, with dimension of L^2, it is possible to find an average value of temperature that represents the WT. See Figure5.8.

5.2.4 Parameter GTP

GTP means Global Thermal Power and indicates the power injected in the aquifer (Courtois and Grisey 2007). To note that the temperature of the water is in Celsius degree because of the consideration of temperature 0 as reference temperature for zero enthalpy. Thus GTP can be given by water temperature, so it follows water discharge temperature trend. The GTP equation is:

$$P_g = \rho_w \cdot c_w \cdot Q_{iorp} \cdot WT \tag{5.3}$$

where:

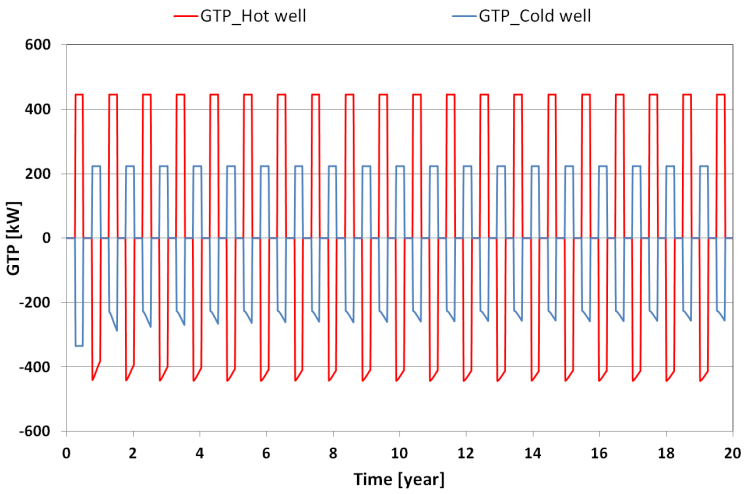

Figure 5.9: GTP evaluation for hot and cold boreholes.

P_g is the GTP $[W]$;

ρ_w is water density $[kg/m^3]$;

c_w is water specific heat $[J/kgK]$;

Q_{iorp} is water volume flow rate i injected or p pumped $[m^3/s]$.

In the Figure5.9 there is GTP trend that is the same of the WT trend. Note that there is a difference between hot and cold power that is due to the temperature reference that is nearest to cold temperature than hot temperature; thus seems that hot power is bigger than cold power, to find the real situation another temperature reference has to be chosen; hence another parameter has to be used.

5.2.5 Parameter UTP

UTP means Useful Thermal Power and indicates surplus of power injected in the aquifer (in a hot form or cold form), compared to a simple exploitation of water (without storage), Courtois and Grisey 2007. To note that there is a new reference temperature, that is the Aquifer normal temperature (15). The UTP equation is:

$$P_u = \rho_w \cdot c_w \cdot Q_{iorp} \cdot |(WT - T_0)| \tag{5.4}$$

where:

P_u is the UTP $[W]$;

T_0 is the undisturbed aquifer temperature $[^oC]$.

In the Figure5.10 there is UTP trend that is the same of the WT trend. Note that there is a modulus to consider cold and hot injection power with a positive number and thus pumped power as negative number (the sign is due only Volume flow rate direction: injection= positive , pumping=negative).

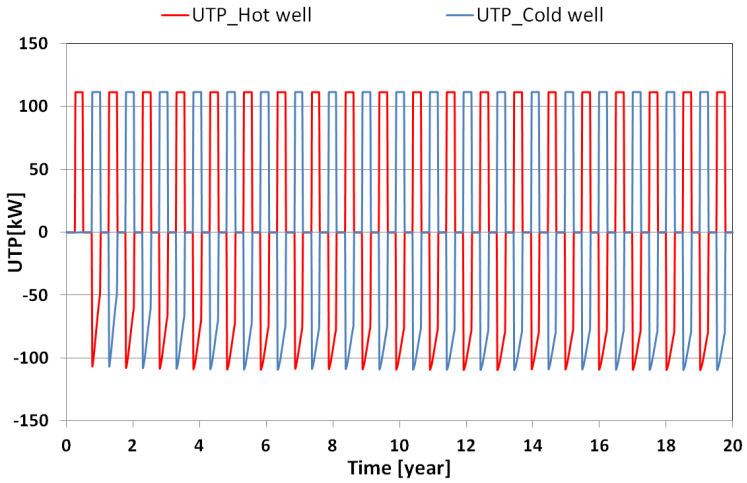

Figure 5.10: UTP evaluation for hot and cold boreholes.

5.2.6 Parameter E

E means Energy and indicates injected and pumped energy (for hot and cold well), in particular indicates Useful Energy with the obvious mean of integral of useful power. It is possible define two Energy coefficient calculated for two distinct periods of the entire cycle : *Energy pumped or Energy Stored*. Useful Stored Energy is associated with injected water during three months injection time. Useful Pumped Energy is that energy extracted by a well during extraction period.(Courtois and Grisey 2007). The E equation are:

$$E = \int_0^{Final-time} P_u(t) \cdot dt \tag{5.5a}$$

$$E_u^{Stored} = \int_0^{Injection-time} P_u(t) \cdot dt \tag{5.5b}$$

$$E_u^{pumped} = \int_0^{Pumping-time} P_u(t) \cdot dt \tag{5.5c}$$

E like P_u take the sign from volume flow rate, positive in injection and negative for pumping.

5.2.7 Parameter r

r means Recovery Factor (Courtois and Grisey 2007) and indicate the fraction of injected energy that can be extracted by the Aquifer system under given conditions. The equation of recovery factor is:

$$r = \frac{E_u^{Pumped}}{E_u^{Stored}} \tag{5.6}$$

5.2.8 Parameter COP

COP means Coefficient of Performance; with this parameter we want to indicate the performance of a inverse Carnot machine used as heat pump. The use of this parameter is very simple, as equation shows, also is very useful to evaluate the potential of ATES exploited with a heat pump

system. The water extracted from hot well is used as cold source of the ideal Carnot machine, the hot source is at 20 ℃, typical temperature of human ambient during cold season [7].

$$COP = \frac{20}{20 - WT_{hot-well}} \tag{5.7}$$

To understand the potentiality of ATES system, COP value has to be compared with others ideal COP values, obtained using air or underground water without any storage mechanism, as cold source [8].

5.2.9 Parameter EER

EER means *Energy Efficiency Ratio*; with this parameter we want to indicate the performance of a inverse Carnot machine used as refrigerator system. This parameter as the same objective of the previous. The water extracted from cold well is used as hot source of the ideal Carnot machine, the cold source is at 10 ℃, typical temperature for sensible heat conditioning systems.

$$EER = \frac{10}{WT_{cold-well} - 10} \tag{5.8}$$

To understand the potentiality of ATES system, COP value has to be compared with others ideal EER values, obtained using air or underground water without any storage mechanism, as cold source [9].

Also *Comsol*® gives the possibility to take pictures and video to have a general view of the results using Thermal map(e.g. in Figure5.11).

5.2.10 Simulation results

Every graphic represents the trend of the three important index: recovery factor, COP and EER. These analysis can furnish a first idea to study and model ATES in a pre feasibility phase; also it gives us some ideas to how ATES systems are favorable to use than normal systems using only normal underground water, without stocking [10]. Below summarized graphics are presented, firstly for Symmetrical case and secondly for Asymmetrical case. Remember that all the simulation cases are illustrated in Table5.1. The results are presented in two distinct ways: one with the three coefficient above nominated versus natural groundwater flow (areal flow) with a fixed wells distance, whereas the second representation shows the three coefficients versus well distance with fixed areal flow value. These two representation types want to show the incidence of the different configurations on the System performances.

[7] We assume to have a ideal heat pump with ideal heat exchangers. None heat loss is considered.

[8] typical values for COP obtained using air or underground water without any storage mechanism are in order: 1.33 using air characterized by constant temperature of 5℃and 4 using underground water at 15℃.

[9] typical values for COP obtained using air or underground water without any storage mechanism are in order: 0.5, using air characterized by constant temperature of 25℃, and 2 using underground water at 15.

[10] See note number 9

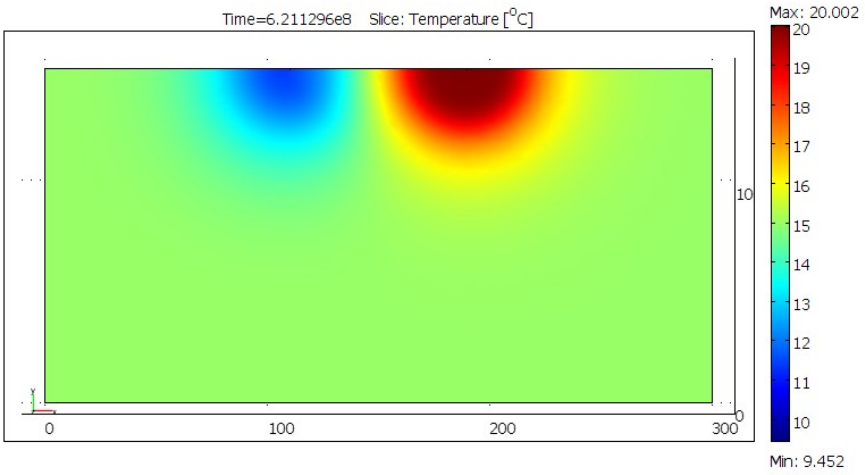

Figure 5.11: Thermal map, horizontal slice in the middle of the wells height; after 20 years of simulation time.

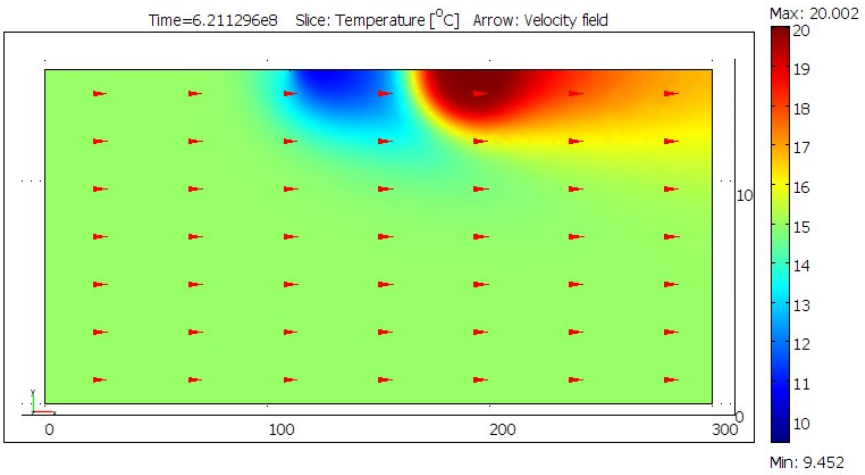

Figure 5.12: Thermal map, horizontal slice in the middle of the wells height; after 20 years of simulation time. Arrows indicate main direction of natural underground water flow.

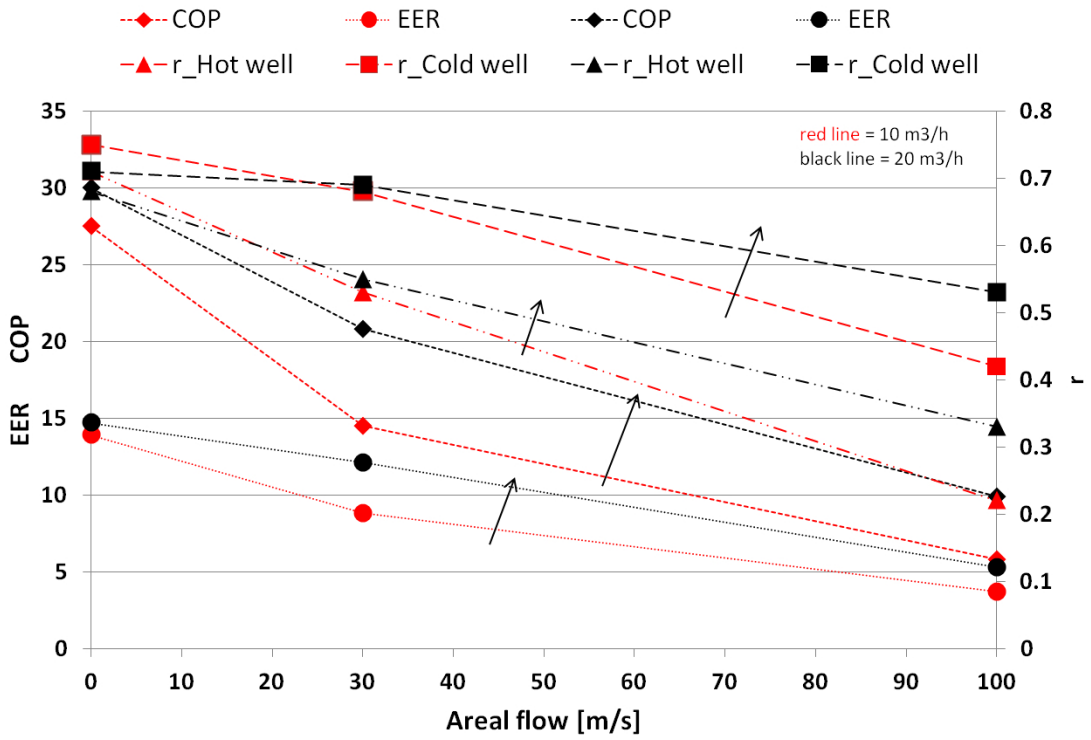

Figure 5.13: COP, EER and r versus areal flow changing, for 40m wells distance and two volume flow rate.

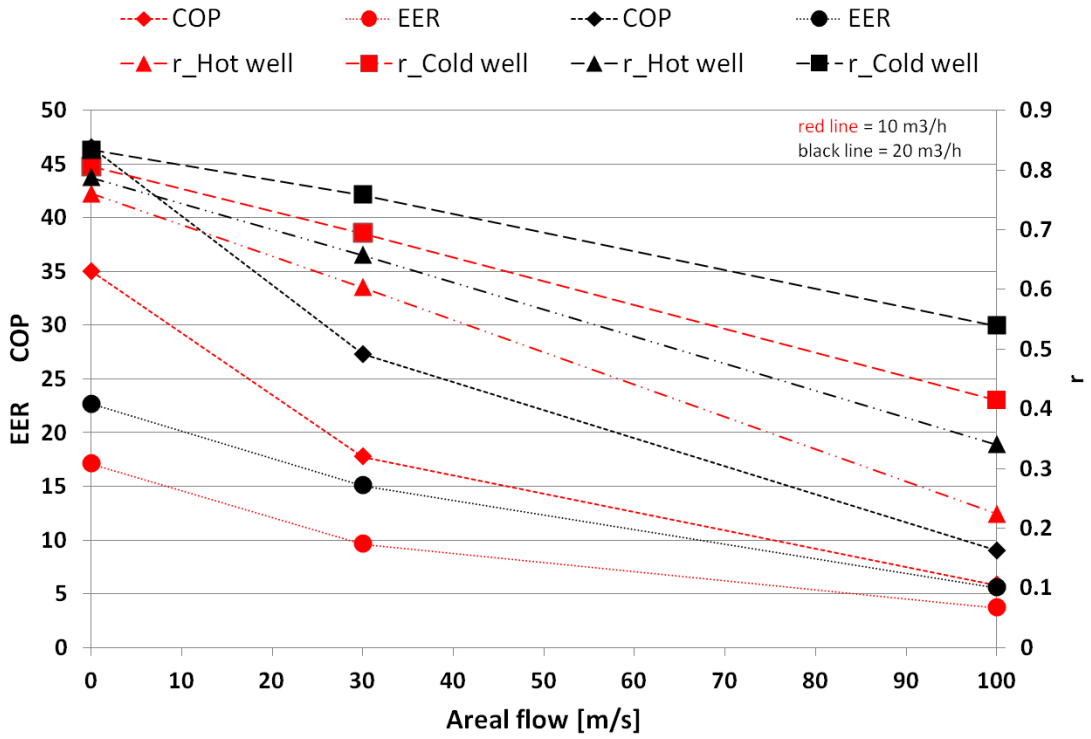

Figure 5.14: COP, EER and r versus areal flow changing, for 80m wells distance and two volume flow rate.

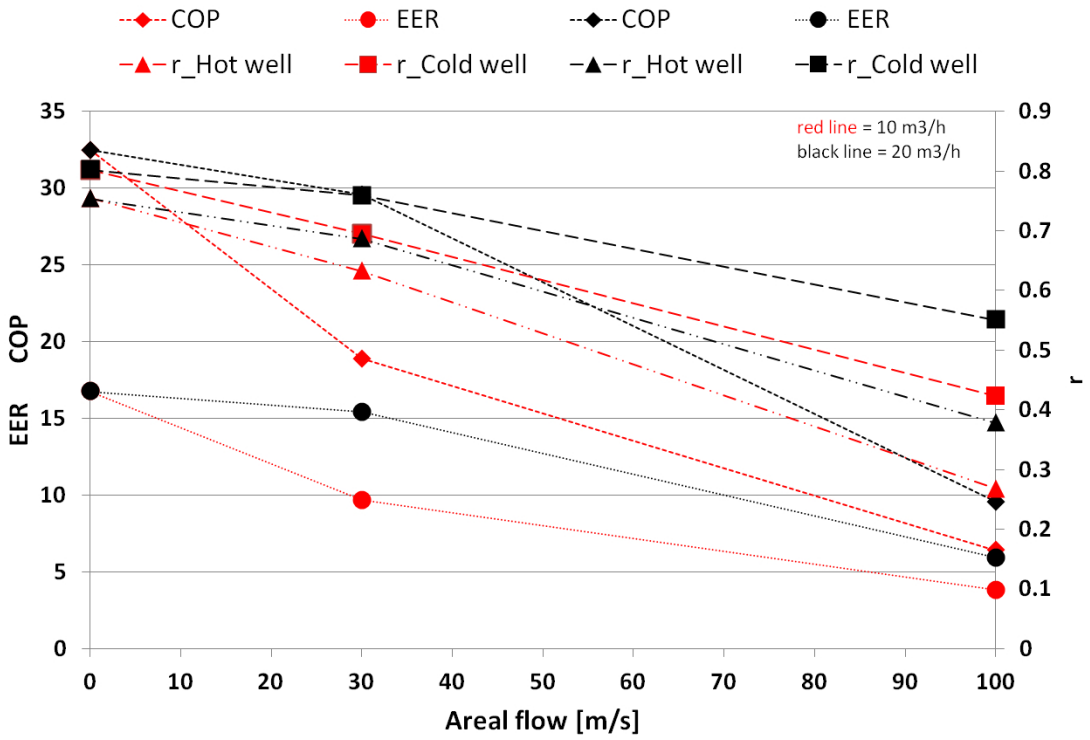

Figure 5.15: COP, EER and r versus areal flow changing, for 120m wells distance and two volume flow rate.

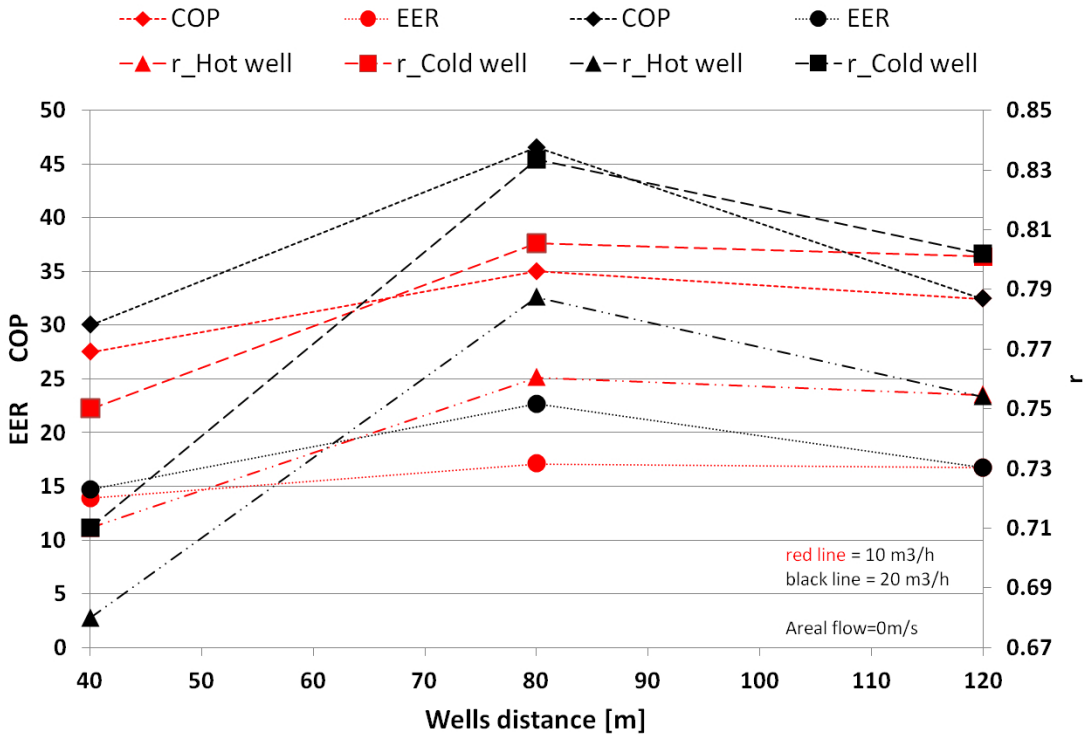

Figure 5.16: COP, EER and r versus distance well changing, for volume flow rate and 0m/s for areal flow.

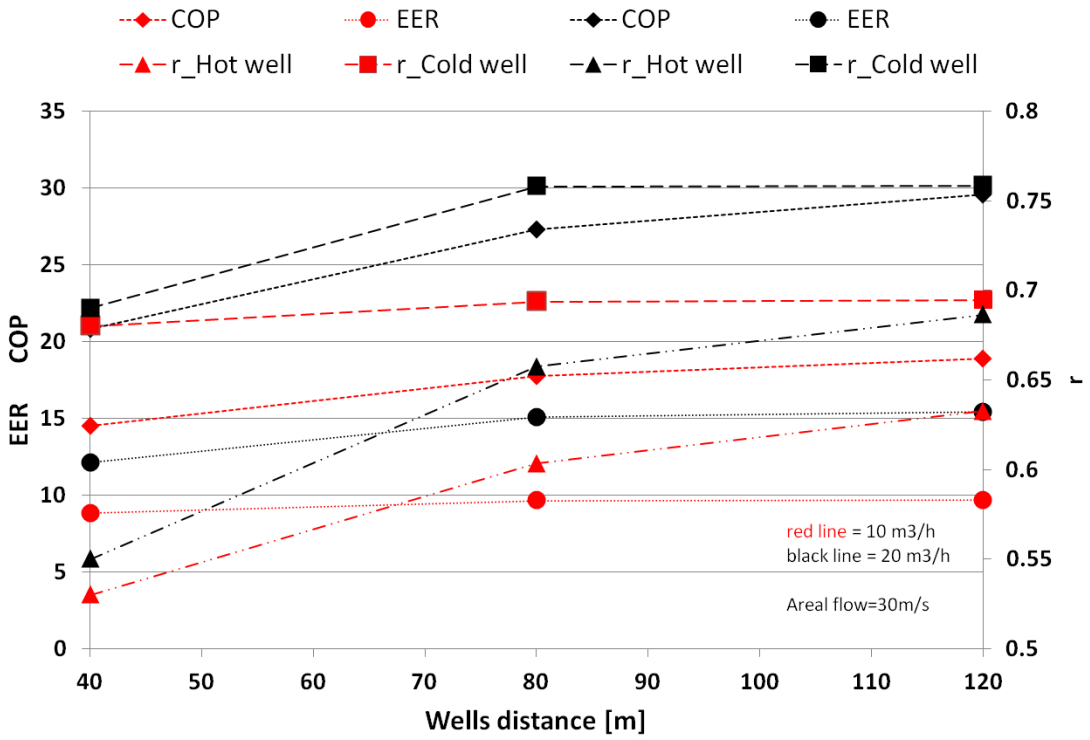

Figure 5.17: COP, EER and r versus distance well changing, for volume flow rate and 30m/s for areal flow.

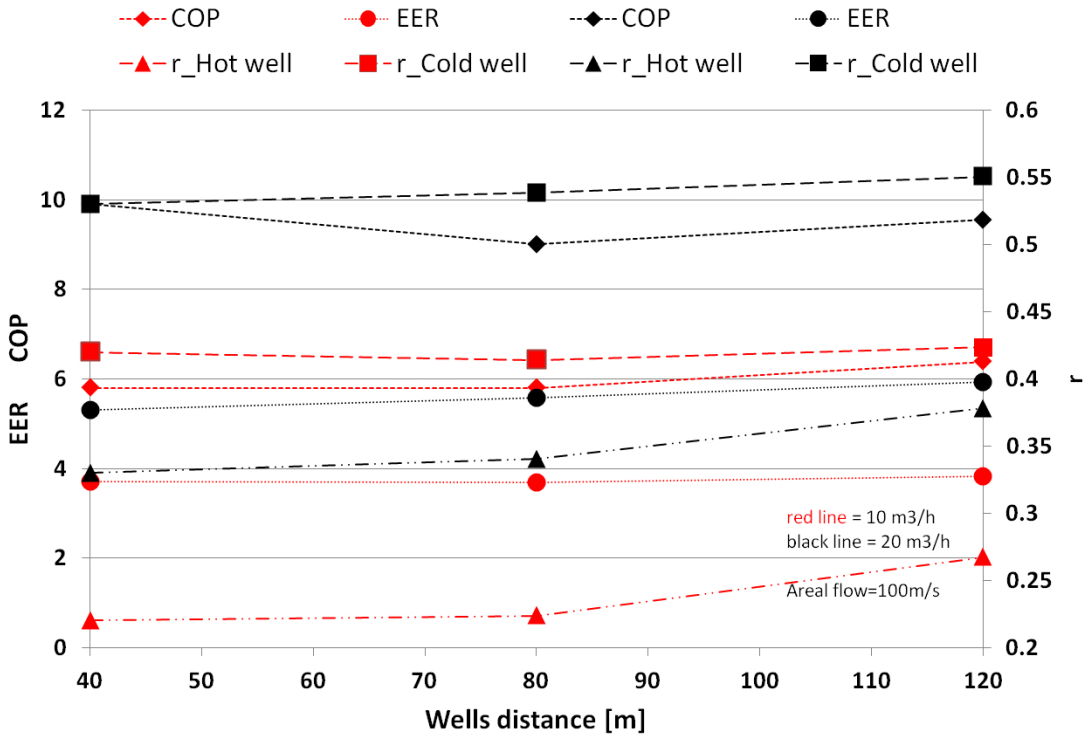

Figure 5.18: COP, EER and r versus distance well changing, for volume flow rate and 30m/s for areal flow.

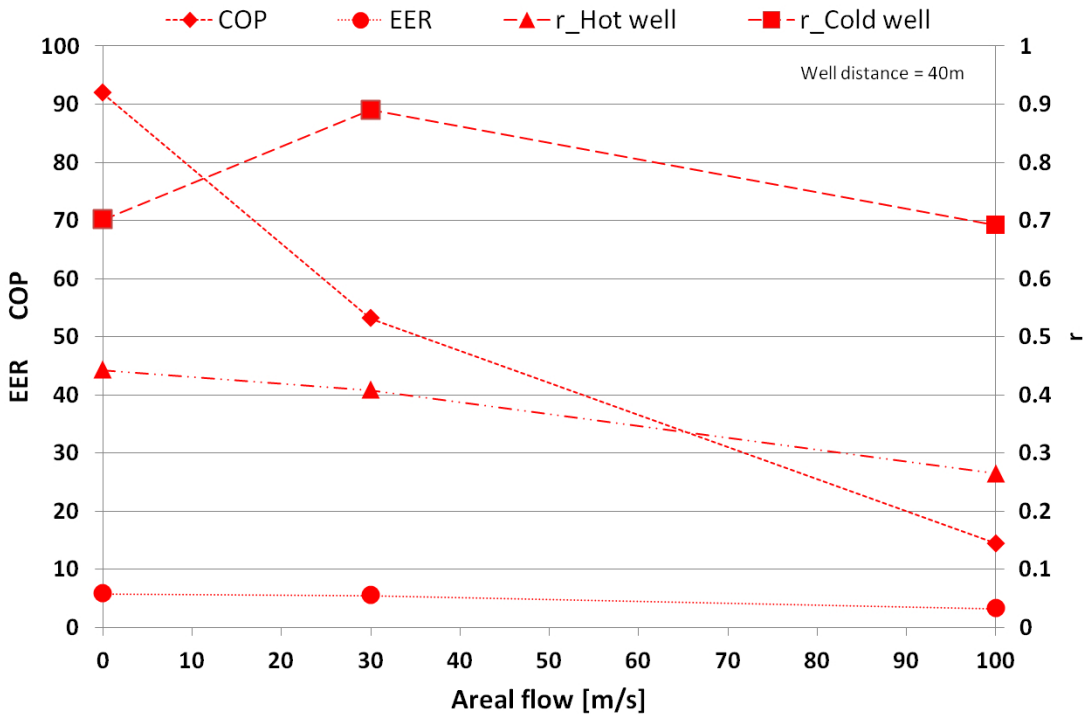

Figure 5.19: COP, EER and r versus areal flow changing, for 40m wells distance.

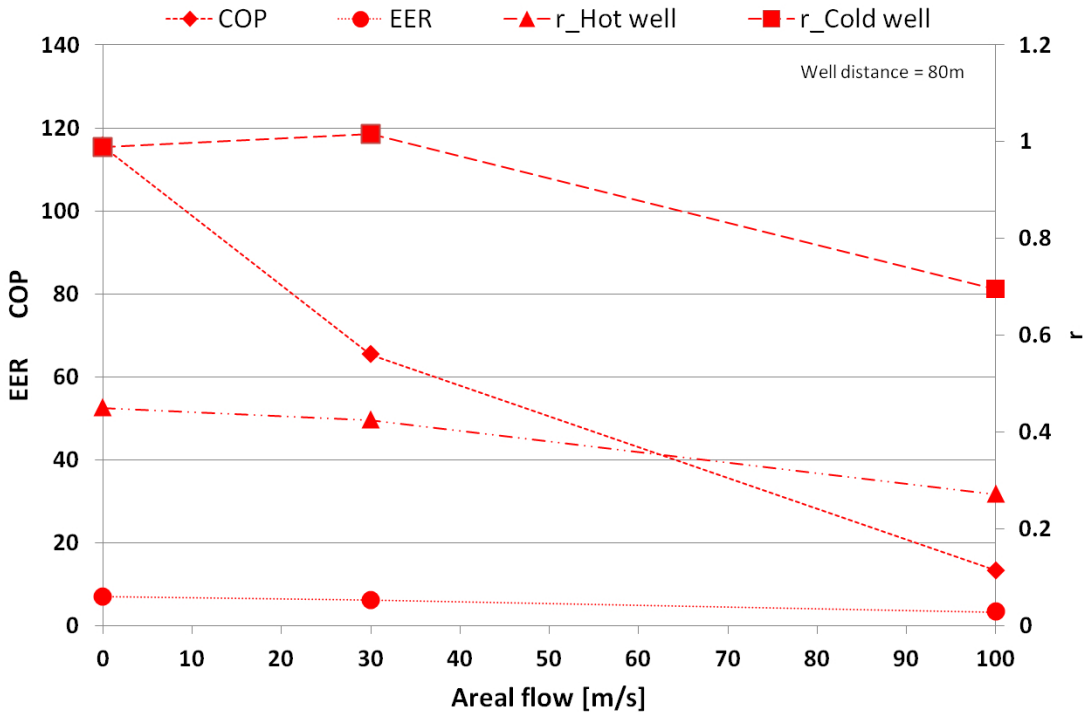

Figure 5.20: COP, EER and r versus areal flow changing, for 80m wells distance.

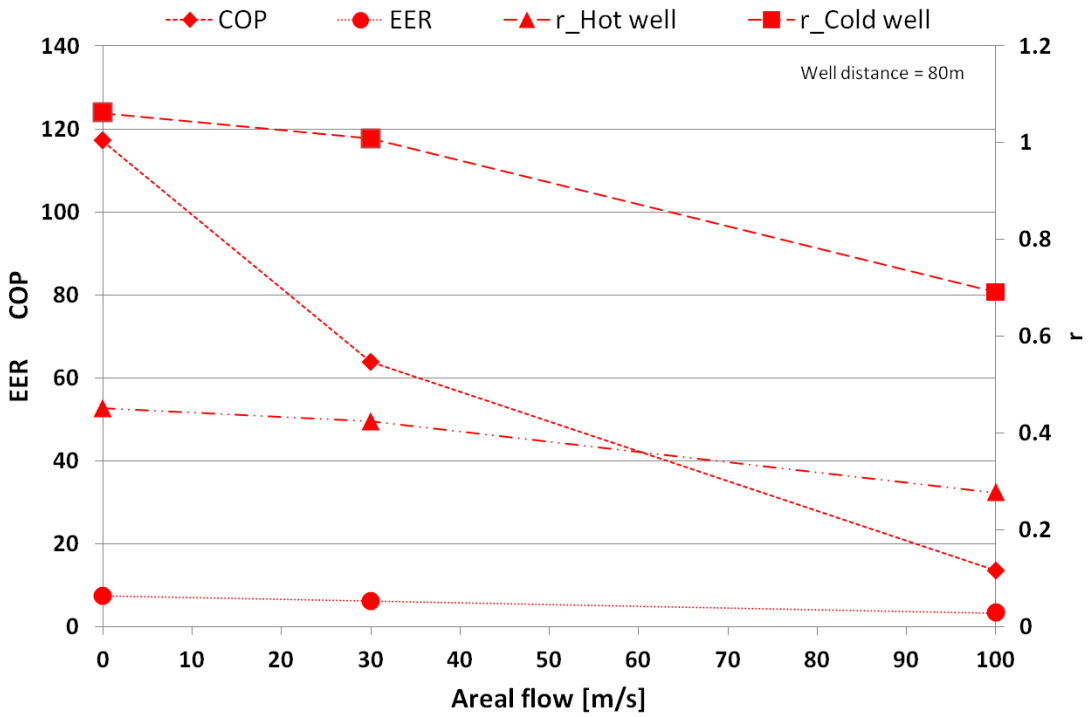

Figure 5.21: COP, EER and r versus areal flow changing, for 120m wells distance.

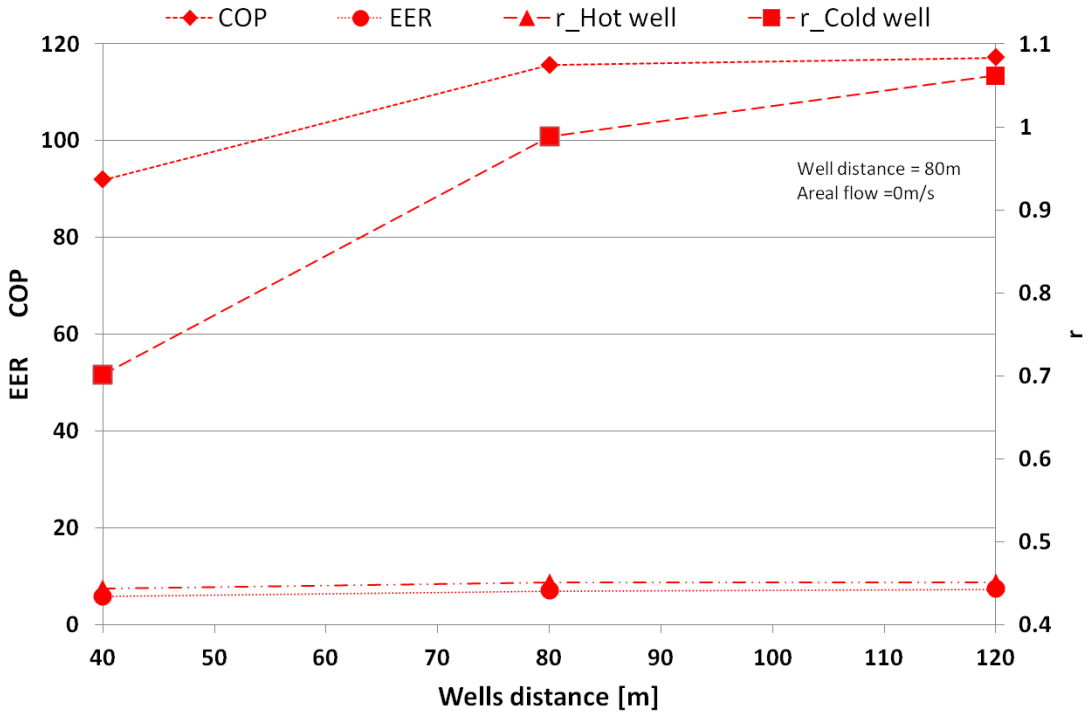

Figure 5.22: COP, EER and r versus distance well changing, for 0m/s for areal flow.

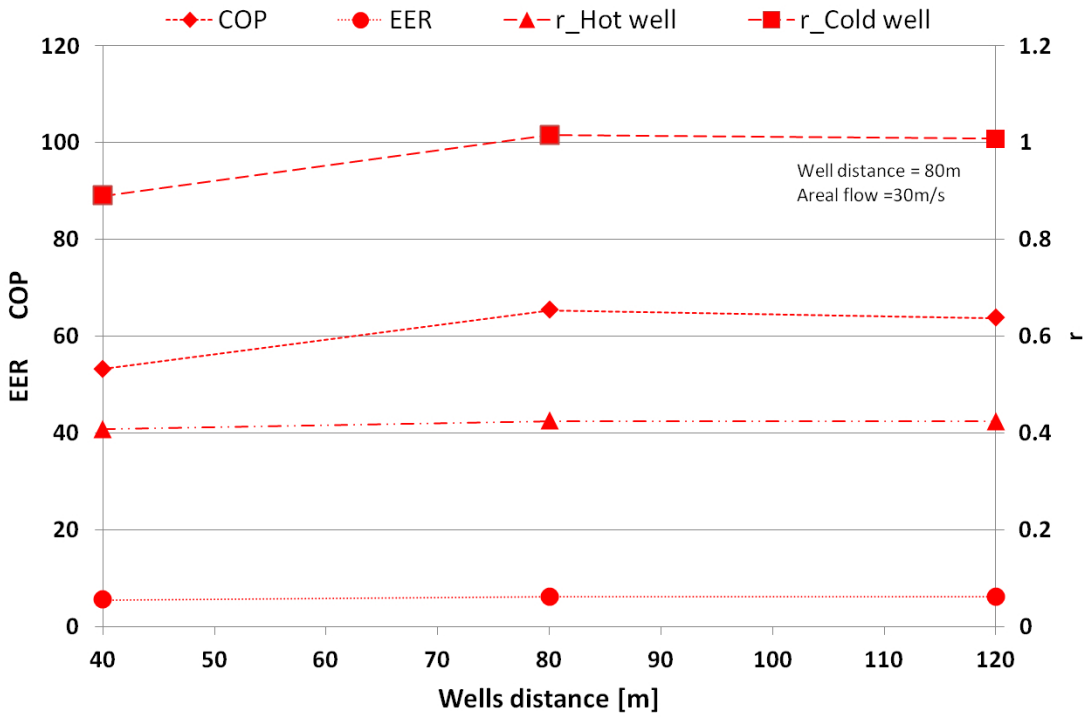

Figure 5.23: COP, EER and r versus distance well changing, for 30m/s for areal flow.

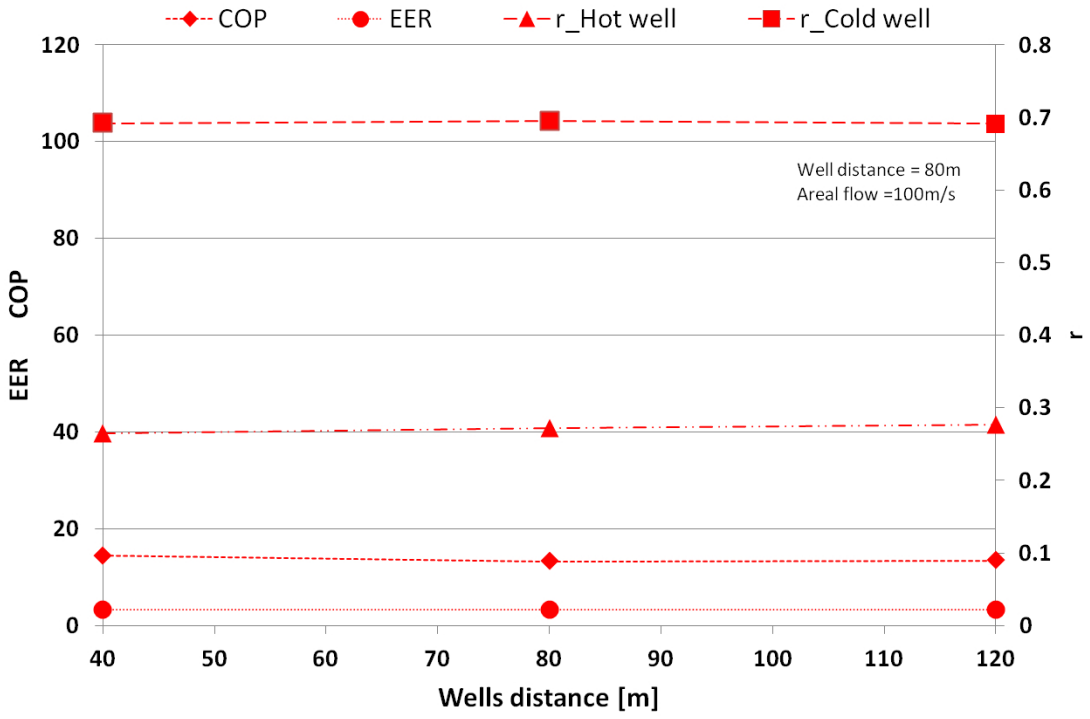

Figure 5.24: COP, EER and r versus distance well changing, for volume flow rate and 30m/s for areal flow.

5.2.11 Synthesis & Conclusions

Below there are some considerations divided in two part; the first part takes into account those graphics with fixed boreholes distance (figures 5.13, 5.14, 5.15)and the second part consider graphics with fixed areal flow value (figures 5.16,5.17,5.18). Note that the direction f areal flow is from cold side to hot side and this direction is parallel to the two boreholes connection line (see Figure5.12).

Symmetric cases

Fixed Distance
- Every coefficient is dropping with areal flow increasing.
- The Cold well is influenced by the areal flow direction (see 5.12), thus the cold coefficient decrease at lower rate than hot coefficients.
- While volume flow rate is increasing and all others conditions fixed, every coefficient is increasing.
- To note that until areal flow magnitude reaches 30m/s coefficients values reduction is not noticeable.

It is possible conclude, if the injected volume flow rate is increasing, less important is the incidence of areal flow.

Fixed Areal Flow
- For graph that include areal flow 0m/s results there is a strange phenomena. Increasing wells distance from 40m to 80m Coefficients value increase; but increasing from 80m to 120m coefficients value decrease. This phenomena is more significant for high value of volume flow rate. This reduction can be associated on the hydraulic gradient. From 40m to 80m wells distance cases, the coefficient increment is due on the major hydraulic head gradient(minor thermal contamination), instead from 80 to 120m wells distance cases, the decrement is caused by the decrement of the hydraulic gradient between two boreholes, which conduces a minor recovery potential of disperse energy.
- With high value of Areal flow the coefficients trend are quite constant, therefor there is an increment caused only by injected volume flow rate increasing.

Increasing Areal flow causes less influence on performance coefficients by the other two variable input parameter.[11]

In a general view increasing well distance and increasing injected water permit to reach great performances for an ATES system.

Asymmetric cases

Fixed Distance
- Increasing on Areal flow causes a parameters decrement.
- An exception can be find for 40 m wells distance; indeed there is an increasing of recovery factor from 0 m/s and 30 m/s of areal flow. This fact can be explained

[11] Obviously the condition of Areal flow direction ini this work is quite restricted. Areal flow direction can be decisive for the ATES system performances.

with the thermal influence caused by hot water. Indeed the cold well temperature, during a 0 m/s areal flow case and during a pumping period, exceeds natural aquifer temperature. Thus using the UTP equation (5.4), some pumped energies assume the value of stored energy. This phenomenon is interrupted when areal flow reaches 30 m/s, but using an areal flow of 100m/s thermal contamination induces a new performance coefficient value decrease.

- Hot parameters reduce more than cold because of the intensive exploitation of hot well than cold well.

So in general, with some exceptions, the increasing of areal flow reduce ATES performance also in Asymmetric cases. In Asymmetric cases COP and EER values are not so important as in Symmetric cases. Reaching a symmetric situation can be used as alternative solution to solve performances devaluation of Asymmetrical cases.

Fixed Areal Flow With well distance there are two parameters behaviour, indeed their values increase or keep constant.

5.3 Analytical Solution in A.T.E.S application

As said in Abstract, in this section of the chapter, the use of analytical solution in A.T.E.S application is treated. The aim of this paragraph is to compare analytical solutions, that are built for continuous flow regime, with ATES solutions obtained by numerical models above illustrated, that are operated with cyclic flow regime. To do that a new concept is introduced: the concept of effective mass flow rate. With a cyclic flow an amount of energy remains into Aquifer (ΔE eq.). It is assumed to have an *Effective mass flow rate* that injects in the aquifer the same amount of energy, ΔE. This energy is injected in the aquifer using continuous flow rate, the Effective mass flow rate, with a temperature that is the same of injection temperature in the numerical simulation used. Below are the equations of *Effective mass flow rate*:

- ΔE

$$\Delta E = (1 - r) \cdot E_i \tag{5.9}$$

- *Effective mass flow rate*

$$m_{eff} = \frac{\Delta E}{\tau \cdot c_w \cdot (T_i - 15)} \tag{5.10}$$

where:

E_i is injection Energy $E_i = m_i \cdot c_w \cdot \tau_i \cdot (T_i - 15)$.

τ is total period of simulation 20years.

τ_i is total period of injection 3 months per 20 years.

r is recovery factor, given by the postprocessing analysis of numerical simulations.

5.3.1 Simulation results

Analytical solutions are already presented in chapter 3. Thus it is clear that the comparison between analytical and numerical solutions concerns a spatial thermal distribution, that is temperature versus distance from well. The numerical solutions temperature profile is chosen to present the maximum extension of thermal bubble all around each well. To do that the temperature distribution is chosen along a line that starts in the middle of the well and parallel to the horizontal surfaces. There are two lines to present two different directions, one to the second boreholes and the other one to opposite direction (obviously the main direction concern the opposite direction). This comparison concern several operational conditions:

- only cases without areal flow are taken into account[12];
- in the Symmetrical cases the comparison concerns only hot well, because of the symmetry of the situation;

[12]Because of the difficulties to use areal flow with analytical solution. To note in literature there are some articles approaching areal flow with analytical solutions.(inserire riferimenti articoli).

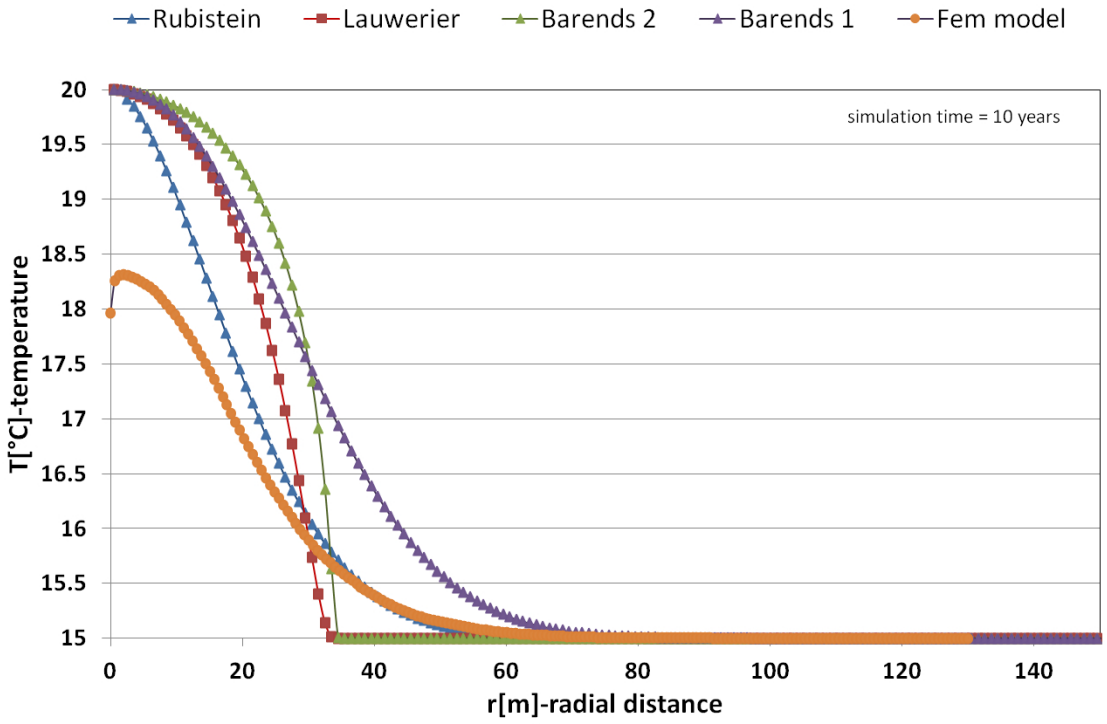

Figure 5.25: Temperature trend vs radial distance from injection hot well. Case: 40 m well distance, 10 m^3/h volume flow rate, simulation time 10 years.

- in the Asymmetrical cases the comparison concerns hot and cold wells with a specific below explanation;
- for every simulation analyzed there are three graphics, every graph is presented for different simulation time; in particular respectively for 10,15,20 years of operation;
- r recovery factor is taken directly from the numerical simulations results.

Below all results are presented, firstly for Symmetric cases and than for Asymmetric case. Every graph refers to the opposite direction. Note: for Asymmetrical case also cold well situation is presented, instead in the symmetrical case the situation is symmetric.

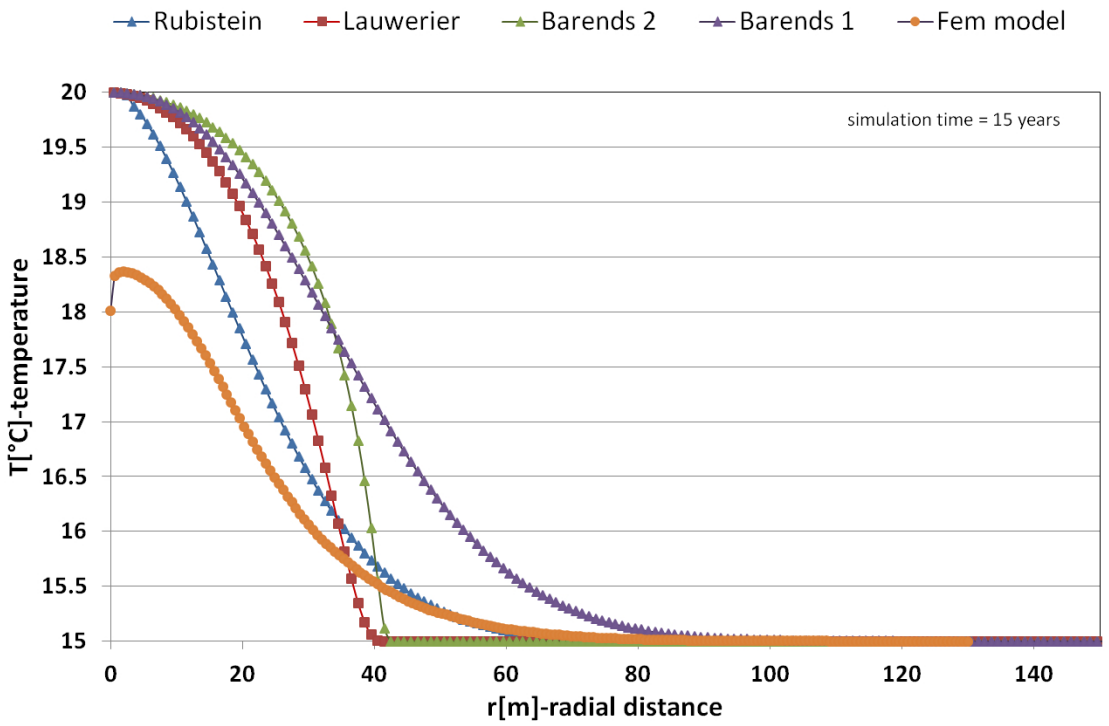

Figure 5.26: Temperature trend vs radial distance from injection hot well. Case: 40 m well distance, 10 m^3/h volume flow rate, simulation time 15 years.

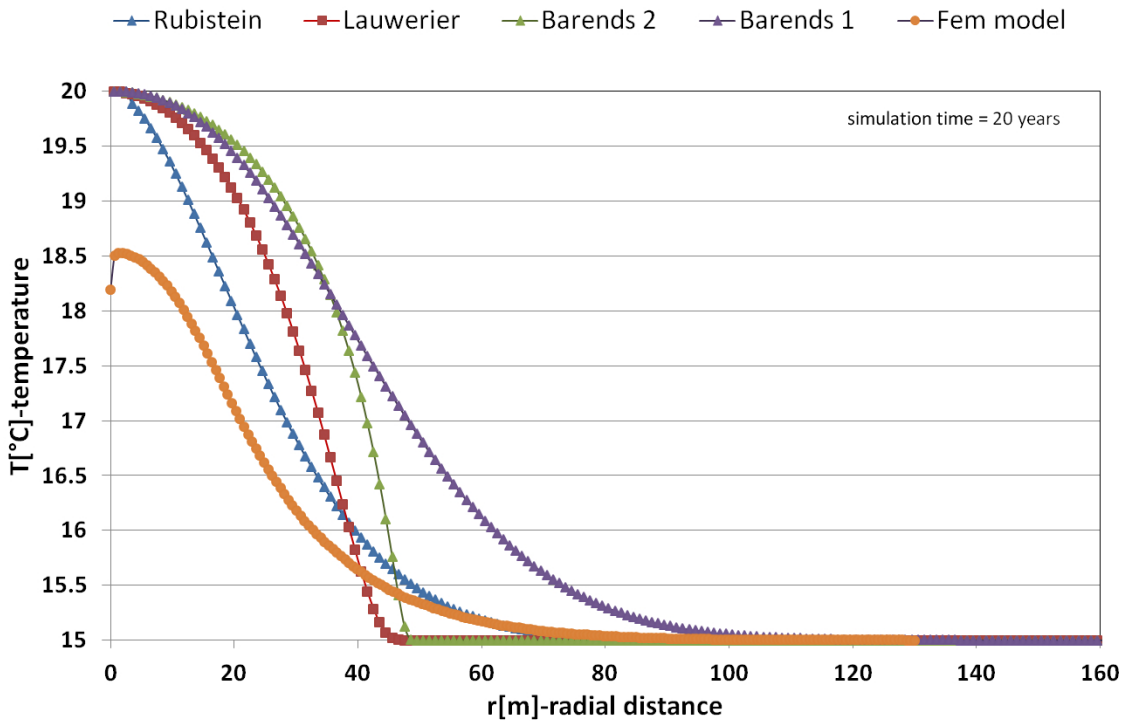

Figure 5.27: Temperature trend vs radial distance from injection hot well. Case: 40 m well distance, 10 m^3/h volume flow rate, simulation time 20 years.

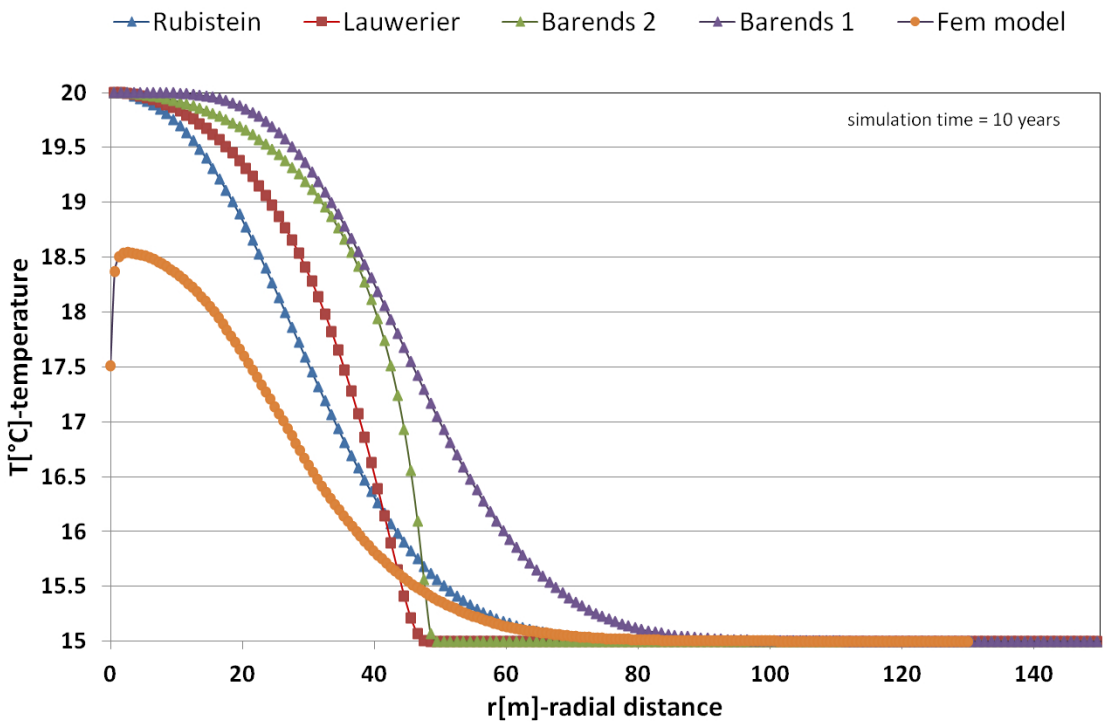

Figure 5.28: Temperature trend vs radial distance from injection hot well. Case: 40 m well distance, 20 m^3/h volume flow rate, simulation time 10 years.

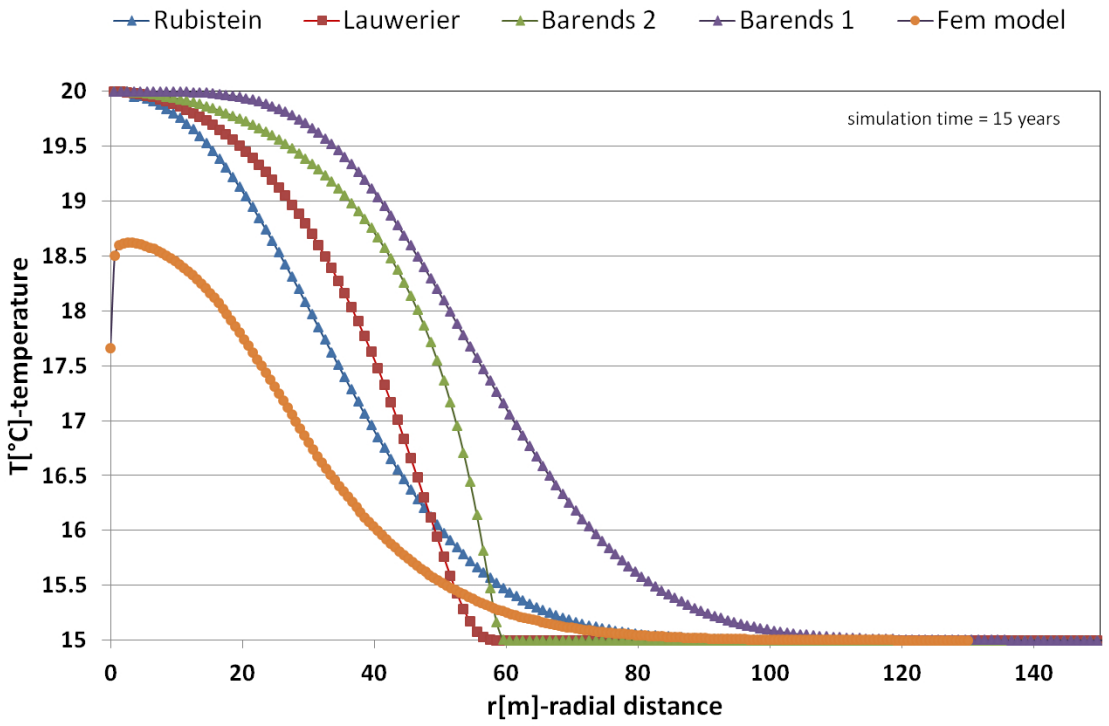

Figure 5.29: Temperature trend vs radial distance from injection hot well. Case: 40 m well distance, 20 m^3/h volume flow rate, simulation time 15 years.

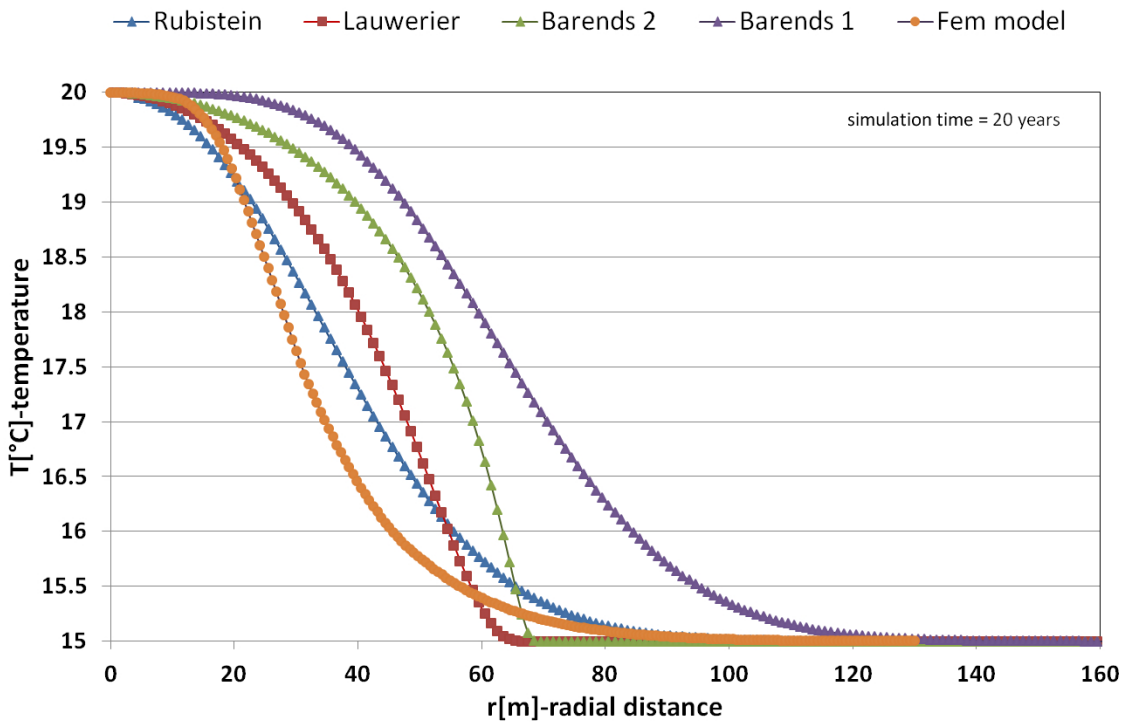

Figure 5.30: Temperature trend vs radial distance from injection hot well. Case: 40 m well distance, 20 m^3/h volume flow rate, simulation time 20 years.

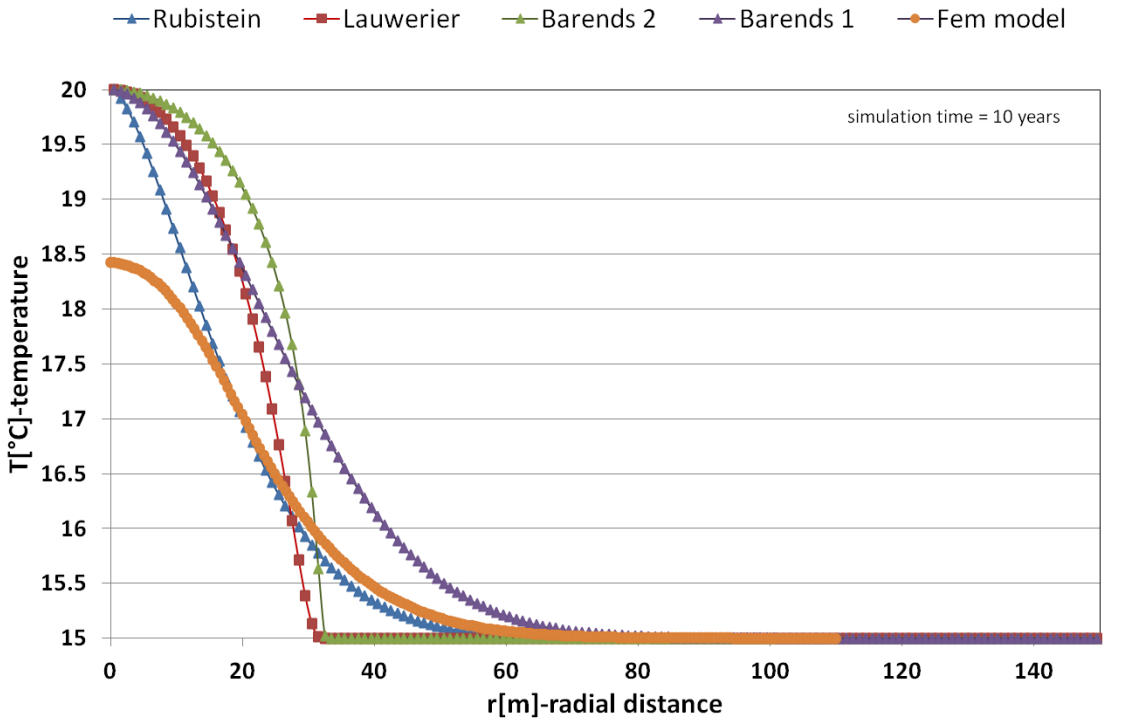

Figure 5.31: Temperature trend vs radial distance from injection hot well. Case: 80 m well distance, 10 m^3/h volume flow rate, simulation time 10 years.

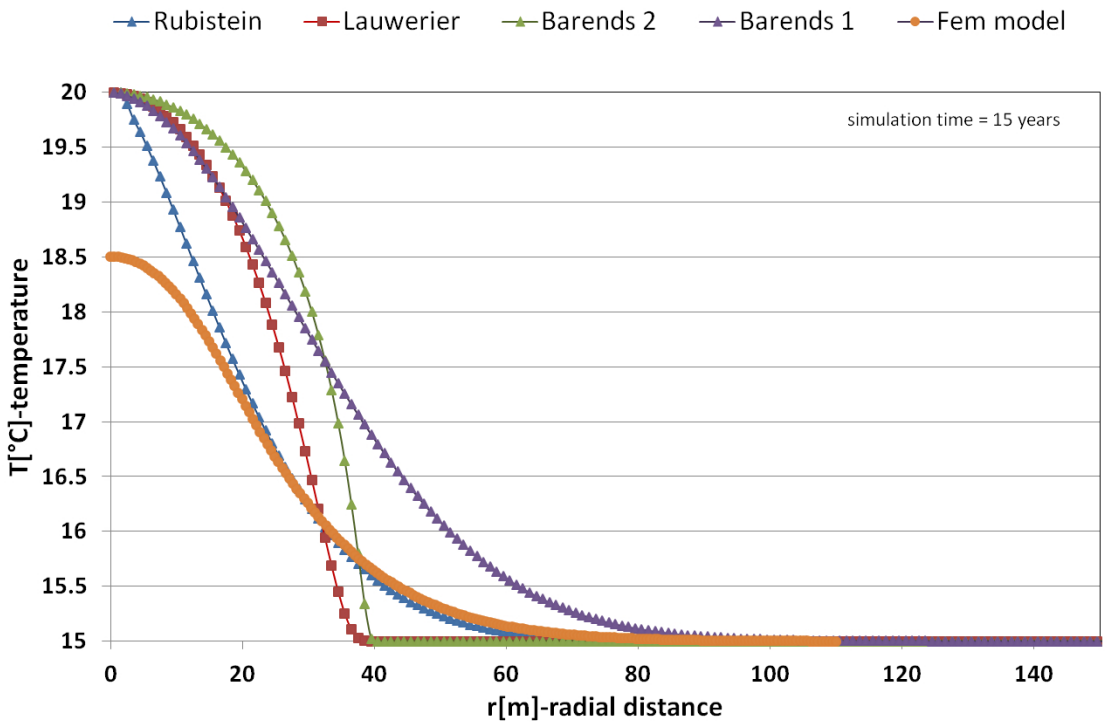

Figure 5.32: Temperature trend vs radial distance from injection hot well. Case: 80 m well distance, 10 m^3/h volume flow rate, simulation time 15 years.

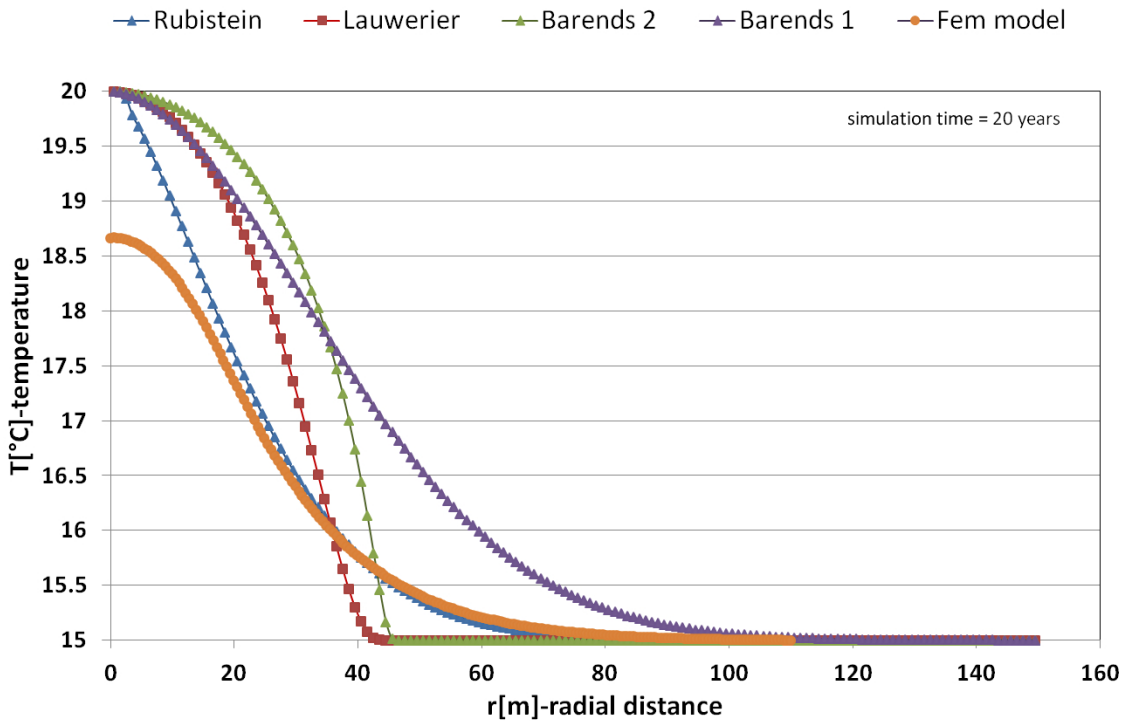

Figure 5.33: Temperature trend vs radial distance from injection hot well. Case: 80 m well distance, 10 m^3/h volume flow rate, simulation time 20 years.

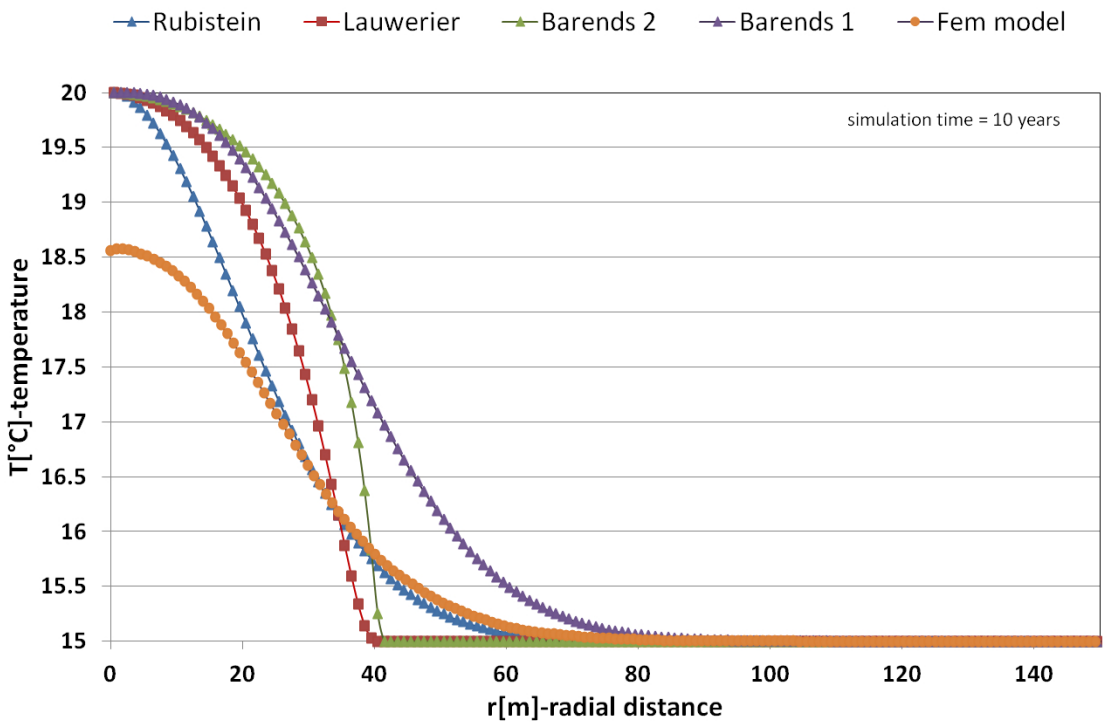

Figure 5.34: Temperature trend vs radial distance from injection hot well. Case: 80 m well distance, 20 m^3/h volume flow rate, simulation time 10 years.

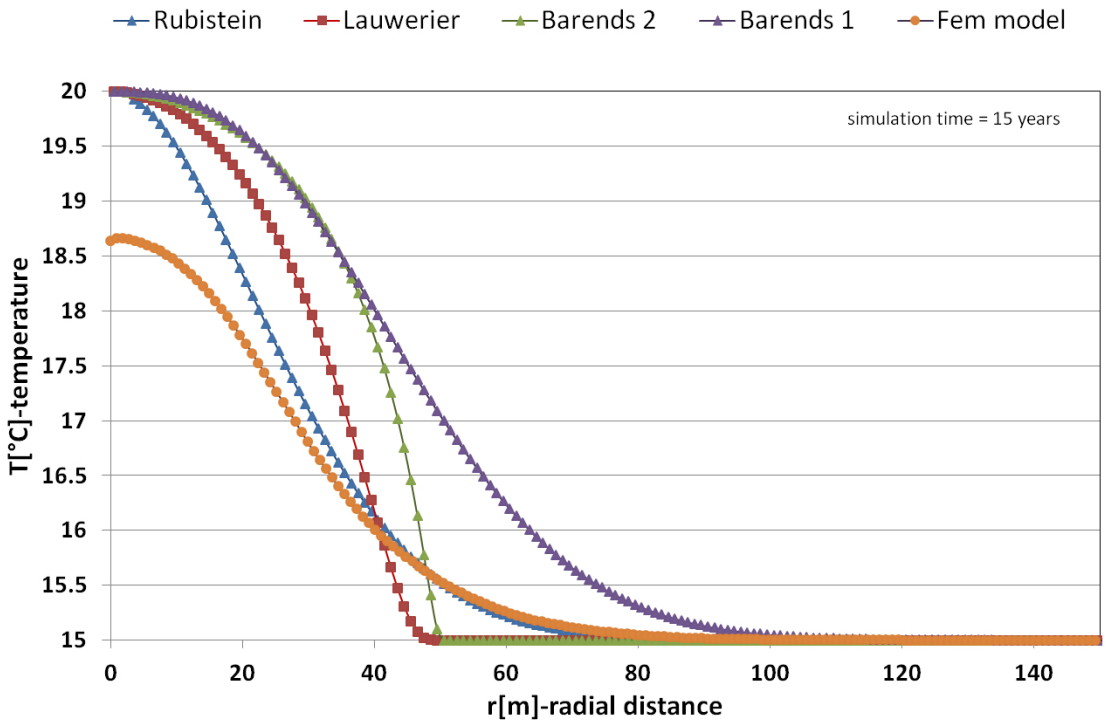

Figure 5.35: Temperature trend vs radial distance from injection hot well. Case: 80 m well distance, 20 m^3/h volume flow rate, simulation time 15 years.

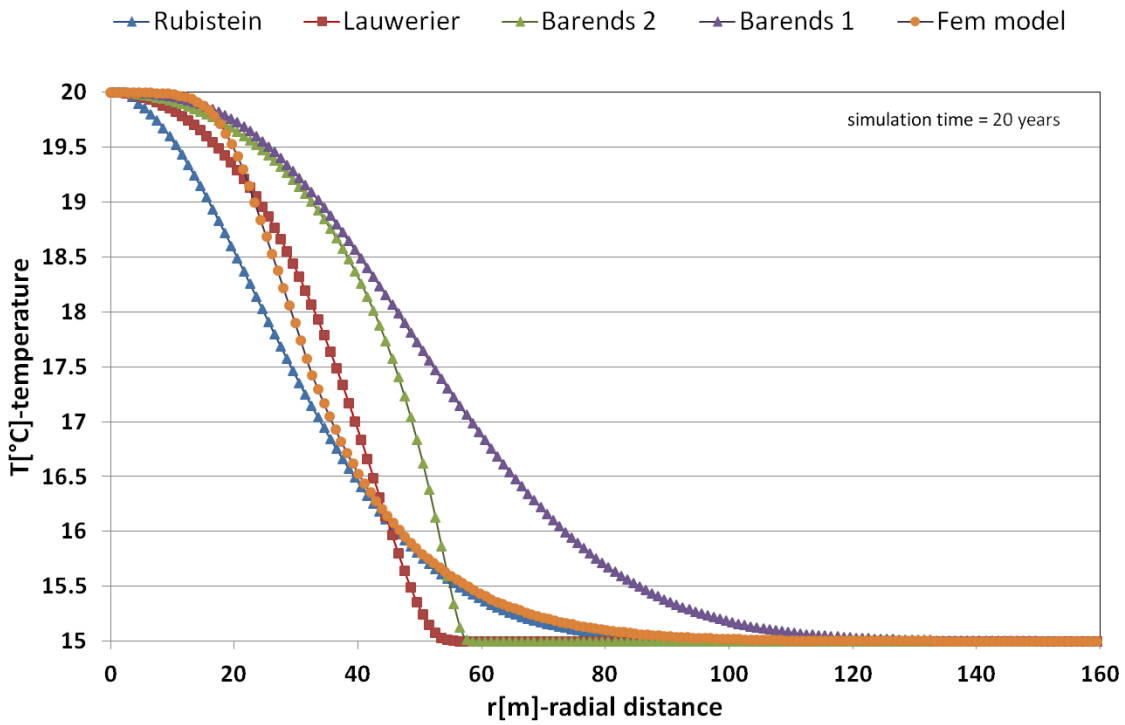

Figure 5.36: Temperature trend vs radial distance from injection hot well. Case: 80 m well distance, 20 m^3/h volume flow rate, simulation time 20 years.

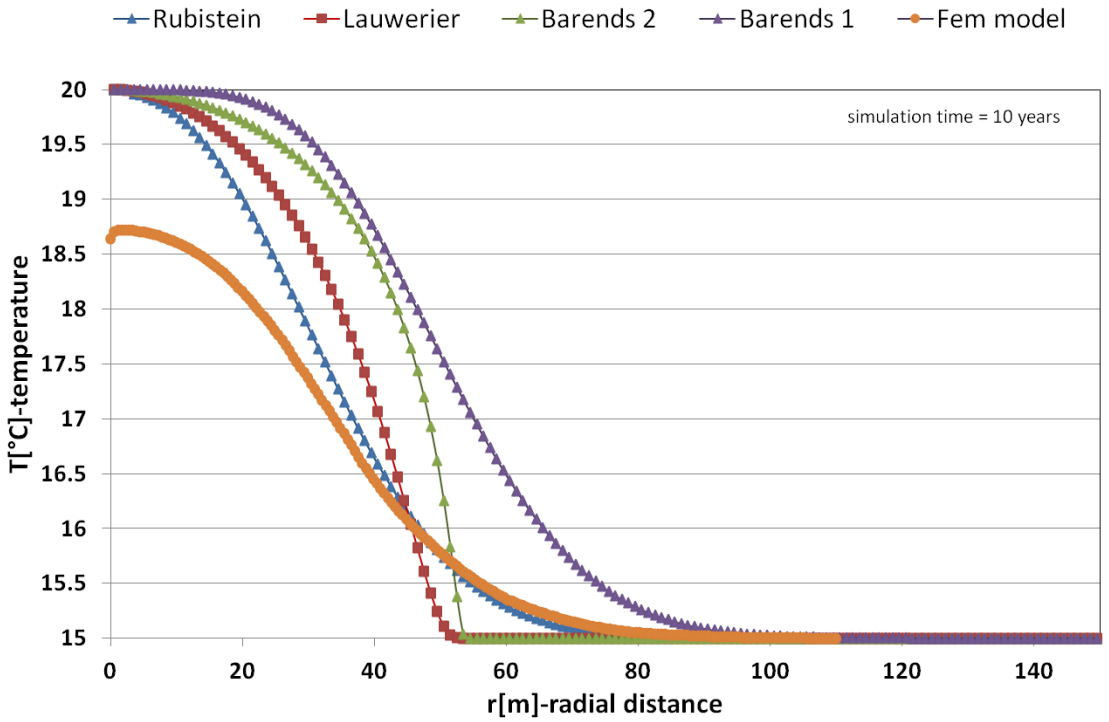

Figure 5.37: Temperature trend vs radial distance from injection hot well. Case: 80 m well distance, 40 m^3/h volume flow rate, simulation time 10 years.

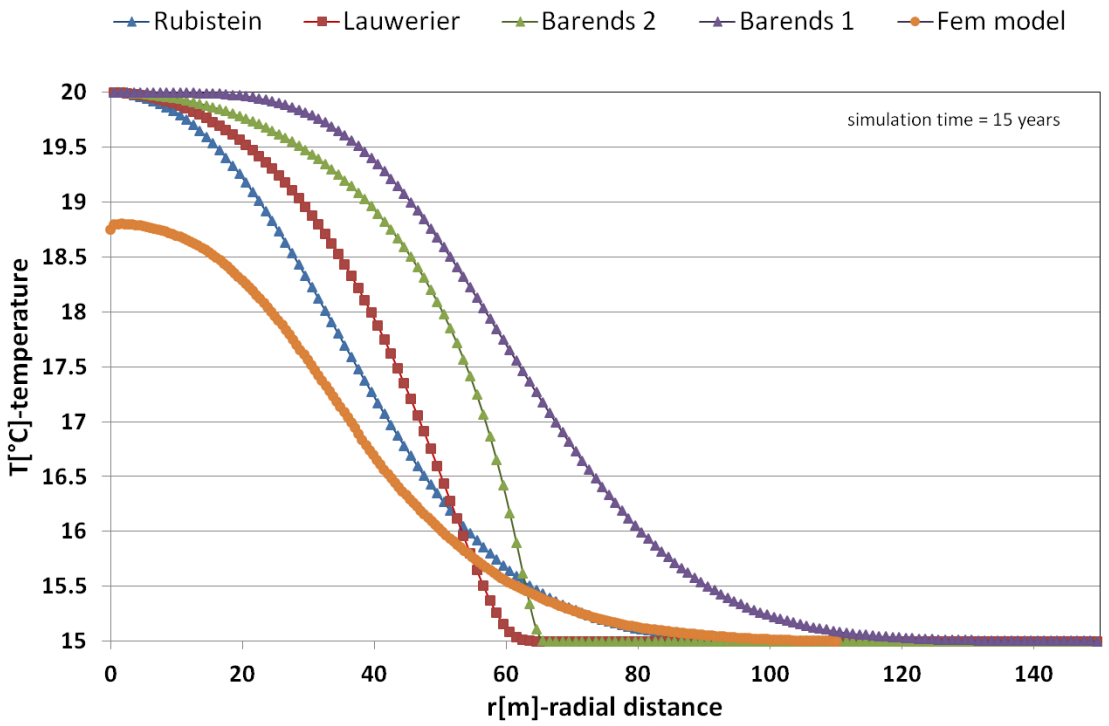

Figure 5.38: Temperature trend vs radial distance from injection hot well. Case: 80 m well distance, 40 m^3/h volume flow rate, simulation time 15 years.

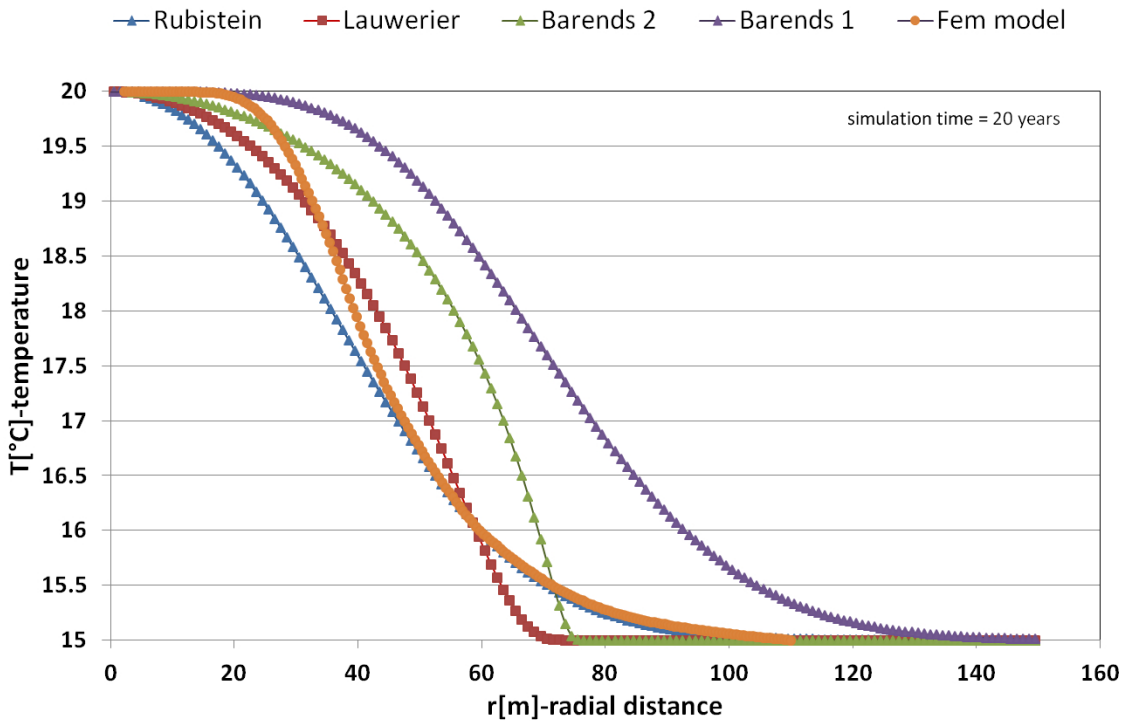

Figure 5.39: Temperature trend vs radial distance from injection hot well. Case: 80 m well distance, 40 m^3/h volume flow rate, simulation time 20 years.

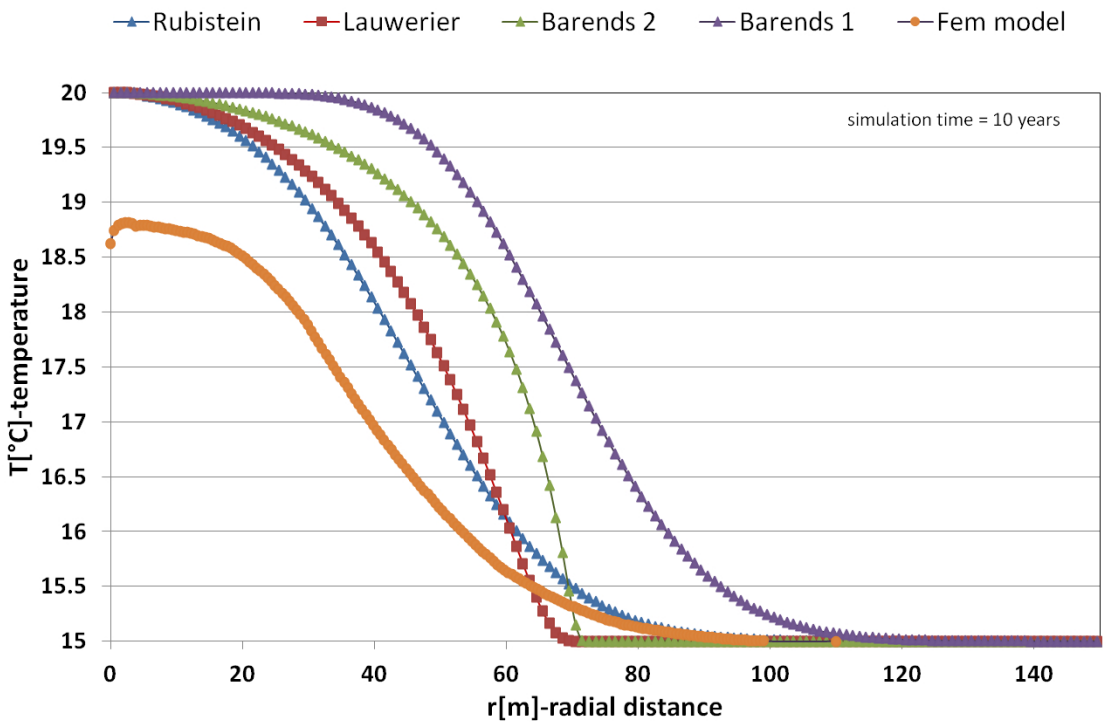

Figure 5.40: Temperature trend vs radial distance from injection hot well. Case: 80 m well distance, 60 m^3/h volume flow rate, simulation time 10 years.

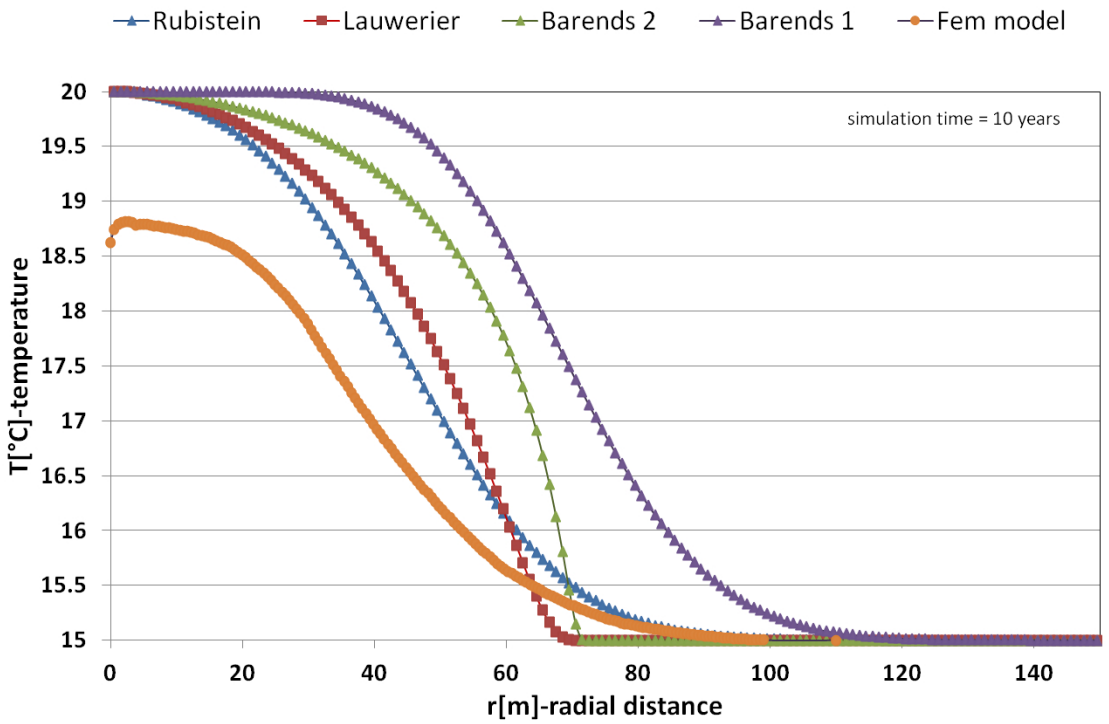

Figure 5.41: Temperature trend vs radial distance from injection hot well. Case: 80 m well distance, 60 m^3/h volume flow rate, simulation time 15 years.

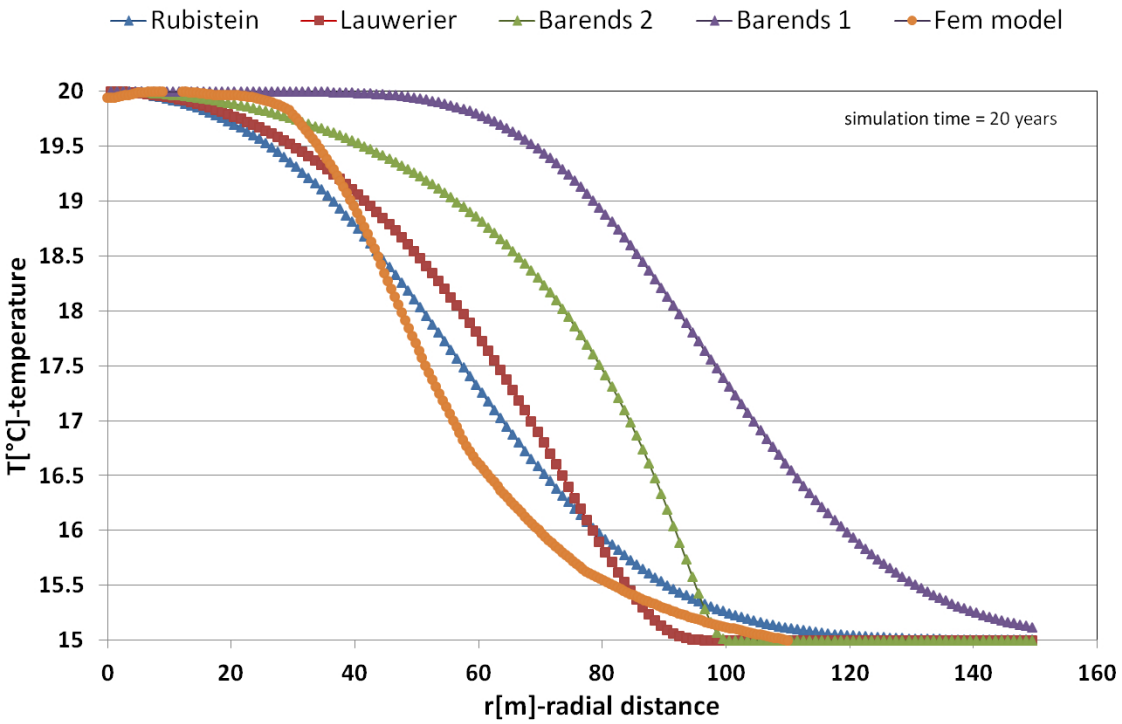

Figure 5.42: Temperature trend vs radial distance from injection hot well. Case: 80 m well distance, 60 m^3/h volume flow rate, simulation time 20 years.

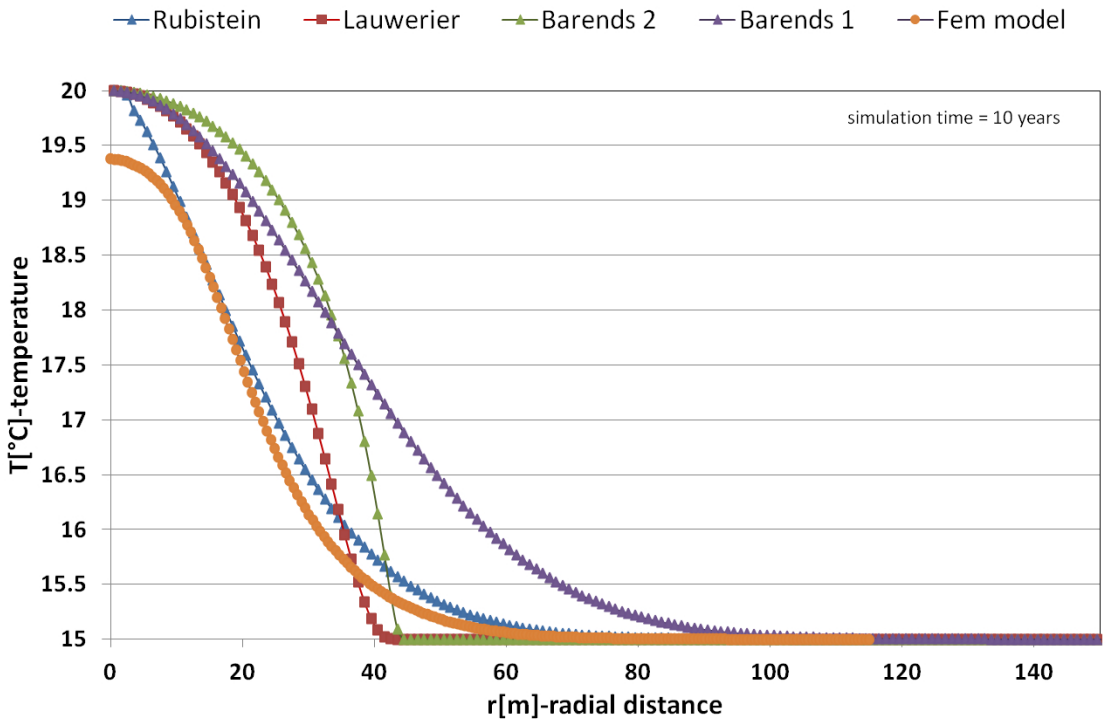

Figure 5.43: Temperature trend vs radial distance from injection hot well. Case: 120 m well distance, 10 m^3/h volume flow rate, simulation time 10 years.

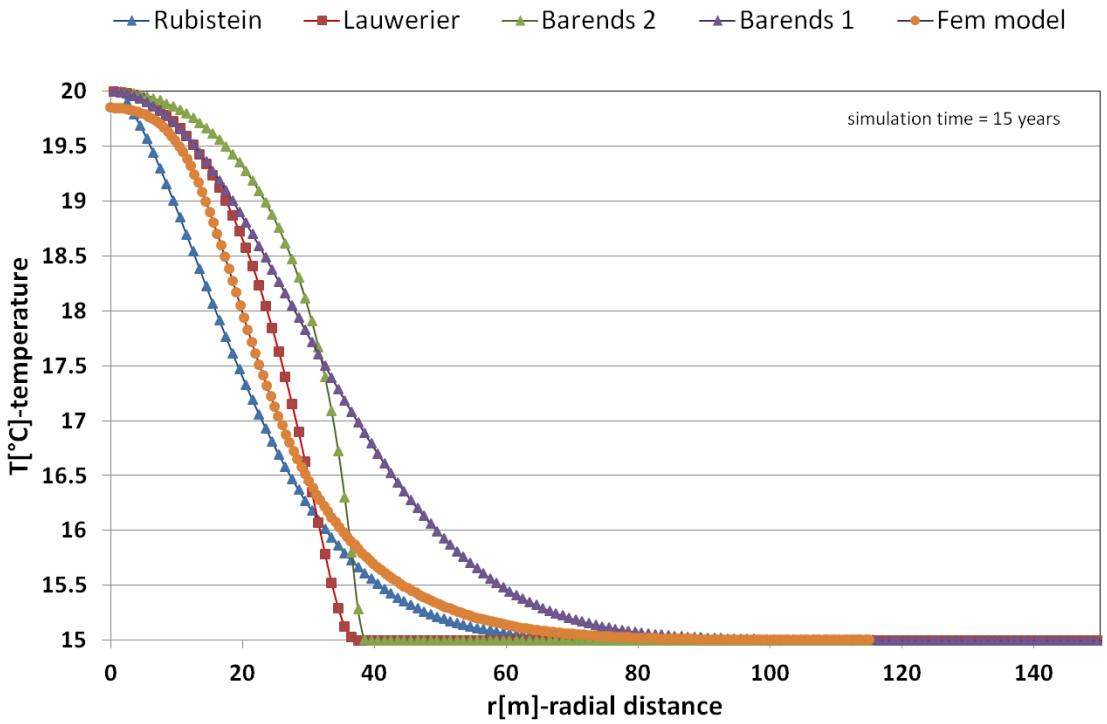

Figure 5.44: Temperature trend vs radial distance from injection hot well. Case: 120 m well distance, 10 m^3/h volume flow rate, simulation time 15 years.

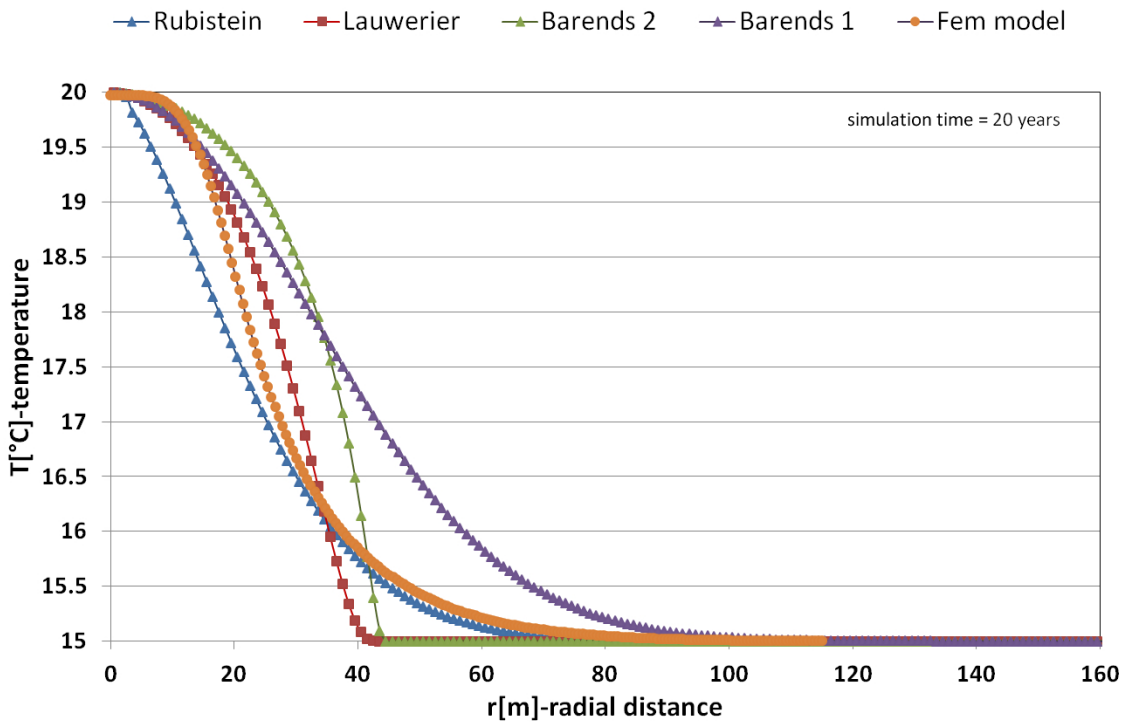

Figure 5.45: Temperature trend vs radial distance from injection hot well. Case: 120 m well distance, 10 m^3/h volume flow rate, simulation time 20 years.

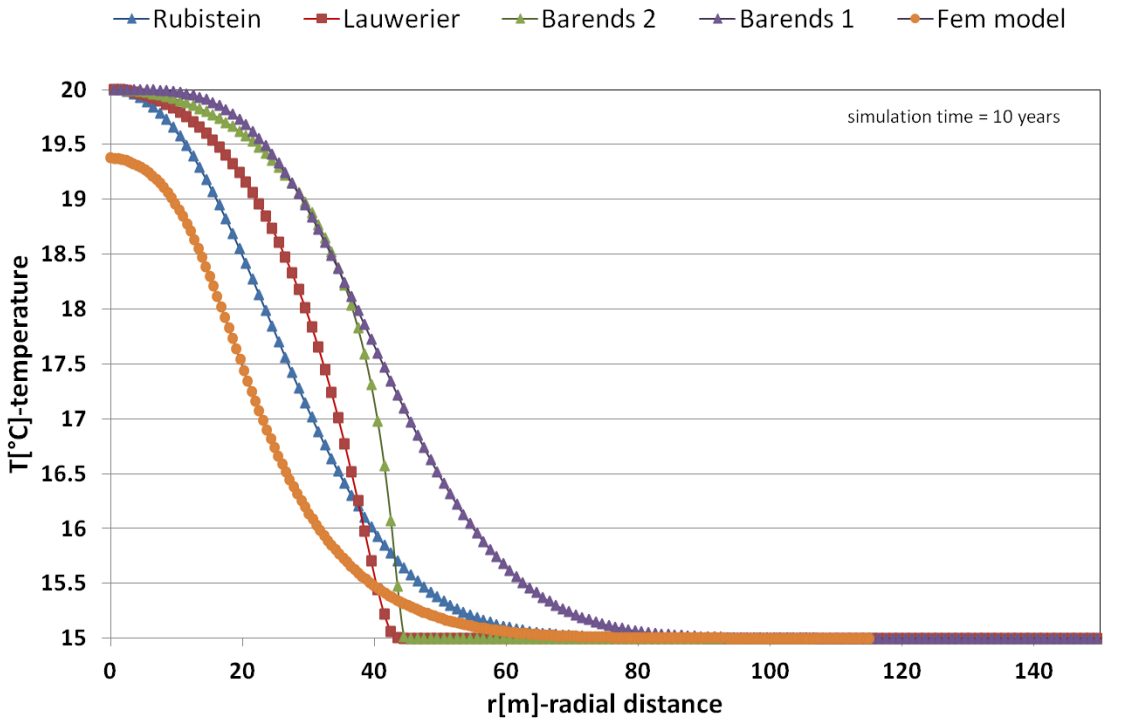

Figure 5.46: Temperature trend vs radial distance from injection hot well. Case: 120 m well distance, 20 m^3/h volume flow rate, simulation time 10 years.

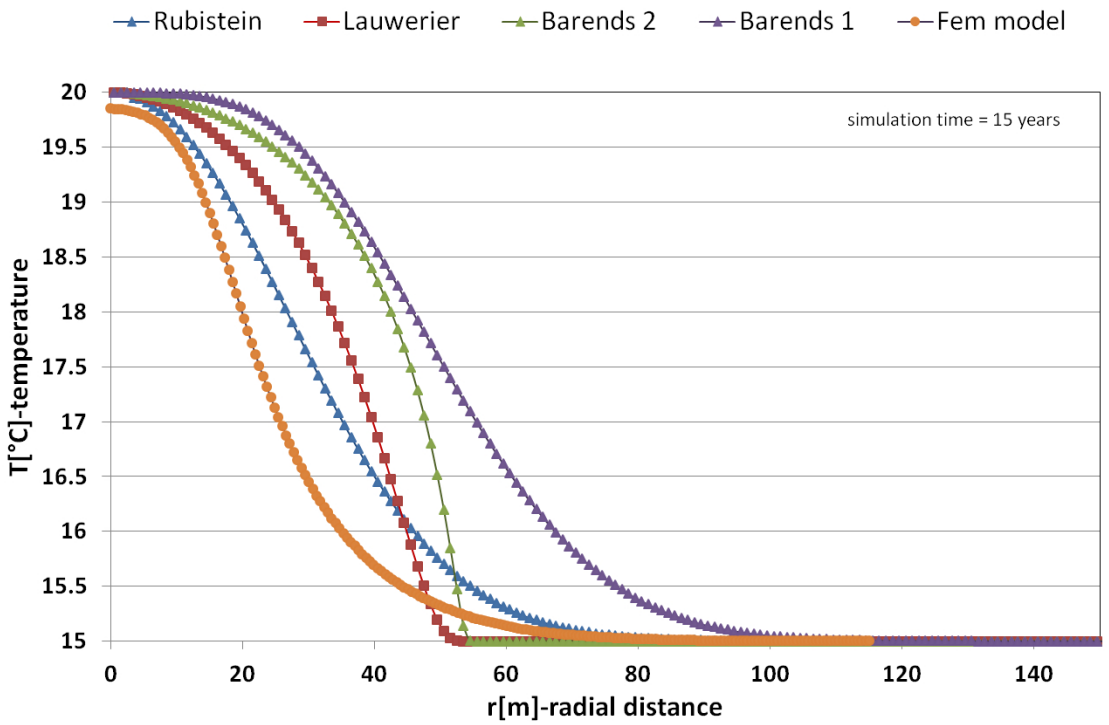

Figure 5.47: Temperature trend vs radial distance from injection hot well. Case: 120 m well distance, 20 m^3/h volume flow rate, simulation time 15 years.

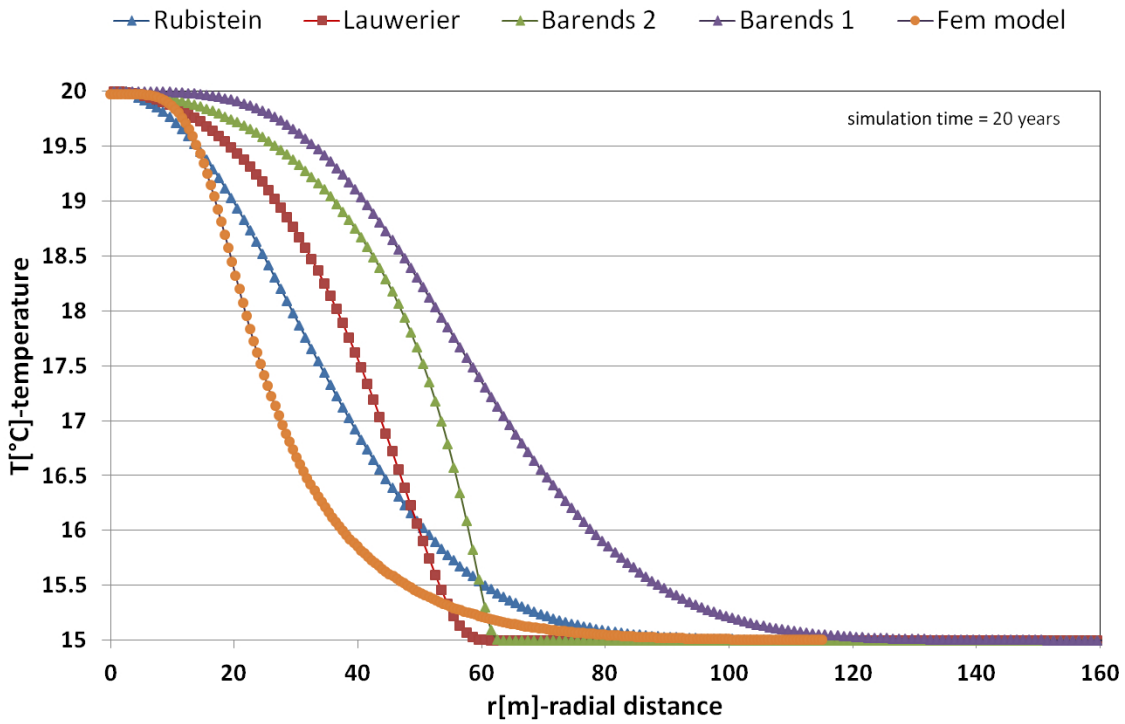

Figure 5.48: Temperature trend vs radial distance from injection hot well. Case: 120 m well distance, 20 m^3/h volume flow rate, simulation time 20 years.

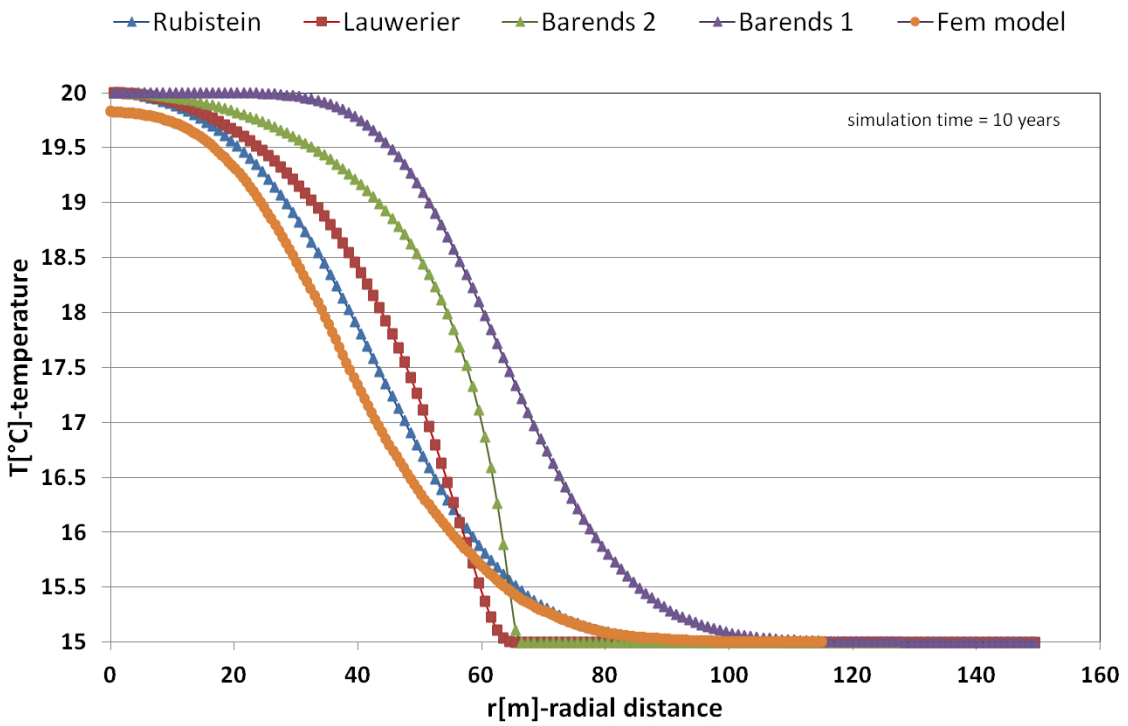

Figure 5.49: Temperature trend vs radial distance from injection hot well. Case: 120 m well distance,simulation time 10 years.

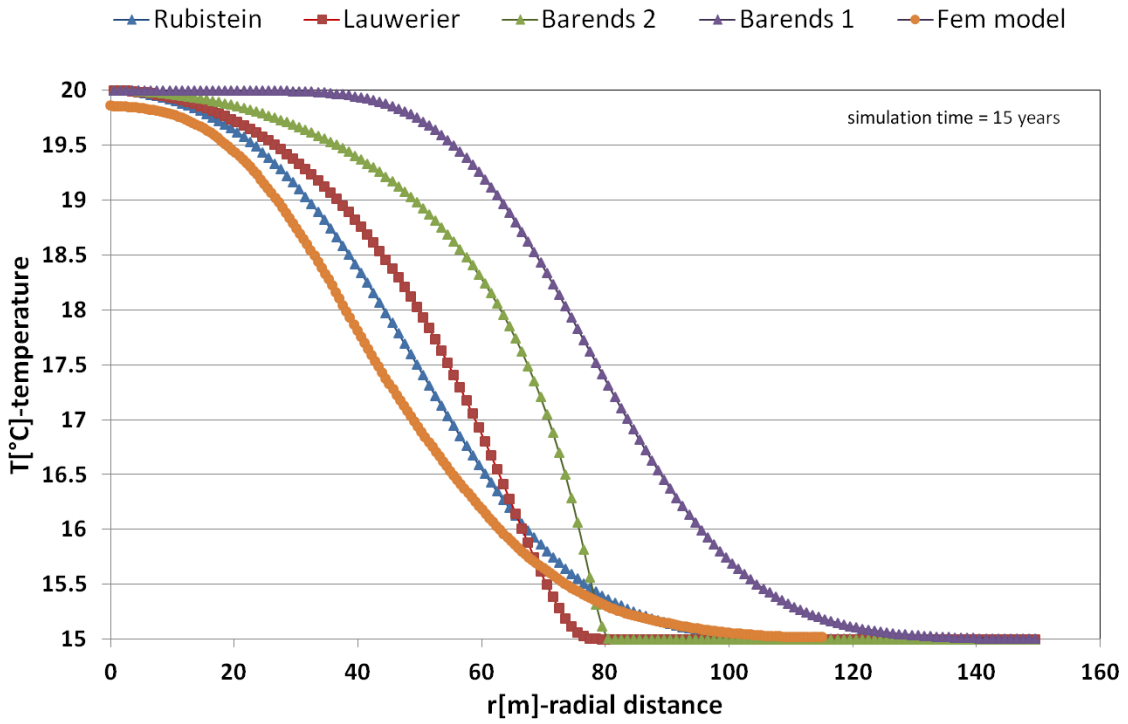

Figure 5.50: Temperature trend vs radial distance from injection hot well. Case: 120 m well distance, simulation time 15 years.

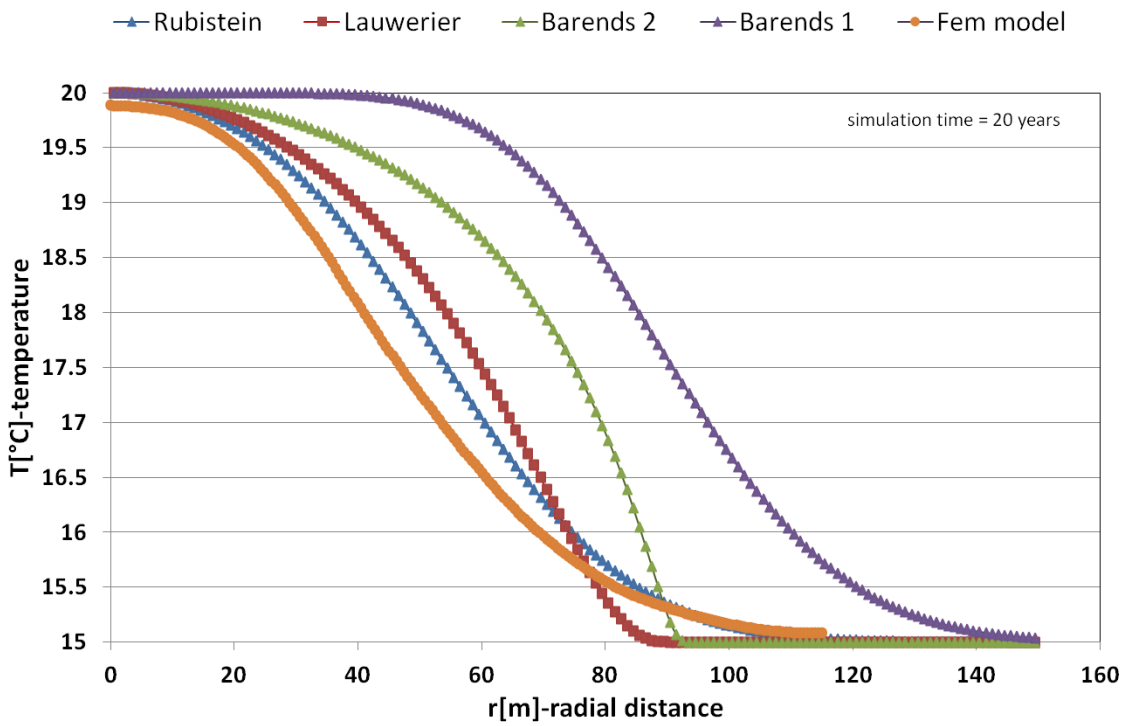

Figure 5.51: Temperature trend vs radial distance from injection hot well. Case: 120 m well distance, simulation time 20 years.

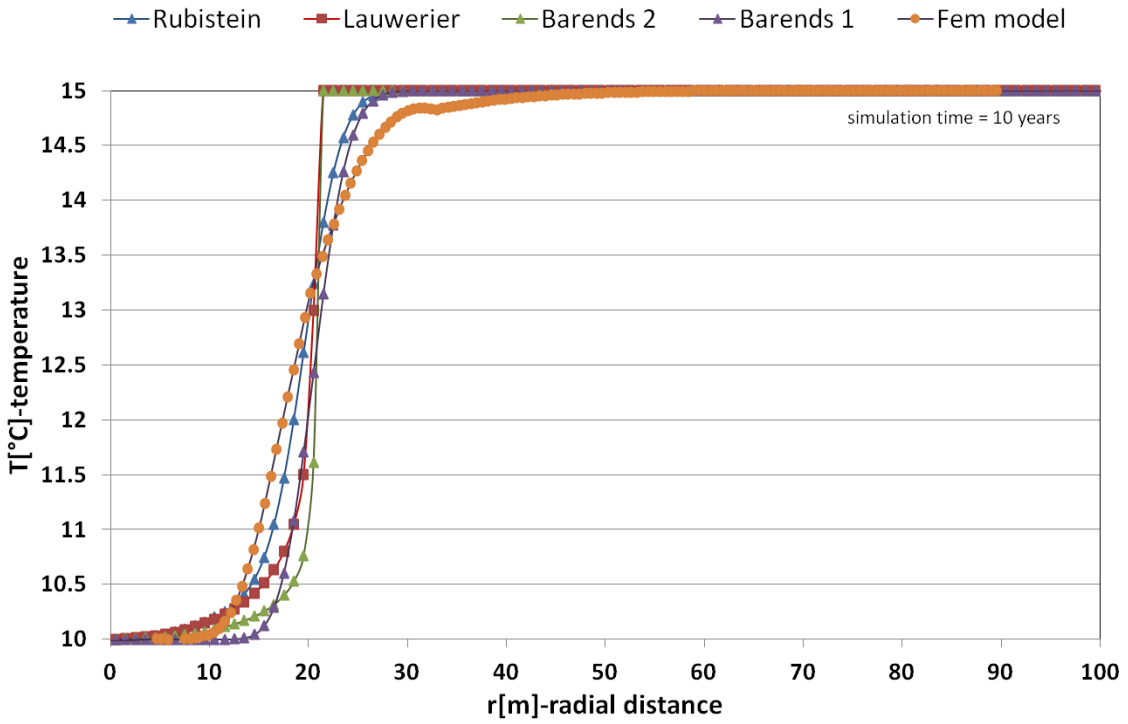

Figure 5.52: Temperature trend vs radial distance from injection cold well. Case: 120 m well distance,simulation time 10 years.

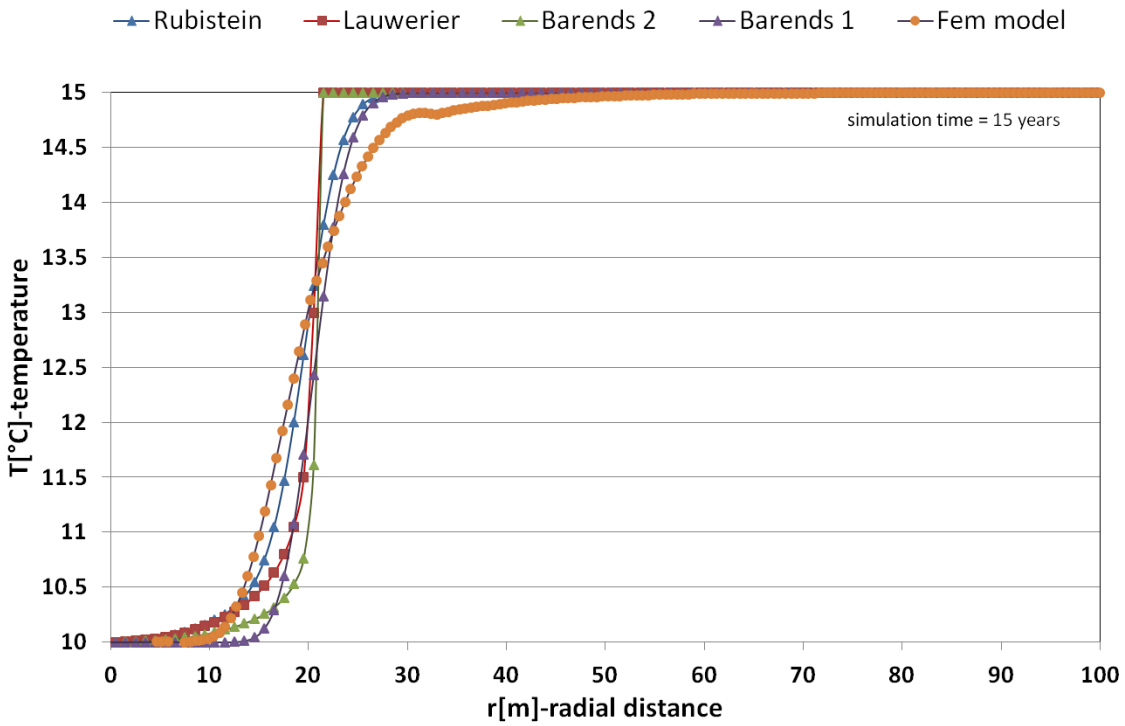

Figure 5.53: Temperature trend vs radial distance from injection cold well. Case: 120 m well distance, simulation time 15 years.

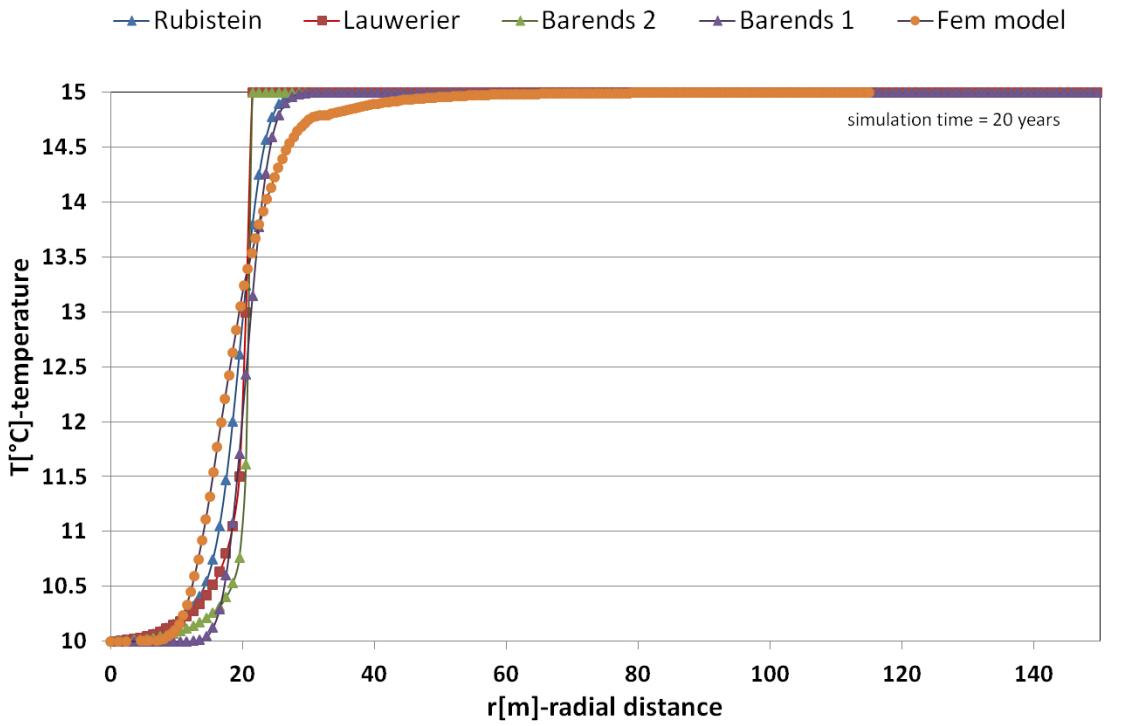

Figure 5.54: Temperature trend vs radial distance from injection cold well. Case: 120 m well distance, simulation time 20 years.

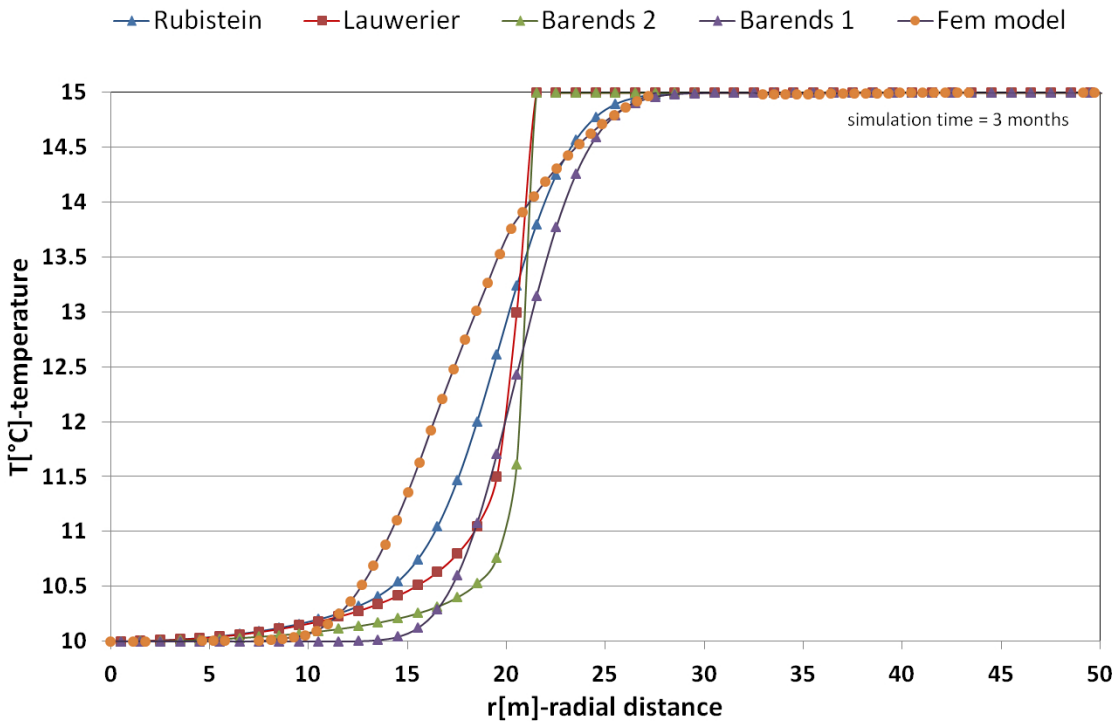

Figure 5.55: Temperature trend vs radial distance from injection cold well. Case: 120 m well distance,simulation time 3 months that is the injection time.

5.3.2 Synthesis & Conclusions

It is possible to talk about two zones, the first one concern a zone near to the well and the other one concerns a zone far than the well (this zone is named *End zone*). This *End zone* identify the maximum dimension of thermal bubble around well. Conclusion are listed below:

- for every result there is a good fitting between analytical and numerical solutions, in particular for the *End zone*;
- the main differences are in the first zone and depend on the period of comparison. If the comparison is taken during injection time, the numerical temperature trend does not coincide with analytical solutions because of the great mass flow rate magnitude difference.

Although there is no best fitting for the first zone, the *End zone* is best fitted by analytical solutions under effective mass solution. Thus this technique is a good method for thermal front evaluation.

Bibliography

Abramowitz, Milton and Irene A. Stegun. *Handbook of Mathematical Functions*. Ed. by Milton Abramowitz and Irene A. Stegun. 10th ed. Washingtor, D.C.: United States Department of Commerce, Dec. 1972.

Andersson, Olof. "Aquifer Thermal Energy Storage (ATES)". In: *Thermal Energy Storage for Sustainable Energy Consumption*. Ed. by H. Paksoy. Dordrecht, Nederlands: Springer, 2007. Chap. 8, pp. 155–176.

— "ATES for district cooling in Malmo". In: *Thermal Energy Storage for Sustainable Energy Consumption*. Ed. by H. Paksoy. Dordrecht Nederlands: Springer, 2007. Chap. 14, pp. 235–238.

— "ATES for district cooling in Stockholm". In: *Thermal Energy Storage for Sustainable Energy Consumption*. Ed. by H. Paksoy. Dordrecht, Nederlands: Springer, 2007. Chap. 15, pp. 239–243.

Banks, David. *An introduction to thermogeology: groundsource heating andcooling*. Ed. by David Banks. 1st ed. Oxford: Blackwell Publishing Inc, 2008.

Barends, F.B.J., Daltares, et al. "Complete Solution for Transient Heat Transport in Porous Media, following Lauwerier's concept". In: SPE International. Florence, Italy: Society of Petroleum Engineers, Sept. 2010.

Comsol, User guide. "COMSOL textsuperscript®Multiphysics user guide".

Courtois, Nathalie and Ariane Grisey. "Application of Aquifer Thermal Energy Storage for heating and cooling of greenhouses in France: a pre-feasibility study." In: *Proceedings European Geothermal Congress* (2007).

Delleur, Jacques W. et al. *The handbook of Groundwater engineering*. Ed. by Jacques W. Delleur. 2nd ed. CRC Press Taylor ampersand Francis Group, 2007. ISBN: 084934316X.

Domenico, P.A. and F.W. Schwartz. *Physical and Chemical Hydrogeology*. New York: John Wiley & Sons Inc., 1990.

Dunn, J.C. and R.H. Nilson. "Transient, radial distribution in a porous medium during fluid injection." In: *Sandia National Lab.* 2 (1981).

Kim, J., Youngmin Lee, et al. "Numerical Modeling of Aquifer thermal energy storage system". In: *Energy* 35 (Sept. 2010), pp. 4955–4965.

Lau, K.C. et al. "Initial experiences with the Canada Centre ATES". In: *21st Intersociety Energy Conversion Engineering Conference* (1986), pp. 676–681.

Lee, Kun Sang. "A review on Concepts, Applications and Models of Aquifers Thermal Energy Storage Systems". In: *Enegies* 3 (June 2010), pp. 1320–1334.

Noyer, M.L. *Simulation des Transferts Thermiques dans les Aquifèrs-(Condition the validité del solutions analytiques)*. Tech. rep. Orléas Cédex: Ministère de l'Industrie, du Commerce et de l'Artisanat-Departement hydrogéologie, Nov. 1977.

Paksoy, H., A. Snijders, and L. Stiles. *State of the Art of Aquifer Thermal Energy Storage Systems for Heating and Cooling Buildings*. Tech. rep. Stockholm, Sweden: Proceedings of Effstock 2009, June 2009.

Schmidt, T., D. Mangold, and H. MullerSteinhagen. "Seasonal Thermal Energy Storage in Germany". In: *ISES Solar World Congress* (2003).

Schneebeli, G. "Expériences sur la limite de validité de la loi de Darcy et l'apparition de la turbulencedans un écoulement de filtration". In: *La Houille Blanche* 10 (1955), pp. 141–149.

Tan, Haochen, Xiaohui Cheng, and Hongxian Guo. "Closed Solutions for Transient Heat Transport i Geological Media: New Development,Comparisons, and Validations". In: *Transp Porous Med* 93 (Mar. 2012), pp. 737–752.

Zienkiewicz, O.C., R.L. Taylor, and J.Z. Zhu. *The Finite Element Method: Its Basis and Fundamentals*. 6th ed. Oxford: Elsevier Butterworth-Heinemann, 2005.